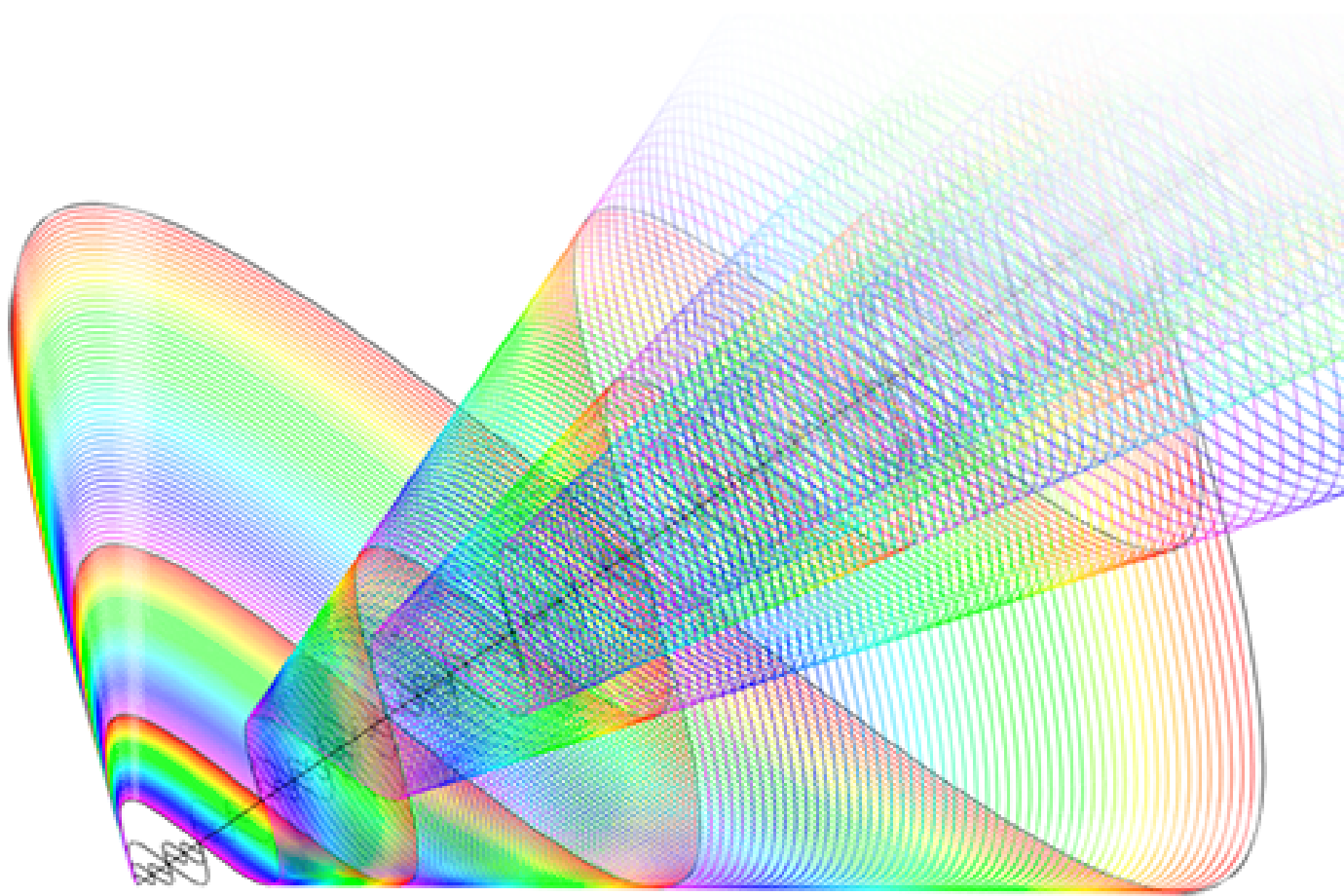


---

# Monitoring of harmonic distortions in distribution grids and their effect on temperature of substation transformers

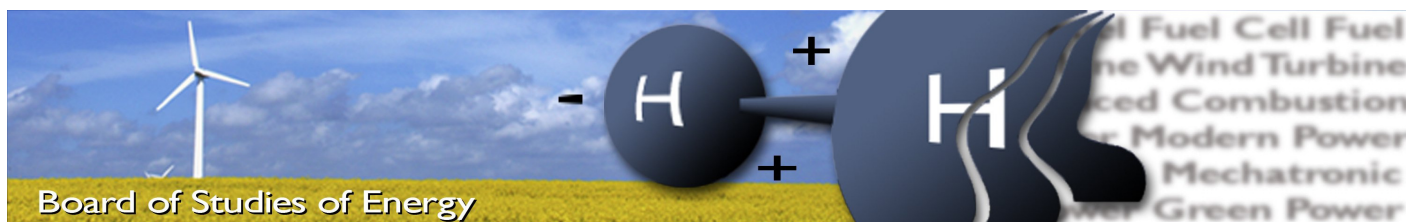
---



Master Thesis



AALBORG UNIVERSITY  
STUDENT REPORT



## Board of Studies of Energy

**Title:** Monitoring of harmonic distortions in distribution grids and their effect on temperature of substation transformers

**Semester:** 10

**Semester theme:** MSc in Energy Engineering

**Project period:** 01.09.2015 - 06.01.2016

**ECTS:** 30

**Supervisor:** Florin Iov, Ewen Ritchie

**Company Supervisor:** Otto Styrbæk

**Project group:** WPS4 - 1053

---

Volodymyr Myagkov

---



---



---

Copies: 3

Pages, total: 120

Appendix: 28

Supplements: -

### SYNOPSIS:

The sales companies of renewable energy sources are competing to get on Danish market. The equipment sold in Denmark must comply with the standards. However, the standards are subject for changing with growing new technologies. Therefore, in some cases the equipment installed 25-30 years back may not be covered by the new standards and the new equipment not reflect their large penetration into the grid. But the DSO task is to insure safe and stable operation of the network together with the equipment installed. It can be done by monitoring the 'health' of equipment. The current work investigates the effect of power electronic based generation and loads on substation transformer. For this purpose a random substation were chosen to perform the measurements. The data gathered during the measurements is used in the electrical-magnetic-thermal model to assess transformer temperature. Finally, the interpretation of the results will be summarized and the guidelines and recommendations will be provided for DSO.

**Keywords:** Condition monitoring, Distribution grid, Distribution transformer, Electrical-Magnetic-Thermal model

By signing this document, each member of the group confirms that all group members have participated in the project work, and thereby all members are collectively liable for the contents of the report. Furthermore, all group members confirm that the report does not include plagiarism.



# Preface and Acknowledgements

This report is about monitoring of harmonic distortions in distribution grids using the alternative methods and software. Moreover it investigate the effect of harmonics on temperature of substation transformers. The report is written by the student studying at the MSc in Wind Power Systems in Aalborg University. The project topic was proposed by the local DSO Thy-Mors Energi and further studied in cooperation with the Department of Energy Technology in Aalborg University.

The Site-Test was performed in order to define and investigate the harmonic emissions from wind turbine, pig farm and substation transformer. The per phase transformer model was developed and consist of the mix of electrical, magnetic and thermal models combined together. This model is used to assess temperature of substation transformers that are loaded with non-linear loads. Finally, the harmonic emissions from different sources was evaluated and analyzed.

The authors acknowledge is addressed to Associate Professors from the Department of Energy Technology in Aalborg University, Florin Iov and Ewen Ritchie for their guidance. The author would like to thank to Ionut Trintis for providing the equipment, guidance and help upon the preparations for test campaign and laboratory setup. Likewise, the authors acknowledge is addressed to employees from Thy-Mors Energi for their support upon the Site measurements.

Aalborg University, January 5, 2016

---

Volodymyr Myagkov  
<vmyagk13@student.aau.dk>



# Contents

<b>List of Figures</b>	<b>iii</b>
<b>List of Tables</b>	<b>vii</b>
<b>Nomenclature</b>	<b>viii</b>
<b>List of symbols</b>	<b>ix</b>
<b>1 Introduction</b>	<b>1</b>
1.1 Background . . . . .	1
1.2 Problem Statement . . . . .	2
1.3 Objectives . . . . .	3
1.4 Scope . . . . .	4
1.5 Content of Report . . . . .	5
<b>2 State of the Art</b>	<b>6</b>
2.1 Online Condition Monitoring . . . . .	6
2.2 Equivalent Circuit Model Representation . . . . .	8
2.3 Magnetic circuit . . . . .	10
2.4 Thermal equivalent model . . . . .	12
2.5 Summary . . . . .	14
<b>3 System Description</b>	<b>15</b>
3.1 Site Description . . . . .	15
3.2 Farm Description . . . . .	16
3.3 Renewable Energy Sources and Their Components . . . . .	21
3.4 Connection Requirements for equipment connected to low voltage grids < 1kV . . . . .	22
3.5 Summary . . . . .	24

<b>4</b>	<b>Site Measurements</b>	<b>25</b>
4.1	Planning of Site measurements . . . . .	25
4.2	Overview . . . . .	26
4.3	Measurement Equipment . . . . .	29
4.4	Data post-processing . . . . .	36
4.5	Summary . . . . .	39
<b>5</b>	<b>Harmonic analysis</b>	<b>40</b>
5.1	Selection of Data . . . . .	40
5.2	Harmonic Content of Farm . . . . .	44
5.3	Harmonic Content of WT . . . . .	49
5.4	Harmonic Content in Substation . . . . .	53
5.5	THD levels in Transformer, WT and PF . . . . .	57
5.6	Summary . . . . .	61
<b>6</b>	<b>Online Monitoring</b>	<b>62</b>
6.1	Transformer Modeling . . . . .	62
6.2	Model Validation . . . . .	65
6.3	Effect of Harmonics on Equipment . . . . .	71
6.4	Summary . . . . .	72
<b>7</b>	<b>Conclusion and Outlook</b>	<b>73</b>
7.1	Conclusion . . . . .	73
7.2	Outlook . . . . .	74
	<b>Bibliography</b>	<b>75</b>
	<b>Appendix A</b>	<b>77</b>

# List of Figures

2.1	Simplified Single-Phase Transformer.[1]. . . . .	8
2.2	A three limb core and its magnetic circuit representation. . . . .	11
2.3	Complex thermal equivalent circuit model used to represent transformer losses[2]. . . . .	13
3.1	Single line diagram of Thy-Mors Energi network . . . . .	15
3.2	Picture of secondary substation, pig farm and PV system n the top of piggery. . . . .	16
3.3	An approximate electrical diagram of the pig farm including main loads. . . . .	17
3.4	Daily operation diagram on a farm. . . . .	18
3.5	Farm feeding and control process. . . . .	19
3.6	Climate control system of one piggery. . . . .	20
3.7	Harmonic levels according to standard DS/EN 61000-2-4. . . . .	23
4.1	Single line diagram of Thy-Mors Energi network including the Points of Measurements. . . . .	27
4.2	Daily cycle for operation of WT and PV . . . . .	28
4.3	Setup for current and voltage measurement using Rogowski coils and High Voltage Differential probes. . . . .	30
4.4	Setup for current and voltage measurement using oscilloscopes, Rogowski coils and High Voltage Differential probes. . . . .	31
4.5	Grouping of harmonics and inter-harmonics according to DS/EN61000-4-7. . . . .	33
5.1	Active power of transformer, wind turbine and pig farm. . . . .	41
5.2	Wind speed for December 2015. . . . .	42
5.3	Levels for harmonic currents phase A Pig Farm for point 493. . . .	45
5.4	Levels for harmonic currents phase B Pig Farm for point 493. . . .	46

5.5	Levels for harmonic currents phase C Pig Farm for point 493. . . .	46
5.6	Levels for harmonic currents phase A Pig Farm for point 550. . . .	47
5.7	Levels for harmonic currents phase B Pig Farm for point 550. . . .	47
5.8	Levels for harmonic currents phase C Pig Farm for point 550. . . .	48
5.9	Levels for inter-harmonic currents phase A Pig Farm for point 550.	48
5.10	Levels for harmonic currents phase A Wind Turbine for point 493. .	49
5.11	Levels for harmonic currents phase B Wind Turbine for point 493. .	49
5.12	Levels for harmonic currents phase C Wind Turbine for point 493. .	50
5.13	Levels for harmonic currents phase A Wind Turbine for point 550. .	50
5.14	Levels for harmonic currents phase B Wind Turbine for point 550. .	51
5.15	Levels for harmonic currents phase C Wind Turbine for point 550. .	51
5.16	Levels for inter-harmonic currents phase A Wind Turbine for point 493. . . . .	52
5.17	Levels for harmonic currents phase A Transformer for point 493. . .	53
5.18	Levels for harmonic currents phase B Transformer for point 493. . .	53
5.19	Levels for harmonic currents phase C Transformer for point 493. . .	54
5.20	Levels for harmonic currents phase A Transformer for point 550. . .	54
5.21	Levels for harmonic currents phase B Transformer for point 550. . .	55
5.22	Levels for harmonic currents phase C Transformer for point 550. . .	55
5.23	Levels for inter-harmonic currents phase A Transformer for point 493.	56
5.24	THD levels for transformer current in three phases for measurement period from 3 December to 4 December. . . . .	57
5.25	THD levels for wind turbine current in three phases for measurement period from 3 December to 4 December. . . . .	58
5.26	THD levels for pig farm current in three phases for measurement period from 3 December to 4 December. . . . .	58
6.1	An equivalent electrical-magnetic-thermal model of three phase transformer. . . . .	63
6.2	Dependence of transformer temperature due to harmonic currents.	68
6.3	Results of simulations done in previous project. . . . .	69
6.4	The visualization of monitoring tool developed during the 9th semester project. . . . .	70
.1	Core and yoke cross section . . . . .	79
.2	Transformer design parameters. . . . .	83

.3	The temperature drop from windings to the ambient in oil filled transformer. . . . .	89
.4	Transformer rated data . . . . .	94
.5	Transformer test report. . . . .	95
.6	Inverter rated data. . . . .	98
.7	Vestas V29 255kW Wind Turbine (1) . . . . .	100
.8	Vestas V29 255kW Wind Turbine (2) . . . . .	101
.9	Vestas V29 255kW Wind Turbine (3) . . . . .	102
.10	The structure of files saved for easy processing using the Matlab script.	104

# List of Tables

3.1	List of main electrical components used on the farm. . . . .	20
3.2	Vestas V29 wind turbine rated data, electrical components and control.	21
3.3	Fronius Agilo 100.0-3 inverter rated data. . . . .	21
3.4	Typical harmonic emission from different equipment. . . . .	22
3.5	Harmonic emission limits for wind power plants with rated power over 25kW to 1.5MW. . . . .	23
4.1	Description of measurement points on the LV side. . . . .	27
4.2	Oscilloscope, probe and channel distribution for test measurements.	32
4.3	The settings for timebase. . . . .	34
4.4	Oscilloscope trigger settings. . . . .	35
4.5	Main settings volt per division and attenuation for voltage and current probes. . . . .	35
4.6	The new file created after processing with Matlab to do DFT. . . .	36
5.1	Test measurements assigned to the day taken. . . . .	42
5.2	Selected points for analysis . . . . .	44
5.3	The amplitude of harmonic current in each phase for transformer, wind turbine and pig farm point 493. . . . .	60
5.4	The amplitude of harmonic current in each phase for transformer, wind turbine and pig farm point 550.5.4 . . . . .	60
.1	Delta to star conversion for winding resistance. . . . .	77
.2	Temperature corrections for winding resistances on HV and LV side.	78
.3	Summary of harmonic levels from DS/EN61000-2-4 for Class 2 . . .	96

# Nomenclature

Acronym	Description
AC	Alternating Current
Dd	Delta-delta
DG	Distribution Grid
DSO	Distribution System Operator
Dyn	Delta-wye neutral
fft	Fast Furrier Transform
HV	High Voltage
HVD	High Voltage Differential
IEC	International Electrotechnical Commission
IT	Ideal Transformer
LED	Light Emitting Diode
LV	Low Voltage
MV	Medium Voltage
OEM	Original Equipment Manufacturer
PCC	Point of Common Coupling
PF	Pig Farm
POM	Point Of Measurements
PV	Photovoltaic
RMS	Root Mean Square
THD	Total Harmonic Distortions
THDI	Total Harmonic Distortions of Current
THDV	Total Harmonic Distortions of Voltage
WT	Wind Turbine
Yd	Wye-delta
Yy	Wye-wye

# List of Symbols

Symbol	Description	Unit
$a$	Transformer turns ratio	-
$C_{fe}$	Thermal capacitance of the core	$J/K$
$C_{mp}$	Thermal capacitance of the tank and other parts	$J/K$
$C_{oil}$	Thermal capacitance of the oil	$J/K$
$C_{th}$	Thermal capacitance	$J/K$
$C_{wdn}$	Thermal capacitance of cooper windings	$J/K$
$F$	Magnetomotive force	$A \cdot turns$
$f$	Frequency	$Hz$
$h$	Harmonic order	-
$H$	Harmonic factor	%
$hc$	Harmonic component	-
$I$	Current	$A$
$i$	Integer number	-
$I_1$	Value of 50 $Hz$ current	$A$
$I_c$	Core loss current component	$A$
$I_h$	Harmonic current	$A$
$I_m$	Magnetizing current component	$A$
$I_o$	Excitation current component	$A$
$I_o$	No-load current (from the data sheet )	%
$I_p$	Primary current	$A$
$I_s$	Secondary current	$A$
$X_m$	Magnetizing reactance	$\Omega$
$X_p$	Primary inductive reactance	$\Omega$
$X_s$	Secondary inductive reactance	$\Omega$
$L_p$	Primary leakage inductance	$H$



*List of Symbols*

Symbol	Description	Unit
$L_s$	Secondary leakage inductance	$H$
$N_p$	Number of turns on primary	-
$N_s$	Number of turns on secondary	-
$\theta_{amb}$	Ambient temperature	$^{\circ}C$
$\Phi$	Magnetic flux	$Wb$
$\Phi_m$	Mutual flux	$Wb$
$\theta_{oil}$	Oil temperature	$^{\circ}C$
$p$	Number of rectifier arms	-
$P$	Active power	$W$
$P_{EC}$	Eddy current losses	$W$
$P_H$	Hysteresis losses	$W$
$P_k$	Short circuit power	$W$
$Pl1n$	Permeances of leakage flux path on primary where $n = phase\ a, b, c$	$Wb/A$
$Pl2n$	Permeances of leakage flux path on secondary where $n = phase\ a, b, c$	$Wb/A$
$P_{LL}$	Load losses	$W$
$P_{loss}$	Core losses	$W$
$P_n$	Magnetic permeance where $n = phase\ a, b, c$	$Wb/A$
$P_{NL}$	No-load loss	$W$
$P_o$	No load power	$W$
$P_{oc-p}$	No-load power related to primary	$W$
$P_{OSL}$	Other stray losses	$W$
$P_p$	Active power on primary	$W$
$P_T$	Transformer total losses	$W$
$Q$	Reactive power	$VAR$
$q_{fe}$	Heat generated by core losses	$W$
$Q_{oc-p}$	No-load reactive power related to primary	$VAR$
$q_{st}$	Heat generated by stray losses	$W$
$q_{tot}$	Total transformer losses due to the heat	$W$
$q_{wdn}$	Heat generated by winding losses	$W$
$R1n$	Winding resistance on primary where $n = phase\ a, b, c$	$\Omega$
$R2n$	Winding resistance on secondary where $n = phase\ a, b, c$	$\Omega$

*List of Symbols*

Symbol	Description	Unit
$R_c$	Core resistance	$\Omega$
$R_{load,n}$	Load resistance where $n = phase\ a, b, c$	$\Omega$
$R_n$	Magnetic resistances where $n = phase\ a, b, c$	$A/(Wb/s)$
$R_p$	Equivalent resistance on primary	$\Omega$
$R_s$	Equivalent resistance on secondary	$\Omega$
$R_{th}$	Thermal resistance	$K/W$
$R_{th-fe-oil}$	Non-linear thermal resistance of core to oil	$K/W$
$R_{th-mp-oil}$	Non-linear thermal resistance of other metal parts to oil	$K/W$
$R_{th-oil-air}$	Non-linear thermal resistance of oil to air	$K/W$
$R_{th-wdn-oil}$	Non-linear thermal resistance of windings to oil	$K/W$
$Sn$	Switch where $n = 1, 2, 3$	-
$T_{constG}$	Ambient temperature	$^{\circ}C$
$V$	Voltage	$V$
$V_p$	Voltage on primary	$V$
$V_s$	Voltage on secondary	$V$
$w1n$	Number of turns on primary where $n = phase\ a, b, c$	-
$w2n$	Number of turns on secondary where $n = phase\ a, b, c$	-
$Z$	Impedance	$\Omega$
$Z_k$	Short circuit impedance	%
$\Re$	Reluctance	$H$
$P$	Permeance	$H^{-1}$
$\mu$	Permeability	-
$l$	Length	$m$
$A$	Cross sectional area	$m^2$
$K_h$	Hysteresis constant	-
$B_m$	Maximum flux density	$T\ (tesla)$
$v$	Volume of the core	$m^3$



# 1 Introduction

## 1.1 Background

*„Learn from yesterday, live for today, hope for tomorrow.*

*The important thing is not to stop questioning.“*

Albert Einstein

Nowadays it becomes more and more challenging to study the distribution grids. The reason for it is the rapid expansion of renewable sources and power electronic based equipment. It becomes accessible to afford e.g. a household WT, PV systems, heat pumps and other renewable generation units. The renewable sources and equipment sold on Danish market is complying with the standards. However, these standards may not reflect their large penetration into the grid. Hence the penetration of renewables is usually seen in terms of harmonic distortion of the voltage and current.

Generally the harmonic issues are caused by power electronic based equipment installed in all network levels such as High Voltage (HV), Medium Voltage (MV) and Low Voltage (LV) network. However, the transmission network is more protected with filtering equipment against harmonic issues compare to distribution network. For example, the Wind Farm on HV or MV grid is supplied with filtering equipment. However, in the LV grid the existing renewable sources may not have any harmonic filters since they were built about 25-30 years ago. Therefore, the current effect of those plants on the network is ' unknown ' due to the absence of information about the harmonics that may come from these plants. Moreover, not only the power generating units but also the loads are the reasons of harmonic issues. These harmonics are causing additional losses and temperature increase. All these have negative influence on the other equipment installed in the grids.

Therefore, it is essential for Distribution System Operators (DSO) to monitor the voltage and current including the harmonic content and also the equipment on the substation level. Consequently, the DSO are installing measurement devices to be up to date about current loading's and harmonic issues. Typically the meters gives big amount of data on Voltage (V), Current (I), power factor , Total Harmonic Distortions (THD) etc. This information can be used to make a forecast for the future transformer loading's or to analyze the past loading's. However, by themselves they do not reflect what is happening with the equipment and how long it will last if there are critical loads with high harmonic content.

There are several diagnostic tools used to monitor the conditions of the equipment in substations. These techniques are described in details in section 2.1.

Taking into account existing diagnostic tools the most effective one involves online condition monitoring. The results of online monitoring can be used to estimate equipment life-time and plan Original Equipment Manufacturer (OEM) maintenance if needed. Most of this equipment is justified in terms of complexity and costs on the primary substations (HV and MV). Notice that the typical number of secondary substations handled by a DSO can go up to 2000.

However these techniques are stand-alone tools expensive and do not interact with meters installed in secondary substations. Thus simple tools for on-line monitoring associated with the existing equipment installed in secondary substations are needed.

## 1.2 Problem Statement

Based on the above mentioned the main attention of this work is paid to the LV Distribution Network (DN) and loads as well as generators (renewable sources). First of all it is the harmonic problems due to the power electronics in loads such as Refrigerators, Television, Light(LED), Motor drives, Automation etc. Secondly the harmonics penetration from the household WT's, PV inverters and heat pumps. The impact of harmonic distortions is seen not only on the secondary substations of LV networks but also reflected into the MV networks.

The substation transformers are the first assets on LV network subject to the adverse effects of harmonic distortions. At the same time the consumers can experience

the effect of harmonics seen as the poor power quality, flickers, maloperation of equipment, resonance effect[3] etc.

The power losses and temperature increase in transformers has negative influence on the transformer lifetime. Therefore, for DSO it is important to monitor these issues. Often the monitoring tools are expensive. Taking into account variety of transformers it is impossible to get and handle these tools from different manufacturers. Since, the DSO has variety of meters it would be more efficient for them to know how to interpret the information taken by these devices. Moreover, the DSO needs the monitoring tools that will account for THD, voltage, current to estimate transformer temperature. It will help to make a forecast for the future transformer thermal behavior and give the information about transformer lifetime which also depends on transformer temperature and other factors.

Therefore, the problem statement is formulated and presented in next section.

### 1.3 Objectives

The main objective of this work is

*to develop a monitoring tool including guidelines for assessment of thermal behavior of distribution transformers exposed to high harmonic content present in LV distribution networks*

#### 1.3.1 Sub Objectives

In order to fulfill the main objective the following sub objectives and tasks are formulated.

1. Investigate the impact of harmonic distortions both from the grid and load side on distribution transformers
2. Develop and validate a per-phase electric-magnetic-thermal equivalent model for distribution transformer
3. Provide a guidelines for DSO regarding the effect of harmonics on LV distribution transformers

### 1.3.2 Tasks

For the Sub Objective 1:

- Investigate different approaches for transformer modeling
- Create a simulation model
- Determine test cases for simulation scenarios
- Model validation and verification using field measurements

For the Sub Objective 2:

- Define the connection requirements for loads, WT, PV, Heat pumps etc.
- Give characterization of the loads and generating units of the LV grid
- Perform on-site measurements

For the Sub objective 3:

- Post processing of measurement data and harmonic analysis

## 1.4 Scope

The project is focusing in condition monitoring of distribution transformers placed in secondary substations. An assessment of the impact of harmonic content on loading and thermal behavior of the distribution transformers is carried out under different scenarios. Based on this impact assessment a combined electric-magnetic-thermal equivalent model is developed in order to estimate the temperature and the loading of the transformer.

The on-site measurements are performed in order to validate the model and give detailed description for the loads and generators. A simple tool for condition monitoring that is using current, voltage and temperature measurements as well as historical data is proposed and developed. This tool is enabling DSOs to monitor effectively the operation of the distribution transformers placed in secondary substations and gather knowledge about the harmonic effect on transformer temperature. Moreover, guidelines for assessment of transformers thermal behavior are suggested.

### 1.4.1 Assumptions and Limitations

Several assumptions and limitations are considered during this project, and they are listed below.

- Only the steady-state operation of transformer is considered;
- Network representation is assumed to be symmetric and balanced;
- MV grid voltage  $10.5\text{ kV}$  is assumed fixed (balanced and without distortions) ;
- Background harmonic content from MV side is not considered;
- Voltage and current sub- and inter-harmonics for both voltage and current are out of the scope;
- Voltage harmonics are not considered;
- Non-linear loads are modeled based on available data from public domain and datasheets;
- Data about ambient temperature is assumed to be equal to outside tank temperature measured using USB thermocouple loggers;
- Off-line condition monitoring tests are not considered;
- Economic aspects are not taken into account;

## 1.5 Content of Report

The project is structured as follows. Chapter 2 gives description of existing online monitoring tools and techniques as well as introduces different modeling approaches. Chapter 3 introduces the problem area, component description and specifications together with the requirements for connection. Chapter 4 explains the test measurements performed on substation transformer also explains the choice of equipment and way the data is treated. Chapter 5 covers harmonic studies and gives characterization for the harmonic content from different sources. Chapter 6 presents the model of substation transformer and simulation results for the predefined simulation scenarios. Moreover, it presents an monitoring tool and also the guidelines and recommendations that are based on the simulation results.



## 2 State of the Art

This chapter provides an overview of the major diagnostic techniques for condition monitoring of transformers and the network equipment. Section 2.1 gives an brief introduction to the online condition monitoring applications and different measurement equipment that is used for monitoring of basic parameters. Moreover, sections 2.2, 2.3 and 2.4 introduce three modeling approaches that are based on the electrical, magnetic and thermal parameters.

### 2.1 Online Condition Monitoring

Transformer is an important asset of any network. The first priority is its smooth and continuous functioning. The second priority is onetime service and maintenance. And last but not least is the planning and control of transformer lifetime (aging and degradation). Therefore, condition monitoring is used to identify possible faults and malfunctioning of transformer and its parts. There are several diagnostic techniques that helps to identify possible faults in transformers.

- Dissolved gas analysis
- Moisture in oil
- Frequency response analysis
- Partial discharge analysis
- Hot spot temperature
- Winding temperatures

The online monitoring systems are used to measure i.e electrical, chemical or physical signals. It has a variety of sensors, data-acquisition units, communications link, computer and data processing software [4]. A wide range of parameters can be monitored since these systems can be used inside and outside the transformer tank and terminals.

The operational principle of such units is based on the sampling of analogue signal that is later transformed to a digital signal. Furthermore, the data can be transferred to control room or PC through the cable or wireless connection.

As an example there are several applications developed by manufacturers that are used for online monitoring e.g. AREVA MS2000 [5], ALSTOM MS3000 [4]. Their typical application is in transmission and distribution grids e.g. monitoring of instrument transformers, bushings and load tap changers.

However, the above techniques are of high cost and often the manufacturer equipment is needed to perform these tests. On the other hand the DSOs has variety of transformers and it could be difficult to have several applications from different manufacturers. Moreover, with increased use of power electronics-based equipment in distribution networks the risk of appearance harmonic distortions is also increased. Hence, these techniques are used to show current conditions of transformer but cannot predict or make a forecast for the future functioning when the harmonic content is present.

In this case the method that can help is monitoring of voltage and current harmonics by use of transducers. It is commonly used in different meters, power analyzers, Rogowski coils, etc. Consequently, this equipment allows evaluation of such parameters as  $I$ ,  $V$ ,  $P$ ,  $Q$ , *power factor*, *THD*. However, it does not show the relation of harmonics on transformer temperature rise.

For example the use of Rogowski coils reflects only the current measurements. The use of differential voltage probes will cover only the voltage. Finally use of thermal sensor will give the thermal readings. All those measurements are time consuming and needs allocation of personal to perform it. The easiest way is to use only the meters and thermal sensors. However, the thermal sensors are costly and not always available or perhaps there is no need to install them. Therefore, the DSO need to know how to use and interpret data only from meters. Since the data analysis is very complicated process the DSO may consider to use a simple model that can process all these data in short time without using extra resources.

For example, a data from meters can be fitted into the model that will estimate the voltage and current levels, harmonic spectra (THDI, THDV) and also the temperature. On the other hand the model can be used to fit historical data to track the previous loading's, make an forecast for the future behavior or to see the changes in current loading's. Based on the previously statments the DSO needs fast and efficient model that is able to determine all parameters.

Therefore, the next following sections 2.2, 2.3 and 2.4 gives characterization for existing model representations that may be used when developing an monitoring tool. The choice of model representations is based on the 9th semester project „*Condition Monitoring of substation transformers in Distribution grids*“ and presented below.

## 2.2 Equivalent Circuit Model Representation

The equivalent circuit models are used to represent the relation between primary and secondary voltage and current. Often in different studies the simplified single phase transformer model is used. Some of the parameters might be neglected such as resistance of windings, leakage inductance, magnetizing current equals to zero and 100% efficiency. Therefore, in this project a detailed model of transformer is utilized. Thereby, the effect of harmonic currents on the core, windings, insulation and transformer oil will be investigated.

The model could be represented as an single phase equivalent circuit. For three phase transformer the three single circuits are combined according to transformer connection type. The equivalent electric circuit model of Ideal transformer (IT)[1] is presented in Figure.2.1.

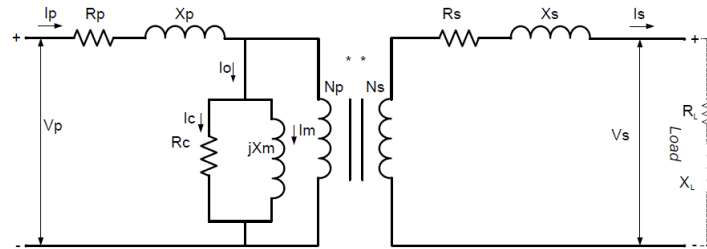


Fig. 2.1: Simplified Single-Phase Transformer.[1].

Where,

$V_p$  voltage on primary and  $V_s$  - voltage on secondary side in  $[V]$

$I_p$  primary current and  $I_s$  - secondary current in  $[A]$

$R_p$  primary winding resistance and  $R_s$  - secondary winding resistance in  $[\Omega]$

$X_p$  and  $X_s$  - primary and secondary inductive reactances in  $[\Omega]$  (or leakage inductance  $L_p, L_s$  in  $[H]$ )

$R_c$  - equivalent core loss resistance in  $[\Omega]$

$X_m$  - magnetizing reactance in  $[\Omega]$

$N_p$  - turn on primary

$N_s$  - turn on secondary and

$I_o$  - excitation current with  $I_m$  magnetizing current component and  $I_c$  core loss component in  $[A]$

It can be seen from the Figure.2.1 that magnetization and core-loss are due to the excitation current component  $I_o$  from that primary current  $I_p$ . Moreover, no-load loss characterized by  $I_m$  and  $I_c$  components. The iron loss due to hysteresis and eddy-currents is characterized by core loss resistance  $R_c$  and copper loss  $I^2R$  loss is vary with load. In the ideal transformer the input power equals to output power but in reality it is not like that due to the loses.

One of the main negative effect of transformer losses is generation of heat that has negative effect on its lifetime and this is depending on loading. The eq.2.1 to eq.2.7 shows relation of No-Load Losses  $P_{NL}$  and Load Losses  $P_{LL}$  to the total losses  $P_T$  eq.2.1 accounting for the non-linear content[6] which is represent by hysteresis  $P_H$  and eddy-current  $P_{EC}$  losses .

$$P_T = P_{NL} + P_{LL} \quad (2.1)$$

$$P_{NL} = P_H + P_{EC} \quad (2.2)$$

Moreover, Open-Circuit and Short-Circuit tests are used to define parameters of the equivalent electric circuit. By the no-load test core losses are defined( $I_s = 0$  and  $P_p = 0$ ) refer to eq.2.3. For no-load test power dissipation is observed in  $R_c$  and  $X_m$  respectively. However, for short-circuit test dissipation in  $R_c$  and  $X_m$  is typically negligible since the required voltage in the secondary coil is less than 5%. Therefore, losses will be seen in terms of copper losses in primary and secondary windings.

$$I_p = I_m = \frac{V_p}{X_m} \quad (2.3)$$

$$P_{LL} = I^2R + P_{EC} + P_{OSL} \quad (2.4)$$

$$I^2 R = R \sum_{h=1}^{h=h_{max}} I_h^2 \quad (2.5)$$

$$P_{EC} = P_{EC-R} \sum_{h=1}^{h=h_{max}} h^2 I_h^2 \quad (2.6)$$

$$P_{OSL} = P_{OSL-R} \sum_{h=1}^{h_{max}} h^{0,8} I_h^2 \quad (2.7)$$

where,

$I^2 R$  - is copper or core losses in  $[W]$

$P_H$  - hysteresis losses in  $[W]$

$P_{EC}$  - eddy current losses in  $[W]$

$P_{OSL}$  - other stray losses in  $[W]$

$I_h$  - harmonic current in  $[A]$

$h$  - harmonic order

However, the use of three single phase circuits does not account for magnetic coupling of the phases and the core geometry. Therefore, another way to represent transformer losses is introduced in the next section.

## 2.3 Magnetic circuit

The magnetic modeling can be used both to represent linear and non-linear behavior of transformer core. The commonly used representation of magnetic circuit by matrix equation eq.2.8 for all three phases. These representation take into account transformer construction parameters namely core geometry as it is seen from eq.2.10. The sum of magnetic fluxes in each limb is represented by eq.2.9 However, it is not easy to get or measure these parameters.

$$[F] = \Phi \cdot [\mathfrak{R}]^{-1} = [P] \cdot \Phi \quad (2.8)$$

$$\Phi = \Phi_1 + \Phi_2 \quad (2.9)$$

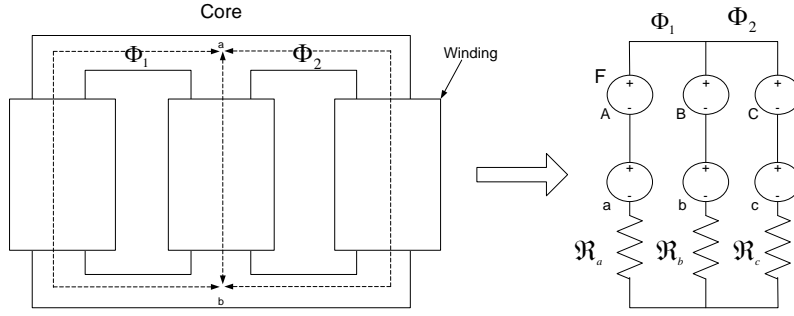


Fig. 2.2: A three limb core and its magnetic circuit representation.

$$\mathfrak{R} = \frac{A}{\mu \cdot l} \quad (2.10)$$

where

$\square$  - matrix notation

$F$  - is the applied mmf in  $[A \cdot turn]$

$\Phi$  - is the developed flux in  $[Wb]$

$\mathfrak{R}$  - reluctance matrix in  $[H]$

$P$  - permeance matrix in  $[H^{-1}]$

$A$ - core cross sectional area in  $[m^2]$

$\mu$ - permeability of material

$l$  - length of limb  $[m]$

In most cases the available measurements are no-load loss and magnetizing current, series or short-circuit impedance. Since the design parameters are the starting point for model definition while the test report and the name plate does not have information about transformer design parameters. Therefore, transformer dimensions and other parameters has to be calculated using the *Transformer design approach*. Simply starting design calculations from the name plate data and validate them using the test reports if available. This is a very important step if no transformer design data are available.

The Fig.2.2 shows a three limb core and its representation in magnetic domain[7]. This figure uses as an help to calculate ideal transformer matrix  $T_i$  (normalized matrix representation of transformer core). However, this project does not include

calculation of ideal transformer matrix for more information refer to Bibliography reference.# . Moreover, the saturation and hysteresis are not considered. The saturation is seen when energizing the transformer and hysteresis depends on the core materials (steel, ferromagnetic). On the other hand the effect of saturation seen as additional heat and the effect of hysteresis is reflected as hysteresis losses. These losses are no-load loss due to the no-load current flowing in the primary windings and the reflected secondary current does not contribute to saturation[8]. However these hysteresis and eddy currents are constant at all the loads since the flux density in the transformer core is almost constant.  $hysteresis\ loss = K_h \cdot B_m^{1.62} \cdot f \cdot v [W] >$  where  $K_h$  - hysteresis constant depends on material,  $B_m$  - maximum flux density  $[T (tesla)]$ ,  $v$  - volume of the core  $[m^3]$ [9]. Saturation appears when the current exceeding rated current. Typically this is not the case of distribution transformers.

The two modeling approaches described in section 2.2 and section 2.3 are supplement each other but they not account for heat transfer. Therefore, an thermal modeling approach is introduced in section 2.4.

## 2.4 Thermal equivalent model

As it was stated earlier the main transformer losses are coming from the core and windings. It leads to temperature rise in the oil and other transformer parts. Either electrical or magnetic model does not show the temperature rise due to the heat. Hence, the thermal modeling is used to cover this part.

In this project a complex thermal circuit model is used. The advantage of this model that it combines several thermal circuits [2]. Each circuit represent different transformer losses.

The model is shown in Figure.2.3 and has following description. It is used to determine transformer oil thermal capacitance. Disadvantages that model does not account for direct heat transfer between transformer parts. For example the windings and the tank, core and the tank etc. Thus to find the oil temperature  $\theta_{oil}$  it is important to find total transformer losses  $q_{tot}$  and the ambient temperature  $\theta_{amb}$ .

The definition of parameters shown in Figure.2.3 is as:

$q_{tot}$  - is the sum of the heat generated by the stray losses  $q_{st}$  in  $[W]$

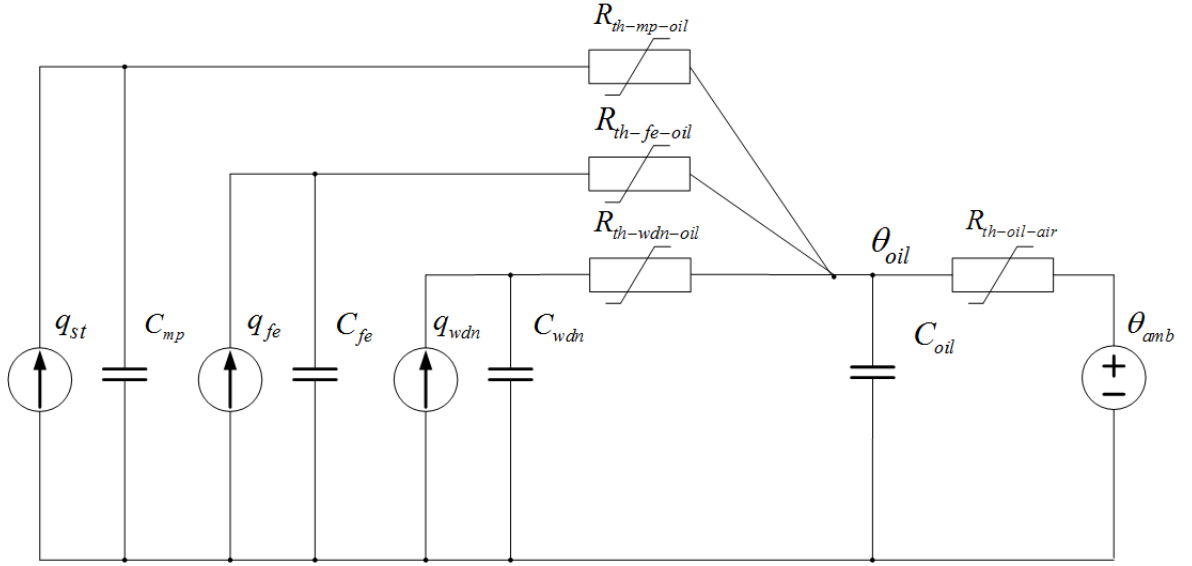


Fig. 2.3: Complex thermal equivalent circuit model used to represent transformer losses[2].

$q_{fe}$  - core losses in  $[W]$

$q_{wdn}$  - winding losses in  $[W]$

$C_{wdn}$  - the thermal capacitance of the copper in  $[J/K]$

$C_{fe}$  - the thermal capacitance of the core in  $[J/K]$

$C_{oil}$  - the thermal capacitance of the oil in  $[J/K]$

$C_{mp}$  - the thermal capacitance of the tank and other metal parts in  $[J/K]$

$R_{th-oil-air}$  - non-linear thermal resistance oil to air in  $[K/W]$

$R_{th-wdn-oil}$  - non-linear thermal resistance winding to oil in  $[K/W]$

$R_{th-fe-oil}$  - non-linear thermal resistance core to oil in  $[K/W]$

$R_{th-mp-oil}$  - non-linear thermal resistance for other metal parts to oil in  $[K/W]$

All thermal resistances are modeled based on the heat transfer theory[2]. In addition to that the transformer design parameters are calculated based on the *Transformer design approach*. Calculation results are attached in Appendix A 7.2.

The last but not least the choice of models depends on the modeling purpose and the model outcomes. Therefore, several equivalent circuit representations can be linked together in order to get better overview of the studied parameters. For example when looking into transformer core losses and temperature effect the magnetic and thermal models can be combined together. When studying non-linearity the electrical and magnetic models can be used.



According to eq.2.1 the total losses are based on the varying loads. Therefore, it is important to get knowledge about existing loads, their characterization and generated harmonic content. Thus the next section 3 gives brief overview of the loads and generators.

## **2.5 Summary**

This chapter presented the existent techniques for condition monitoring of the network equipment, electrical parameters such as voltage, current, harmonics etc. Moreover, it gives the summary for these techniques and introduces an advanced technique that is based on the modeling approach. Furthermore, there are presented several model representations that can be used for development of an advanced model. Finally, this chapter defines the need of combination of three models in order to cover electrical, magnetic and thermal behaviors in one model.

## 3 System Description

The System Description chapter gives a detailed description of the pig farm including the electrical equipment and renewable energy generation sources. This chapter defines main sources for the harmonic distortions and specifies their harmonic content. Moreover, it determine the harmonic and voltage limits based on the Danish standard and technical regulations for the equipment in distribution grids.

### 3.1 Site Description

The topology of Thy-Mors Energi network is shown in Figure.4.1. It represents a part of the radial feeder where primary substation is connected through the cable to the secondary substation and to the single consumer at the end of the feeder.

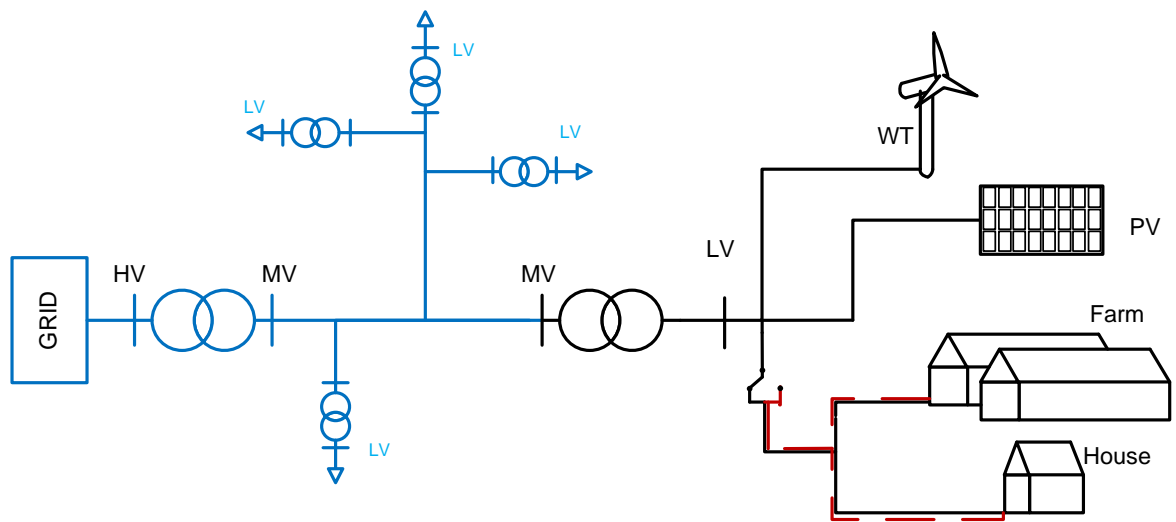


Fig. 3.1: Single line diagram of Thy-Mors Energi network

The MV grid highlighted in blue is unknown due to the company policy and cannot be described in the present report. Therefore, it is assumed that the MV grid

voltage is constant  $10.5\text{ kV}$  and the harmonic content from the grid is out of the scope due to the absence/lack of the data for MV grid. However, the secondary substation together with the loads and generation units is chosen for investigations and following description is given below.

The substation is situated in Nykøbing Mors it is a North-West Jylland (Danmark). The secondary substation transformer is connected to the customer that produce energy by *Vestas V29 255kW* WT, the PV system with rated power  $255\text{ kW}$ . Moreover, the loads are connected to the transformer. It is an pig farm and private house. Furthermore, the consumer has its own generator to ensure safe operation for the pig production since it is required that farm is supplied with power 24/7. The substation is placed next to the pig farm, house and PV system. Moreover, the PV system is mounted on the roof of the piggery refer to Figure.3.2 The WT is placed on the remote distance about 230m therefore the cables connecting the WT, PV and pig farm with transformer are assumed neglect and not used in simulations.



Fig. 3.2: Picture of secondary substation, pig farm and PV system on the top of piggery.

## 3.2 Farm Description

This section includes description of the electrical equipment, weekly operations, including food preparation, ventilation and climate control and the main electrical components

installed on pig farm.

### 3.2.1 Pig farm electrical diagram

The electrical diagram of the farm is not available. Therefore, an approximate diagram is shown in Figure.3.3 with main electrical components. As it is seen from

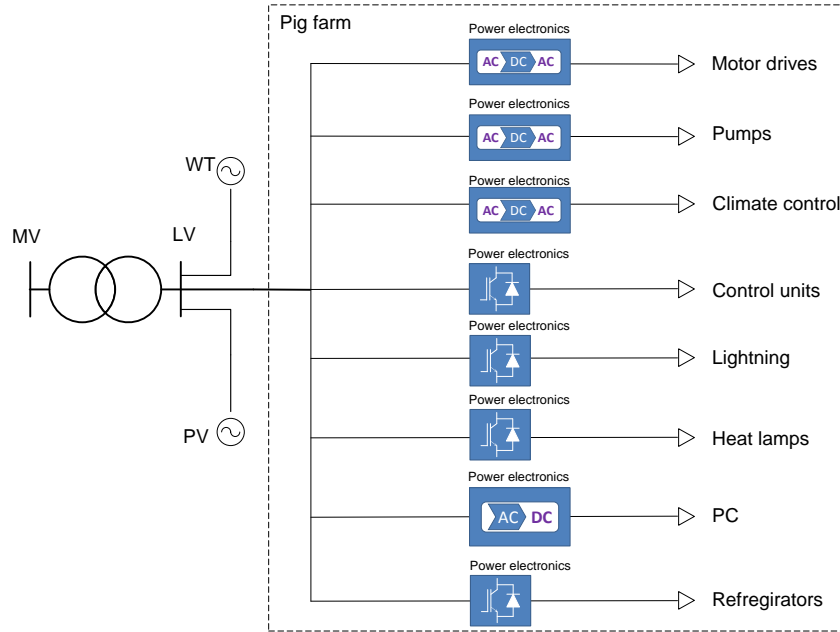


Fig. 3.3: An approximate electrical diagram of the pig farm including main loads.

Figure.3.3 the load connected to distribution transformer is the Pig farm. The main load (PF) consists of number of loads as the motors, pumps, control units, pc's and other. There is also present generators such as WT and PV system. The private house is not shown in this figure and assumed to not contribute to the main harmonic issues.

The farm is specialized on the breeding of pigs. Some of the basic operations involved in this process are feeding, animal treatment, cleaning, climate, etc. It involves use of electrical equipment. For example, the feeding involves food preparation and food distribution. The climate is regulated by exhaust ventilation, ceiling and wall inlets and high pressure system for humidity control. The cleaning process involves use of high pressure pumps to wash piggery or other places. The other important processes are lightning on the farm, heating/infrared lamps in farrowing unit/pen and many other.

### 3.2.2 Typical weekly operations

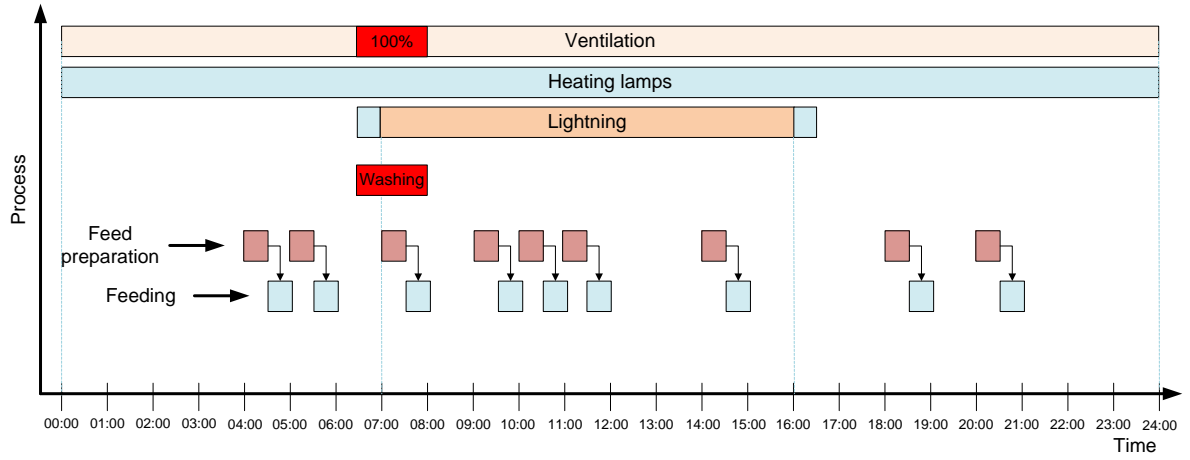


Fig. 3.4: Daily operation diagram on a farm.

On the Figure.3.4 is shown the main operations on the farm during one day. The same is applicable for rest of the week. Some of the tasks might be shifted, but in general the sequence of operations remain the same. It is seen from the Figure.3.4 that the Ventilation and Heating lamps are working constantly. The ventilation depends on the inside and outside temperature and is running full power during the hottest time and at low level in the cold periods. However, every Tuesday when the piggery is cleaned using the high pressure washer it is required to run the ventilation at full power for outflow of vapor and dusty air (Red box Washing and 100% in Figure.3.4).

The lightning on the farm is to be on at 07:00 and to be off at 16:00 however there is an extra margin  $\pm 30 \text{ min}$  in case of some delay or other situations related to maintenance and animal treatment. The food mixes and distributes nine times within 24 hours to the different piggery sections. In addition, twice a week Monday and Friday the manure has to be removed/pumped out. The time is not specified and will be corrected during the data analysis.

### 3.2.3 Food preparation

The visualization of liquid feeding system is shown in Figure.3.5.

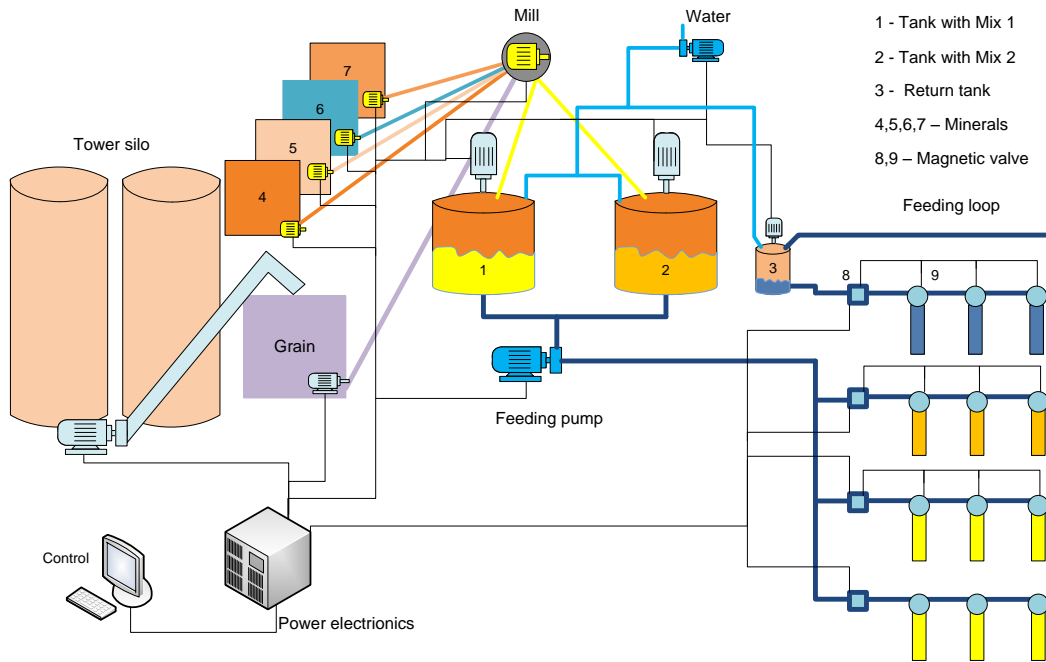


Fig. 3.5: Farm feeding and control process.

The Figure.3.5 gives description of complex processes that require switching on and off of electrical equipment involved in the food preparation. Moreover, all operations are managed and controlled from the PC then the Power Electronic is in charge for the switching. For example, to prepare one kind of food the Tank-1 will be filled with water. Then the grain goes from Tower silo or Grain silo to the Mill where the grain is finned/catted. Then different minerals from silo 4, 5, 6,7 are added to the main mix in Tank-1. Finally, Finished food is distributed through the specific feeding loops(different pig sections needs various food type) to the animals and doses by the help of magnetic valves and feeding pump.

#### 3.2.4 Climate control

So called climate control computer, installed on the farm, is used for the climate, ventilation and humidity control. It is based on the same switching principle as for the liquid feeding and can be controlled both from the PC or climate control computers. The visualization of climate control is shown in Figure.3.6. It can be observed that the basic components of climate control system are the Exhaust ventilation(variable speed), steering motor(fixed speed) for air inlet and the cooling system(pump with fixed speed) to keep the humidity and cool down the area.

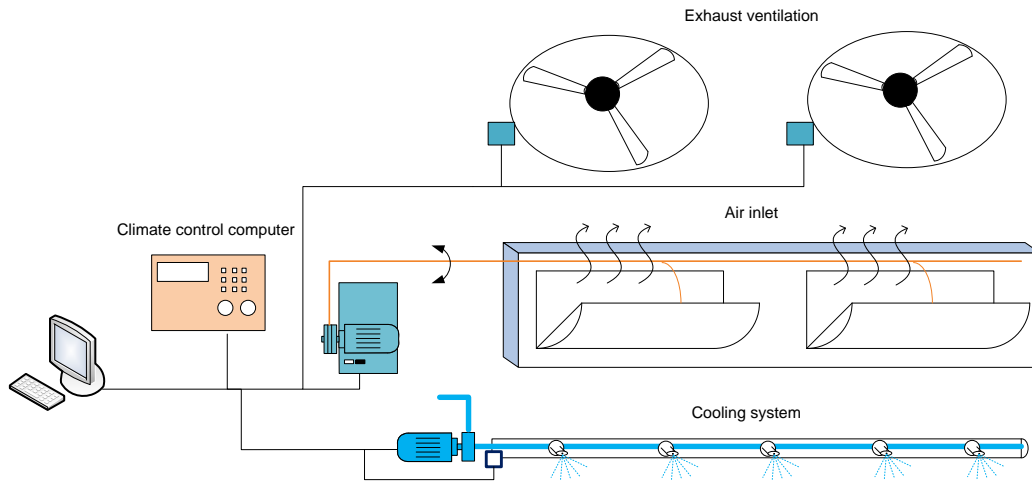


Fig. 3.6: Climate control system of one piggery.

#### 3.2.5 Main electrical components

Most of equipment on the farm is supplied with electrical motors, since they are involved in food preparation and distribution, ventilation, high pressure and water pumps. According to Figure.3.3 the power electronics is used for the control in almost all devices. Description of main components and its application is listed in Table.3.1 For example, the motors involved in food preparation are directly connected and has a fixed speed but for the food distribution the variable speed drives are used. Moreover, the climate control involves variable speed drives since the ventilation is depends on the inside and outside temperature, humidity and other factors. Thus the control is done by use of power electronics in PC's, climate control computers, different control units engaged in feeding sequences. Consequently, the impact of the power electronics might be seen in terms of harmonic distortions(inter-harmonics might be present) that will influence the power quality. The same for the farm lightning that can affect the voltage but mainly when the light is turned on around 6:30am in Figure.3.4.

Tab. 3.1: List of main electrical components used on the farm.

Equipment	Application
Motor	Pumps/ventilation/mills/drum cleaner/storage silo/agitator
Fluorescent lamp	Farm lightning
Infrared lamp	Heating in pigsty
Power electronic	Control units

### 3.3 Renewable Energy Sources and Their Components

The remaining assets are Vestas V29 wind turbine and PV system. The main electrical components of WT are Generator, Yaw control, VMP-top control unit and listed in Table.3.2. The PV system connected to the grid through the

Tab. 3.2: Vestas V29 wind turbine rated data, electrical components and control.

Generator								
Rated power, 6 poles [kW]	Voltage [V]	Frequency [Hz]	Rated current [A]	Power factor	Reactive power no load [kVAR]	Power factor correction [kVAR]	Current cut in	
225	3x400	50	390A/225	0.83	95	100 kVAR	Via Thyristor	

Top processor control						Bottom processor control		
Yawing	Hydraulic	Wind - Temperature	Rotation	Generator	Pitch system	Grid	Power factor correction	Thyristors

inverter *Fronius Agilo 100.0-3*. The main electrical data is depicted in Table.3.3. Refer to Appendix 7.2 and 7.2 for more information regarding general specifications of PV and WT.

Tab. 3.3: Fronius Agilo 100.0-3 inverter rated data.

Input data		Output data						
Voltage range DC [V]	Max. input current [A]	Nominal output power [kVA]	Nominal grid voltage [V]	Grid voltage tolerance	Frequency [Hz]	THD [%]	PF	
460-820	227	100	3~400 /230	$\pm 10 / \pm 5\%$	50	< 3	1	

#### 3.3.1 Typical harmonic content

Since the studied components may generate harmonics it is important to get basic understanding of generated harmonic spectra. An typical harmonic spectrum



produced by different equipment is shown in Table.3.4. The information regarding harmonic emission is taken from the public domain. The data sheet for Vestas V29 WT and PV inverter does not include the information regarding harmonics. However, for PV inverter *Fronius Agilo* the harmonic content generated is less than 3% refer to data sheet 7.2. Table.3.4 gives description of different harmonic generators and their typical content. Hence, next section gives characterization of existing standards and requirements for connection of loads and equipment.

Tab. 3.4: Typical harmonic emission from different equipment.

Equipment	Harmonic emission (harmonic order)
WT	odd not multiple of 3 - 5, 7, 11, 13, 17...49, even not multiple of 3 - 2, 4, 8...50
PV Inverter	$n = 6 \cdot k \pm 1$ where $k = 1, 2, 3, 4...$
Motors	5, 7, 11, 13, 17, 19
Transformer energization	2, 3, 4, 5, 7
Fluorescent and Infrared heat lamp	3, 5, 7, 9, 11, 13
Thyristor based power electronics	2, 4, 6, 10, 20, 40 single thyristor 3, 5, 11, 21, 41 triac

## 3.4 Connection Requirements for equipment connected to low voltage grids < 1kV

The general connection requirements are taken from Danish Standard DS/EN61000-2-4 ( IEC 61000 series) Compatibility levels in industrial plants for low frequency conducted disturbances. Furthermore, Technical Regulation 3.2.5 for wind power plants greater than 11 kW (Energinet) is taken as the base for Vestas WT harmonic injections. The standard regulations for motors are taken from the regulations for manufacturers. In this case it is Schneider Electric (since it was available on public domain).

### 3.4.1 Harmonic Content Limits

The harmonic limits are presented in Figure.3.7 and evaluated at PCC. Moreover, Electromagnetic environment *Class 2* is taken into consideration. It is due to the fact that this *Class 2* is generally similar to the compatibility levels of public network. General compatibility levels for harmonics are listed in Figure.3.7. Description

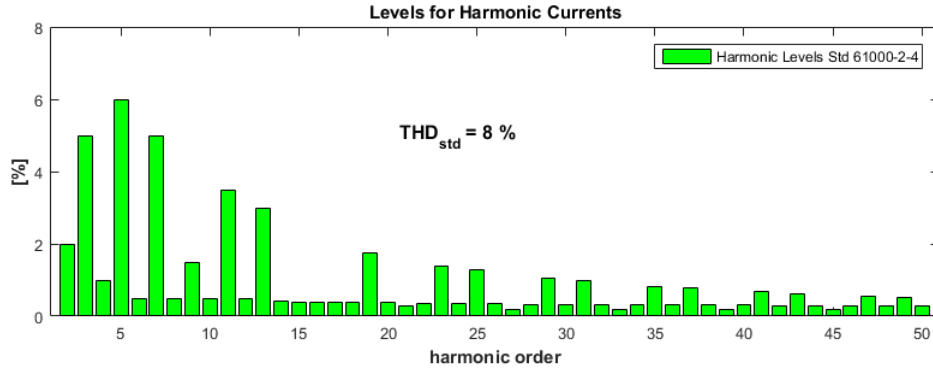


Fig. 3.7: Harmonic levels according to standard DS/EN 61000-2-4.

Tab. 3.5: Harmonic emission limits for wind power plants with rated power over 25kW to 1.5MW.

Voltage level	Harmonic order $h$				
	5	7	11	13	THDi
$U_N \leq 1kV$	3.6	2.5	1.0	0.7	4.5

for each harmonic level is given in Appendix A section 7.2 Table..3. The Total Harmonic Distortion (THD) for *Class 2* is 8%.

According to Teknisk forskrift 3.2.5 „for vindkraftværker større end 11 kW“ the limits for emission of harmonic currents are shown in Table.3.5

### 3.4.2 Voltage Limits/Variations

In this project the standard DS/EN61000-2-4 and Recommendation 16 „Spændingskvalitet i lavspændingsnet“ are used as a reference for voltage limits.

According to DS/EN61000-2-4 the voltage deviations for *Class 2* is  $\pm 10\%$  resulting in supply voltages in the range  $0.85 U_C$  to  $1.1 U_C (\Delta U/U_N)$ . A voltage increase can last from 10 ms to 1 min. The nominal voltage  $U_N$  is a standard 230V between phase and neutral. Voltage unbalance ( $U_{pos}/U_{neg}$ ) is 2% long-term effect ( $\geq 10$  minutes) and power-frequency deviations ( $\Delta f$ ) is  $\pm 1 Hz$ . For the lightning equipment the compatibility levels of IEC 61000-2-2 for *Class 2*.

According to General specification for Vestas V29-225 kW Wind Turbine the variation for nominal voltage 400V is +6% as the highest. And the voltage deviations for PV system according to Energinet.dk „Teknisk forskrift 3.2.2 for

*solcelleanlæg større end 11 kW*“ is  $\pm 10\%$  of  $U_N = 0.40kV$  thus  $U_{min} = 0.36kV$  and  $U_{max} = 0.44kV$  .

## 3.5 Summary

This chapter focused on the detailed description of the Test site electrical components and renewable generation sources. Moreover, the cycle of daily operations on the pig farm were presented with the electrical equipment involved in i.e. food preparation or climate control. In addition to this the typical harmonic content generated by the electrical equipment and renewables was highlighted. Finally, the chapter has covered the connection requirements for the equipment that is connected to the LV grid rated for maximum voltage of  $1kV$ .

## 4 Site Measurements

This chapter describes the general purpose of the Site-Test measurements defining the places where the measurements are performed. The planning and preparations for the site measurements are also important and included in this chapter. The overview and choice of equipment, main settings, measured values, bandwidth and other specifications are described in section 4.3. Furthermore, the literature review is carried out to highlight the process of data handling according to Danish Standard using the Discrete Furrier Transform.

### 4.1 Planning of Site measurements

One of the important steps in any work is to develop an plan it could be the actions plan with the tasks, timing and milestones, assignment and allocation of resources. Additionally, the planning process involve the communication between student and different parties DSO, project managers and network and control staff and consumes.

In this case the planning of site tests started as follows. First of all the student and DSO has arranged meeting to discuss the problem topic and develop the actions plan. The action plan was divided into three parts

- 1) site preparation
- 2) laboratory tests and training
- 3) measurement campaign

Upon the meetings there were discussed preferable size of substation that might be interesting for study. The next topic was to chose and find the equipment at AAU. Moreover, the choice of the site was made by DSO since the requirements from the student was to arrange the place (shelves) for setting up all measurement equipment.

While choosing the place the DSOs task was to get acceptance from the owner in order to use the properties. Typically, if it is a large consumer the substation can be 'shared' between DSO and the owner. Therefore, the access should be given and approved by these parts. After several meetings with DSO an estimated date for site measurements was chosen. This process is very complicated since the student has to account for many details starting from the choice and availability of equipment, substation, space requirements for the equipment, man power from DSOs side to cut the power on substation and put equipment. The most important part of the planning is personnel safety, therefore one of the meetings was to announce the safety rules and the procedure in case of emergency situation.

In order to get the site description the student has contacted the owner. The information from interview with the owner was summarized and presented in the above section 3.2. Consequently, the laboratory training was done in order to prepare for measurement campaign. Additionally, the labeling of all equipment was done in order to keep the structure.

The challenges on setting up all measurement equipment are

- that the measurement campaign could be done using only one attempt. This is due to the limited amount of man power allocated for this project
- the substation transformer can be powered off only once
- the measurement equipment could be taken for one week only

Just to describe the complexity of the planning process one will show the time spent on planning. The project started on 1<sup>st</sup> September 2015 but the date for test campaign was scheduled after all negotiations and preparations on 31 November 2015. However, due to the forced need of changing the equipment the date for test campaign was rescheduled on 1<sup>st</sup> December 2015.

## 4.2 Overview

The description of the Point's Of Measurements(POM) is listed below in Table.4.1. Where *POM1* is taken to measure three phase current and voltage on the LV terminals of transformer, *POM2* is for the measurements of current injections from WT. The following *POM3* is to measure current injections from pig farm and *POM4* is to measure inside transformer oil temperature  $T_{oil}^o$  as well as top and

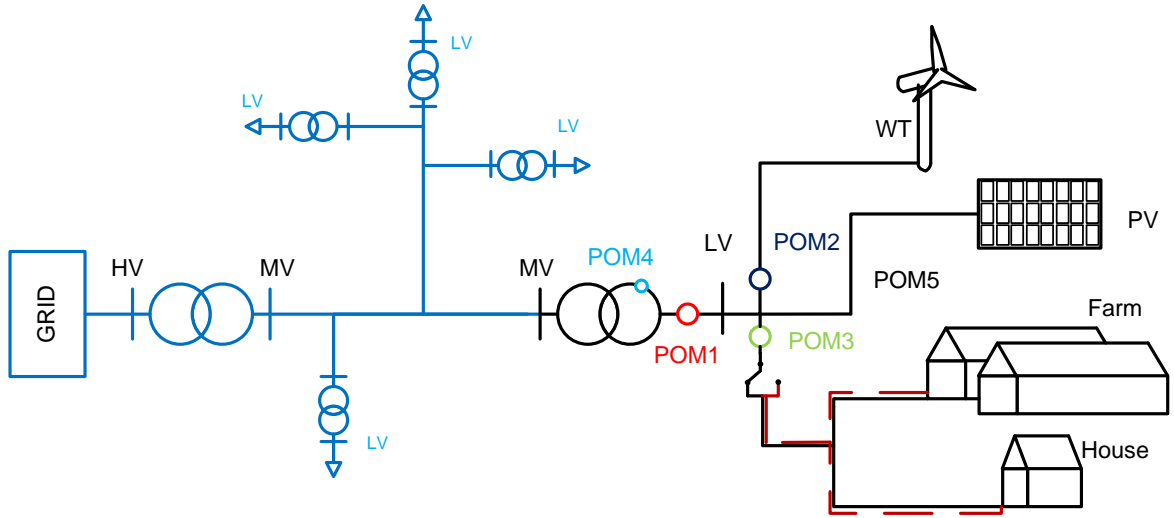


Fig. 4.1: Single line diagram of Thy-Mors Energi network including the Points of Measurements.

bottom tank temperature respectively  $T_{top}^{\circ}$  and  $T_{bott}^{\circ}$ . Further measured data will be processed to get the spectrum for the harmonic currents in each of the point of measurement.

Tab. 4.1: Description of measurement points on the LV side.

Measurement points	To be measured	Consequence
POM1	$V, I$	$I_{h-T}$
POM2	$I$	$I_{h-WT}$
POM3	$I$	$I_{h-Farm}$
POM4	$T_{oil}^{\circ}, T_{top}^{\circ}, T_{bott}^{\circ}$	$T_{ave}^{\circ}$
POM5	<i>not measured</i>	$I_{h-PV}$

As it is seen from the Figure. 4.1 there is no measurements from PV system it is due to the limit of equipment and the space in transformer house. However, later on one can extract data using the following equation 4.1.

$$I_{h-PV} = I_{h-Tot} - I_{h-WT} - I_{h-PF} \quad (4.1)$$

where

$I_{h-PV}$  - current harmonic generated by PV in [A]

$I_{h-Total}$  - total current harmonics generated by WT, PV and Farm in [A]

$I_{h-WT}$  - current harmonics generated by WT in [A]

$I_{h-PF}$  - current harmonics generated by the equipment on Pig Farm in [A]

$T_{ave}^{\circ}$  - average temperature of transformer in  $C^{\circ}$

Meaning that the information for current harmonics from PV system will be found by subtracting measured harmonics at *POM2* - WT and *POM3* - Farm from the total harmonic injections measured on *POM1* - Transformer. One has to note that injection from PV will be found assuming that the start for energy production by PV at the sunrise and stop at the sunset. The data for sunrise and sunset is taken from public domain for the period starting from 30 November 2015 to 8 December 2015. The approximate sunrise time is at 8:00am and sunset is about 16:00pm. The visualization example of daily power cycle of WT and PV system is shown in Figure.4.2(not real values are plotted).

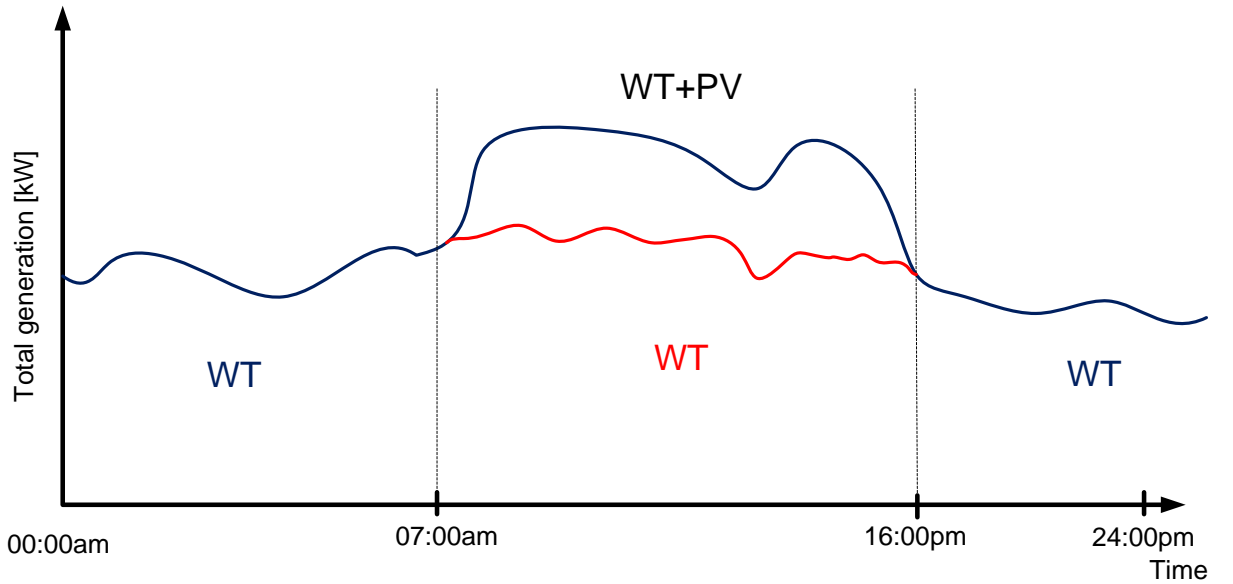


Fig. 4.2: Daily cycle for operation of WT and PV .

The points for sunrise and sunset has been chosen in order to figure out what harmonic injections are coming to transformer from PV system. The active and reactive power of transformer( $P_{TR}$  ,  $Q_{TR}$ ), WT( $P_{WT}$ ,  $Q_{WT}$ ), and PF( $P_{PF}$ ,  $Q_{PF}$ ), will be calculated using the general equation 4.2 and 4.3.

$$P = V_a \cdot I_a + V_b \cdot I_b + V_c \cdot I_c \quad (4.2)$$

$$Q = (V_a + V_b) \cdot I_c + (V_b + V_c) \cdot I_a + (V_a + V_c) \cdot I_b / \sqrt{3} \quad (4.3)$$

where

$P$  - active power [W]

$Q$  - reactive power [var]

$V_{a,b,c}$  - voltage in phase a, b, c [V]

$I_{a,b,c}$  - current in phase a, b, c [A]

However, the power generated by PV will be found first calculating  $I_{PV} = I_{Total} - I_{WT} - I_{PF}$  since the current in *POM5* is unknown and then calculate  $P_{PV}$  and  $Q_{PV}$ . Where  $I_{PV}$  - is the current on PV [A],  $I_{Total}$  - total current generated by WT, PV and Farm [A],  $I_{WT}$  - current generated by WT [A],  $I_{PF}$  - current generated by the equipment on Pig Farm [A].

Further on it will give ability to investigate the temperature rise in transformer due to the harmonics. Moreover, it will be possible to give guidelines if the harmonics are on the safe level or they need some attention.

## 4.3 Measurement Equipment

On the site the measurement equipment was placed in shrank



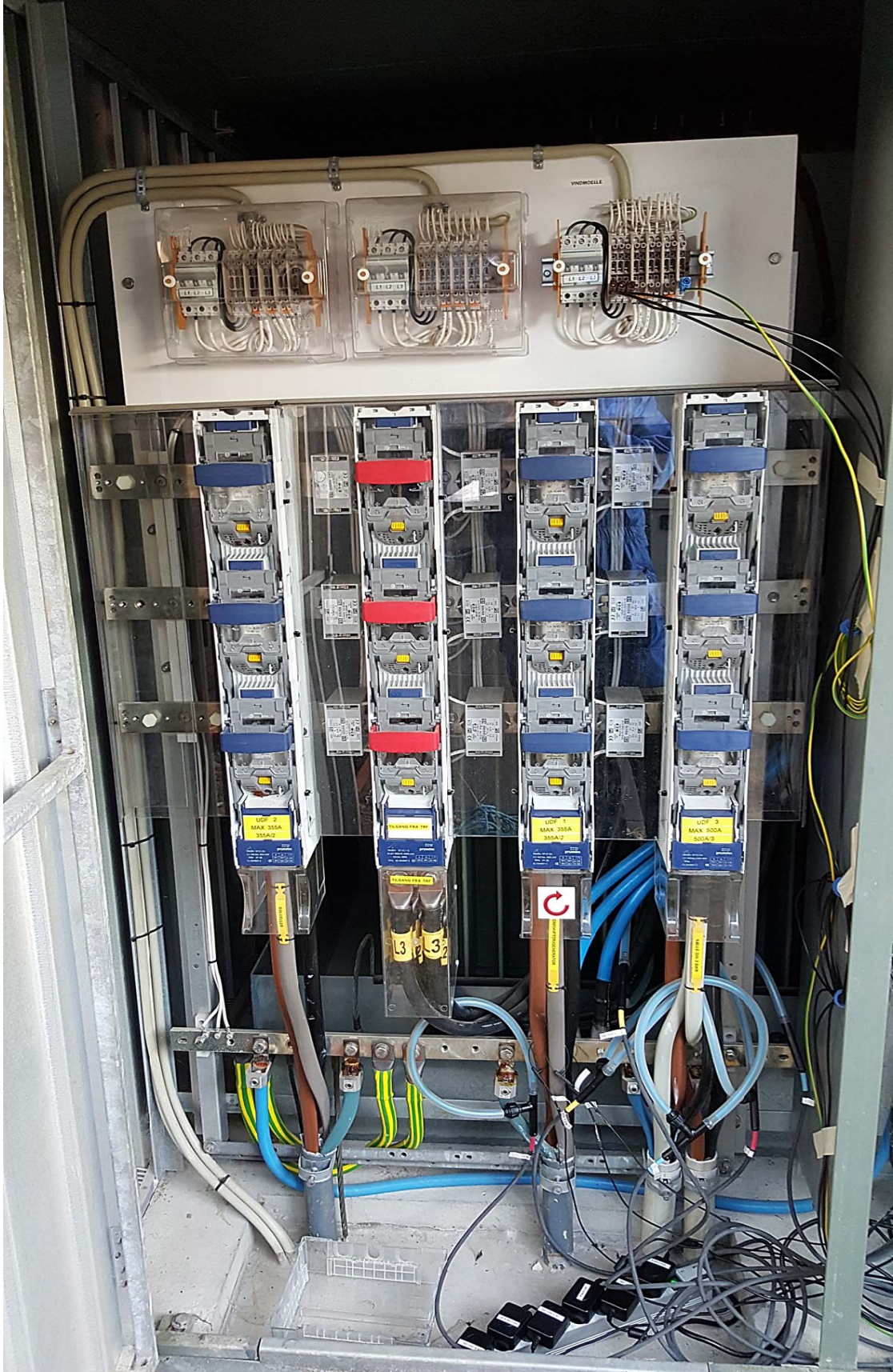


Fig. 4.3: Setup for current and voltage measurement using Rogowski coils and High Voltage Differential probes.



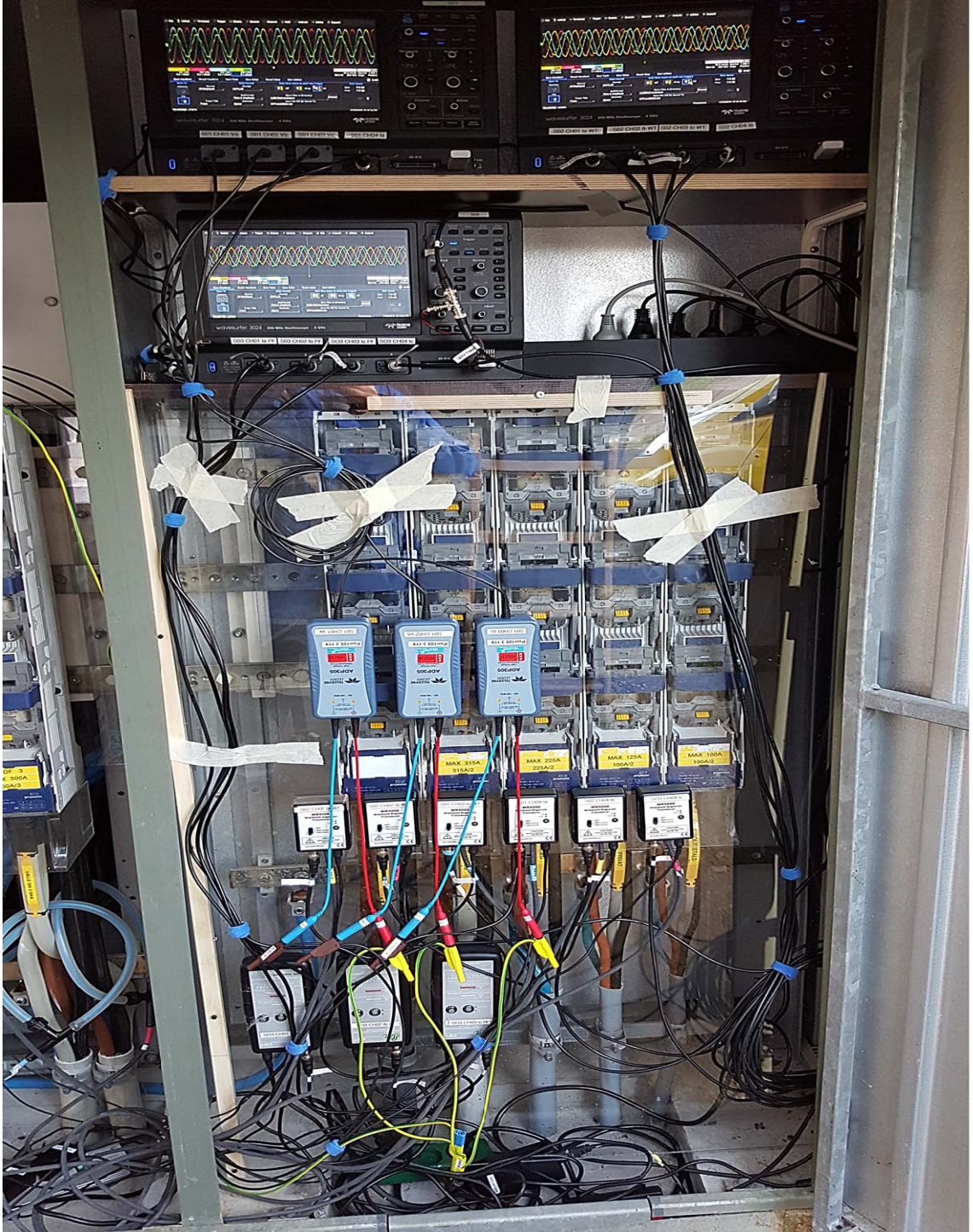


Fig. 4.4: Setup for current and voltage measurement using oscilloscopes, Rogowski coils and High Voltage Differential probes.

### 4.3.1 Description

The following equipment is used to perform measurements. It was decided to use three 200 MHz oscilloscopes Lecroy WaveSurfer 3024 with 4 GS/s (giga samples per second). The reason for using three oscilloscopes is that each of them has only 4 input channels. Hence, in total there are 12 channels to measure 3xVoltage and 3xCurent of transformer, 3xCurent of Pig Farm, 3xCurent of WT. The current of PV is not measured due to the restrictions for the area in transformer house. Moreover the measurements for the current and voltage are performed on LV terminals of a transformer, WT and Pig Farm. Refer to Table. 4.1 to see the POM's.

The voltage and current probes are assigned to each of the channels in oscilloscopes. The assigned probe, channel and oscilloscope are depicted in Table.4.2. Where  $V_{a,b,c}$ ,  $I_{a,b,c}$  - voltage and current measured on each phase of transformer,  $I_{a,b,c-WT}$ ,  $I_{a,b,c-PF}$  - current measured on WT and Farm respectively.

Tab. 4.2: Oscilloscope, probe and channel distribution for test measurements.

Phase	Channel	Oscilloscope 1	Probe	Oscilloscope 2	Probe	Oscilloscope 3	Probe
Phase A	Channel 1	SO1	SO1 CH01 Va	SO2	SO2 CH01 Ia WT	SO3	SO3 CH01 Ia PF
Phase B	Channel 2	SO2	SO1 CH02 Vb	SO2	SO2 CH02 Ib WT	SO3	SO3 CH02 Ib PF
Phase C	Channel 3	SO1	SO1 CH03 Vc	SO2	SO2 CH03 Ic WT	SO3	SO3 CH03 Ic PF
A,B,C	Channel 4	SO1	SO1 CH04 Ia	SO2	SO2 CH04 Ia	SO3	SO3 CH04 Ia
	Ext.	Trigger		Linc to Ext1		Linc to Ext2	

The following channels 1 – 4 from Table.4.2 has analog input and *Ext* used for connecting Digital Signal Processor (DSP) module that is an external trigger device. A DSP module is used for triggering all oscilloscopes at the same time, meaning that measurements will have same sampling rate, length etc. Further it will give ability to selet the most important points i.e. current of WT and correlate it with measurements from other oscilloscopes.

For the voltage measurements the High Voltage Differential(HVD) probes *ADP 305* is used rated for maximum 1000V<sub>RMS</sub>. For current measurements *WR5000* Ro-

gowski High Frequency Current Transducer with flexible coil and *PEM CWT6 mini* are used. The current probes are rated for maximum 1000A and 1200A respectively for *WR5000* and *PEM CWT6 mini*. The attenuation of *WR5000* Rogowski current probe is 2mV and 5mV for *CWT* current probe.

In order to measure transformer temperature two EL USB TC thermocouple loggers are used. Both thermocouples are attached to the tank side one on the top and second on the bottom of transformer. They are used to find the average outside temperature of transformer tank. Moreover, an fiber optic temperature sensor *Temperature Guard* from SensorCLIP is mounted to measure oil temperature inside the transformer. The rated data for *Temperature Guard* is not available and the rated data for other devices is attached in Appendix #.

### 4.3.2 Measurement bandwidth for harmonic analysis

The bandwidth of 12 kHz is chosen for harmonic analysis. Within this bandwidth the harmonics up to the 50<sup>th</sup> order will be covered. The harmonic order is selected based on DS/EN 6100-2-4 standard. Sampling frequency for one measurement is calculated taking into consideration the highest number of samples equals to 1024 samples. According to DS/EN 61000 4-7 the samples are taken from 10 fundamental cycles of 50 Hz. It will give a 5 Hz bins for using Discrete Furrier Transform (DFT) analysis meaning that the harmonics and inter-harmonics are captured. Refer to Figure.4.5 to see the grouping of harmonics and inter-harmonics.

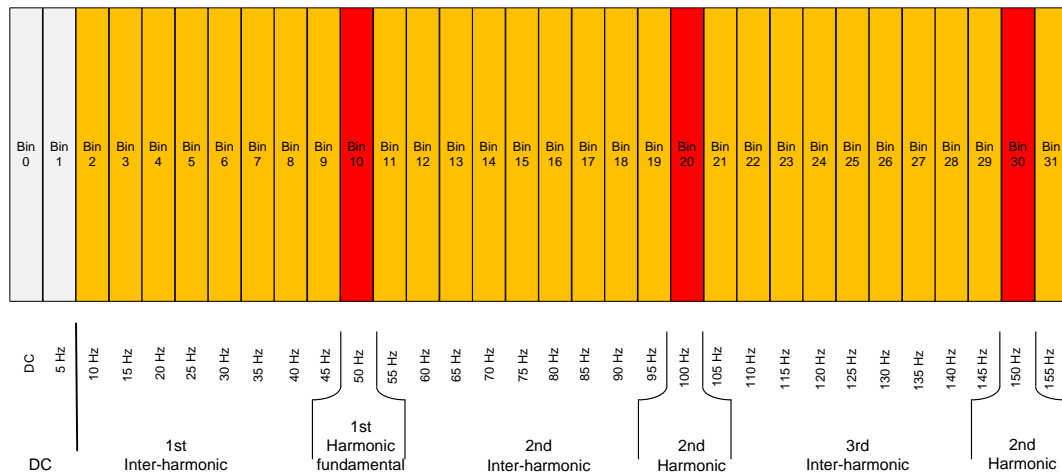


Fig. 4.5: Grouping of harmonics and inter-harmonics according to DS/EN61000-4-7.

The sampling frequency for ten cycles is obtained using eq.4.4, 4.5 and 4.6 and the minimal length of the vector to be saved is equals to 51200 *points*.

$$\Omega = 2\pi f = 2\pi \cdot \frac{1}{\frac{0.02}{1024}} = 2\pi \cdot 51200 [Hz] \quad (4.4)$$

$$f_{sampling} = \frac{N_{samples}}{f} = \frac{1024 \text{ samples}}{0.02 \text{ sec}} = 51200 [samples/sec] \quad (4.5)$$

$$f_{sampling-10} = 51200 \cdot 10 = 512000 [samples/sec] \quad (4.6)$$

where

$\Omega$  - angular frequency [*Hz*]

$f_{sampling}$  - sampling frequency for one period [*samples/sec*]

$f_{sampling-10}$  - sampling frequency for ten periods [*samples/sec*]

### 4.3.3 Main settings

The oscilloscopes are manually programmed and the main settings are shown in Tables. 4.3, 4.4 and 4.5. The timebase and trigger settings are programmed in descriptor boxes. Since oscilloscope has 10 horizontal divisions the timebase is set to 20 *ms/div* to have 10 fundamental cycles. An Real time sampling mode with sample rate is set to 250 *kS/s* and number of samples is 50 *kS* (50000 samples in 10 cycles, 5000 samples in one cycle, which is better than minimum number 1024 samples ). The timebase settings are depicted in Table.4.3

Tab. 4.3: The settings for timebase.

Sampling mode	Timebase	Number of samples	Sample rate	Offset
Real time	20 <i>ms/div</i>	50 <i>kS</i>	250 <i>kS/s</i>	0

In the trigger descriptor box an external trigger source is chosen to provide an external trigger signal from DSP module to all oscilloscopes. The trigger settings are shown in Table.4.4

The following settings for voltage and current probes are listed in Table.4.5

Tab. 4.4: Oscilloscope trigger settings.

Trigger mode	Trigger type	Setup source	Level	Slope	Coupling	Ext. Aux. Trigger	Impedance
Normal	Edge	External	1.5 V	Positive	DC	$\div 5$	1 M $\Omega$

Tab. 4.5: Main settings volt per division and attenuation for voltage and current probes.

Settings for SO1	V/div	Attenuation	Settings for SO2	V/div	Attenuation	Settings for SO3	V/div	Attenuation
SO1 CH01 Va	100 V/div	$\div 100$	SO2 CH01 Ia WT	200 V/div	2 mV/A	SO3 CH01 Ia PF	200 V/div	5 mV/A
SO1 CH02 Vb	100 V/div	$\div 100$	SO2 CH02 Ib WT	200 V/div	2 mV/A	SO3 CH02 Ib PF	200 V/div	5 mV/A
SO1 CH03 Vc	100 V/div	$\div 100$	SO2 CH03 Ic WT	200 V/div	2 mV/A	SO3 CH03 Ic PF	200 V/div	5 mV/A
SO1 CH04 Ia	200 V/div	2 mV/A	SO2 CH04 Ib	200 V/div	2 mV/A	SO3 CH04 Ic	200 V/div	2 mV/A

#### 4.3.4 Selection of sampling time and measurement interval

The measurements are performed during one week starting on 01.12.15 to 08.12.15. This interval is chosen in order to capture different weather conditions and pig farm operations. The measured window of 10 cycles (DS/EN 61000 4-7) is saved every 5 minutes. The 5 minutes interval is taken due to the number of data files that needs to be processed and analyzed. With these settings the data file from one oscilloscope will be more than 8Gb. Temperature measurements from thermocouple loggers are taken every 1 minute to match with data from oscilloscopes and data from thermal sensor measured top oil temperature. Moreover, the data from fiber optic sensor is saved with 15 minutes interval. The sampling time in this case is fixed by the provider (Sensorclip) and cannot be adjusted to have smaller sampling time. However, these data will be interpolated to have same format as for other measurements.

#### 4.3.5 Saving data and data files format

The data from oscilloscopes is automatically saved on each trigger. The stored data is saved on USB flash drive that has an specific name similar to one on the oscilloscope. The following format is used to save the data *XXTrace000000.dat*

Tab. 4.6: The new file created after processing with Matlab to do DFT.

Transformer Voltage	Transformer Current	WT Current	PF Current
rawDada.mat	rawDadaCurrent_tr.mat	rawDadaCurrent_wt.mat	rawDadaCurrent_pf.mat
Voltage_rms.mat	rmsDadaCurrent_tr.mat	rmsDadaCurrent_wt.mat	rmsDadaCurrent_pf.mat
Voltage_rms_vec.mat	rmsDadaCurrent_tr_vec.mat	rmsDadaCurrent_wt_vec.mat	rmsDadaCurrent_pf_vec.mat

where

$XX$  - is the Source, in this case it is channel  $C1$ ,  $C2$ ,  $C3$ ,  $C4$

$Trace$  - trace title

00000 - the counter of saved files on each trigger

$.dat$  - extension for Matlab text files

Moreover, the sub format for each data file is chosen to save time and amplitude of voltage or current. The total amount of data collected is  $25\text{ Gb}$  with the length of single file equal to  $1\text{ Mb}$ . Since the file format is identical on all scopes the saved files are transferred from USB drives to separate folders on PC to avoid their mixing.

Furthermore, the data is organized using Matlab scripts. The new file names are assigned such that on the latter stage harmonics can be extracted using DFT analysis. The new file names are depicted in Table.4.6. This table has files with  $.mat$  extension for raw data, RMS (root mean square) data and vectorized RMS data. It is done for easy access of these data for future analysis. Moreover the  $.mat$  files has substructure inside which is described in Appendix A 7.2.

More about data handling is written in next section.

## 4.4 Data post-processing

The data is processed in accordance to DS/EN 6100-4-7 (Electromagnetic compatibility (EMC) – Part 4-7: „Testing and measurement techniques – General guide on harmonics and inter-harmonics measurements and instrumentation, for power supply systems and equipment connected thereto“).

Based on the information of section 4.3 the data processing is done for the harmonic current spectra obtained from measurements.

The following is achieved

- The wide bandwidth of the spectra is covered for the resolution of 1024 points per each 20 *ms* period.
- The current spectra is processed using Discrete Fourier Transform (DFT) in Matlab '*fft*' (Fast Furrier Transform )
- The function is employed fast radix-2 FFT algorithm for faster computations since the fastest algorithms occur when N is power of 2.[10]
- The calculation is done considering inter-harmonics, since the load may have some inter-harmonics due to the use of motor and pumps.

Based on the [3] the DFT algorithm has the errors in its computation. There are three main types of DFT errors: *averaging at the endpoints*, *aliasing* and “*leakage*”.

When averaging at the end points the result of DFT will be filled with DC component errors. Therefore, for DFT calculations the average values of the function  $f(x) = x$  must lie in the interval  $[-\frac{A}{2}, \frac{A}{2}]$  thus the periodic extensions not continues anymore. Simply, the DC-link current will be replaced by the average value of this vector  $A$ .

The next important factor is aliasing. The aliasing occurs when the signal sampling rate is to small (*undersampled*). To avoid aliasing the sampling rate must be twice the highest frequency present in the signal (Nyquist frequency). The function is called band-limited if the sampling has a finite interval  $[-\frac{\Omega}{2}, \frac{\Omega}{2}]$  and it is used to prevent aliasing[3] and the sampling interval must satisfy relation  $\Delta x \leq \frac{1}{\Omega}$ .

The spectral leakage is an issue [3] when the DFT is performed. Since the signal or frequency components occur between the frequencies which is not an integer multiple of the period. To reduce the leakage the time window should be an exact multiple of the period of the waveform (fundamental frequency). Moreover, the different filters can be applied to remove leakage e.g the Hamming or Hanning windows [3].

#### 4.4.1 Scaling of measurements

In order to do the DFT analysis and calculate THD the sampled data should be processed. As the sampled input signal  $V$  and  $I$  is transformed to the output voltage by attenuation the original amplitude must be restored. It is done by the computation of the attenuation factor. The following relation eq.4.7 is used to get the value of the real signal.



$$I_{real} = I_{meas} / probe\ att \cdot scope\ att \quad (4.7)$$

where

$I_{real}$  - transformed real value of current [A]

$I_{meas}$  - measured value of current [A]

$scope\ att$  - attenuation of oscilloscope  $\div 500$

$probe\ att$  - attenuation of WR5000 Rogowski current probe 2 mV and 5 mV for CWT current probe [mV]

The scaling of measured values of Voltage is done taking into account the oscilloscope attenuation and attenuation of HVD probes ADP 305. The HVD probes are automatically detected by oscilloscope and the measured voltage  $V_{meas}$  is equal to the real voltage  $V_{real}$ . Therefore, the eq.4.8 is used for calculations of real value. One has to note that  $I_{real}$  and  $V_{real}$  are the peak values. Therefore these values must be transformed to RMS. Refer to 5.1.1 for information about transformation to RMS. Moreover, the  $v/div$  settings are not used in the calculations since the output signal is already multiplied by the  $v/div$  value ( $v/div$  is used to set up the margin on the oscilloscope to be sure that the measured signal will be captured on the screen and further saved without losing the peaks.).

$$V_{real} = V_{meas} \quad (4.8)$$

#### 4.4.2 Total Harmonic Distortion calculations

After the data is selected the eq.4.9 is used to calculate THD. Since it is most common index that relate to the voltage and current waveform. The THD is calculated as the RMS value of all the harmonic components of the current, to the fundamental current  $I_1$ . The eq.4.9 is implemented in Matlab script. Results of the calculations are plotted and presented in the report section 5.

$$THD = \sqrt{\sum_{h=2}^{h=H} \left( \frac{I_h}{I_1} \right)^2} \cdot 100[\%] \quad (4.9)$$

where

$I_h$  - amplitude of current of harmonic order  $h$  in [A]

$I_1$ - amplitude of current  $50Hz$  in  $[Hz]$

$h$  - harmonic order

$H$  - is 50 according to DS/EN 6100-2-4

The process of data selection and harmonic sharing is described in next section 5.

### 4.5 Summary

In this chapter presented overview of the Thy-Mors Energi network topology where the points of measurements are defined. Moreover, it follows with description of the equipment chosen to perform the measurements and the measured quantities/values. Furthermore, this chapter highlights general settings for the equipment, scaling, measured bandwidth, sampling time etc. Thus the measurements and data processing are performed according to DS/EN 6100 2-4 and IEC 6100 4-7 standards(DS/EN).

## 5 Harmonic analysis

This chapter gives argumentation for choosing the data for DFT analysis. The considered aspects are the pig farm daily operations, weather conditions (wind and solar irradiation) and power generation. Moreover, the results of DFT analysis are presented in sections 5.2, 5.3 and 5.4.

### 5.1 Selection of Data

The preparations listed in this section are acquired to perform analysis of measured data. Since the data measured by the oscilloscopes is showing the Peak for current and voltage. For further processing it must be recalculated to RMS values. In order to see the whole power production the active P and the reactive power Q must be calculated. Furthermore, these data are plotted and analyzed to perform harmonic studies.

#### 5.1.1 Calculations of RMS values

The RMS values are calculated using the equation 5.1 (using Matlab  $I_{RMS} = rms(I)$ ). The equations described in section 4.2 and 4.3 are implemented to calculate active and reactive power. The power is calculated for Transformer, WT and PF.

$$I_{RMS} = \sqrt{\frac{1}{N} \sum_{n=1}^N |I_n|^2} \quad (5.1)$$

#### 5.1.2 Considerations for selecting the data for DFT analysis

The measurement campaign was way intensive (section 4.3.4) and a large amount of data was saved. Due to time limitations it was decided to select only a few sets of data for analysis which are relevant for validation of transformer model. The

following aspects are considered when the points are picked: the power profile, weekly schedule for the pig farm operations, wind conditions, solar irradiation and the measured temperature of transformer.

a) Power profile

In order to chose the proper points one have to look at the power profile plotted in Figure.5.1.

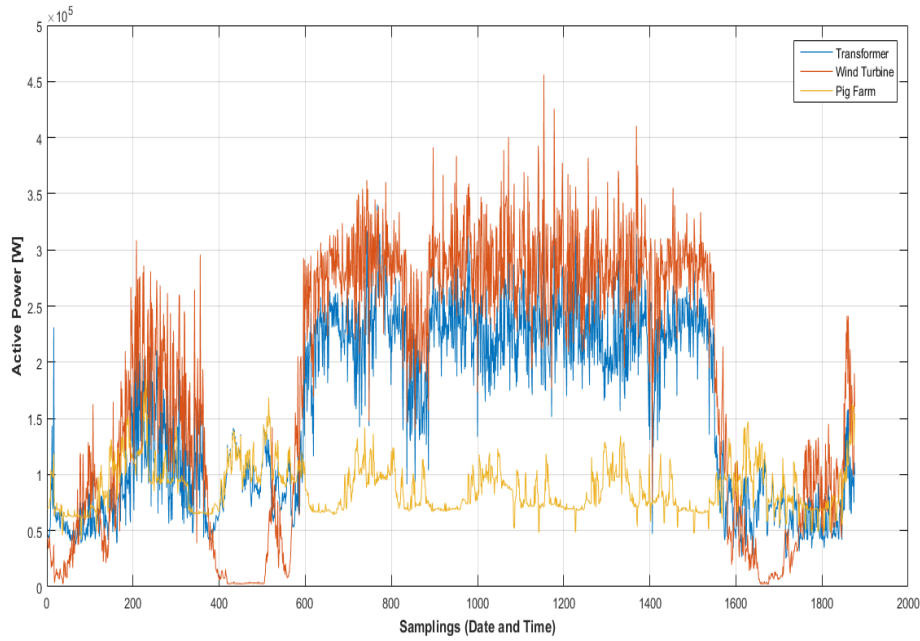


Fig. 5.1: Active power of transformer, wind turbine and pig farm.

By looking at the power peaks and power dips one can define whether the current have maximum or minimum amplitude. Therefore, it would be good to look at those points to find a link with the transformer temperature. Moreover, the power profile together with farm weekly schedule will be used to define the spots where the most processes are involved. For example, the food preparation process is overlapped with running pump to remove the manure or other daily operations.

b) Weekly schedule

Since the measurement campaign is performed for one week it was decided to take two different week days accounting for 24 hours per day. According to Figure.3.4 the basic daily operations are the same during the entire week and differ only on Tuesday. However, during the test campaign the measured data for Tuesday are

lost due to some technical problems. Therefore, the other days will be considered taking into account the weather and wind conditions.

The measured data is sorted out as follows. The set of files is assigned for the specific day according to the samples taken. For example, the number for measurements taken on 1 December starts from 1 to 53 for the 2 December the files stored as follows starts with 55 to 342 etc. The files distribution according to the days are depicted in Table.5.1.

Week day	Tuesday	Wednesday	Thursday	Friday	Saturday	Sunday	Monday	Tuesday
Date	1 December	2 December	3 December	4 December	5 December	6 December	7 December	8 December
File number (from...to)	1...53	54...342	343...628	629...916	917...1203	1204...1490	1491...1778	1779...1876
Files Total	53	288	285	287	286	286	287	97

Tab. 5.1: Test measurements assigned to the day taken.

### c) Wind conditions

Upon the tests the different whether and wind conditions were captured. The information about wind speed was taken from public domain namely DMI (Danmarks Meteorologiske Institut).

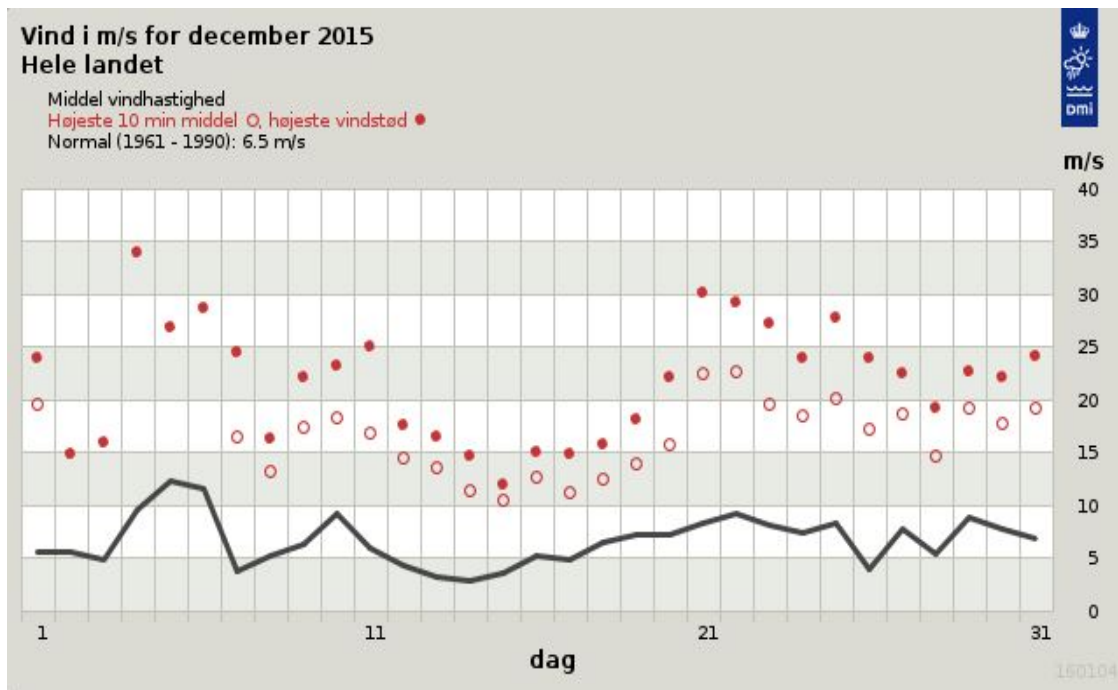


Fig. 5.2: Wind speed for December 2015.

Figure.5.2 shows the wind speed for the entire week when the measurements are performed. It can be seen that there were days with no wind and days when the area was hit by the storm. Therefore, the storm day might be taken into consideration since the WT is running full power. The other day with no wind is also interesting since the WT was not in operation and therefore the main attention can be drawn to PV array.

### d) Solar irradiation

This aspect is taken to consideration since the PV generations is fully depends on the solar irradiation. Due to the absence of information about solar irradiation the time for sunrise and sunset was taken into account. The data is taken from <http://www.torbenhermannsen.dk/almanak/almanak.php#>. Based on this data the time for the dark and bright time is defined assuming that the PV generates the power during the bright time starting from 8:00am to 16:00pm.

### e) Transformer temperature

Finally, all the mentioned above considerations will be accomplished with the information about transformer temperature. The temperature measurements available are the top oil temperature also top and bottom tank temperature for the entire week.

## 5.1.3 Selected points

The following days selected for DFT analysis are 3 December with no wind and 4 December stormy day with the highest wind speed of 35m/s. The farm operations seems to be same for both days and need deeper look into the data. Moreover, the transformer temperature for these days is varying from 25 to 30 C. The sunrise and sunset for both days is 08:18am to 15:52pm and 08:19am to 15:51pm respectively for 3rd and 4th December.

## 5.1.4 DFT analysis

The DFT analysis starts for the selected days and performed for the whole 24 hours time interval. The Current harmonic levels for 24 hours window are collected and plotted refer to section 5.2, 5.3 and 5.4. In case the current harmonic levels of 8% are exceeded the studied sample is compared with the daily schedule, wind

Tab. 5.2: Selected points for analysis

	Date of measurements	Time
point 493	03.12.2015	12:39
point 550	03.12.2015	17:24

conditions etc. to give the explanation for the harmonic content and the factors that may influence its generation. Even though the harmonic levels are not exceed there might be situations where some of the harmonics i.e. 3rd, 5th or other are exceed their limits. Moreover, the inter-harmonics can be present in the network. Therefore, the entire day needs to be studied and analyzed.

The results of DFT will be plotted to highlight the harmonic content and compare it with the harmonic levels. Furthermore, if the harmonic content is present the results will be analyzed to give the explanation for the harmonics and possible sources of harmonic distortions. Moreover, the data from the DFT will be fitted into the model described in Chapter 6 to run the simulations and validate the results of simulations with temperature measured.

## 5.2 Harmonic Content of Farm

Some of the data is chosen to highlight the harmonic content in substation. The chosen points are listed in Table. . Both points are for the no wind conditions and WT does not produce the power, however for the second point 550 the PF has some activities. Refer to the power profile in Figure.5.1. All figures structured according to phase (A, B, C) for point number.

Moreover, for the same points the DFT analysis is done without removing the inter-harmonics from the Matlab script. The results of DFT for the point 493 are shown in Figure.5.3, Figure.5.4 and Figure.5.5 where the THD are below the limit and only the 17<sup>th</sup> harmonic exceed the level. Results for point 550 are presented in Figure.5.6, Figure.5.7 and Figure.5.8. The THD in this case are exceeded in all three phases and the harmonics of order 3, 5, 7, 11, 13, 17, 21 are present.

For the DFT when the inter-harmonics are considered the results are shown in figures starting from Figure.5.9 to ?? for the point 493 and 550. The THD limit for point 493 is not exceeded in all three phases however the harmonics of the?? are present and above the level Figure.5.9, Figure.?? and Figure.?. For point 550

the THD limits are 12.9%, 14% and 11.8%. The content is harmonics of the order ?? which above their limits. Based on the information from the figures the possible harmonic sources are Motors with power electronics, Fluorescent and Heat lamps also the Thyristor based power electronics i.e in ventilation and climate control.

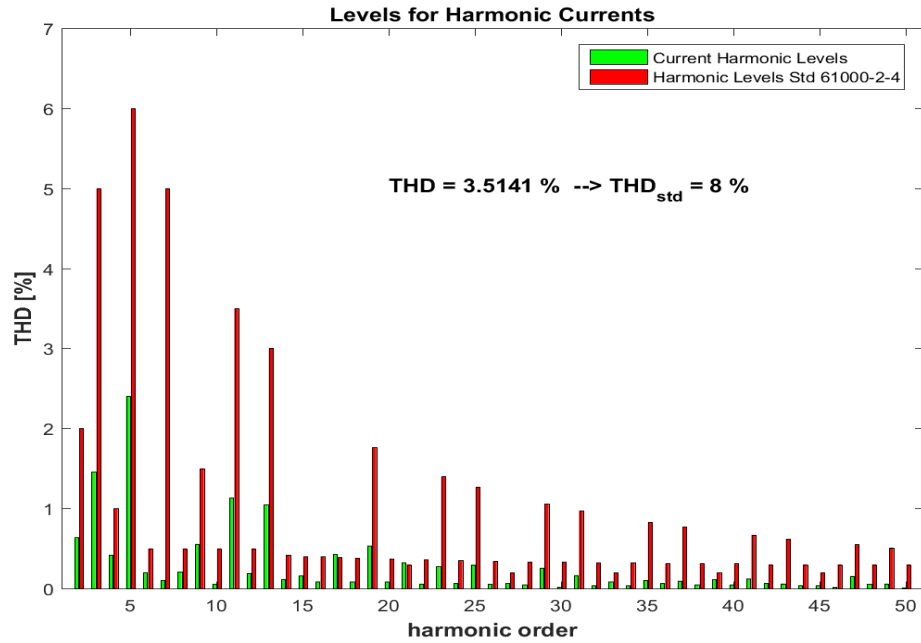


Fig. 5.3: Levels for harmonic currents phase A Pig Farm for point 493.



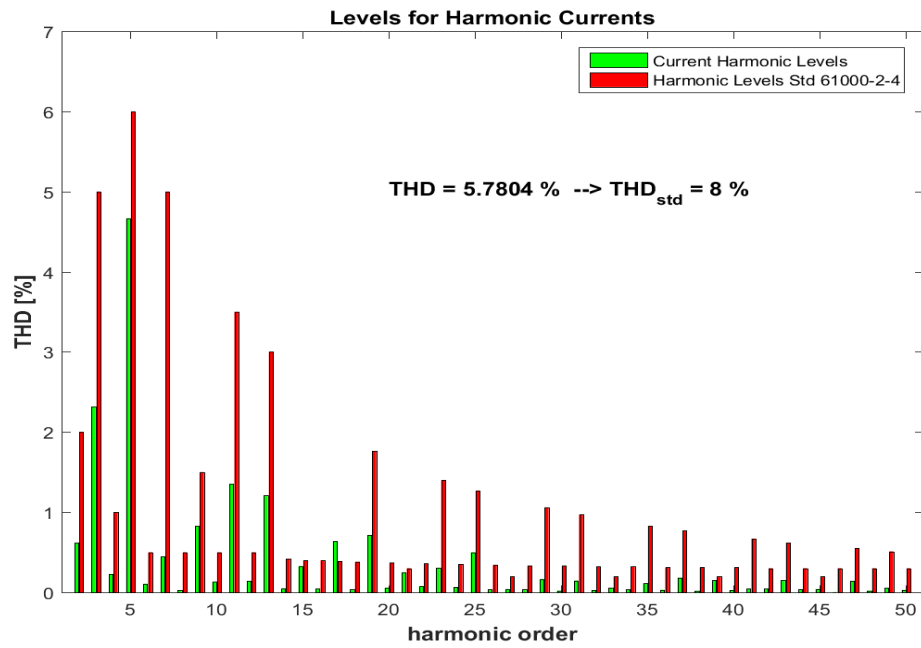


Fig. 5.4: Levels for harmonic currents phase B Pig Farm for point 493.

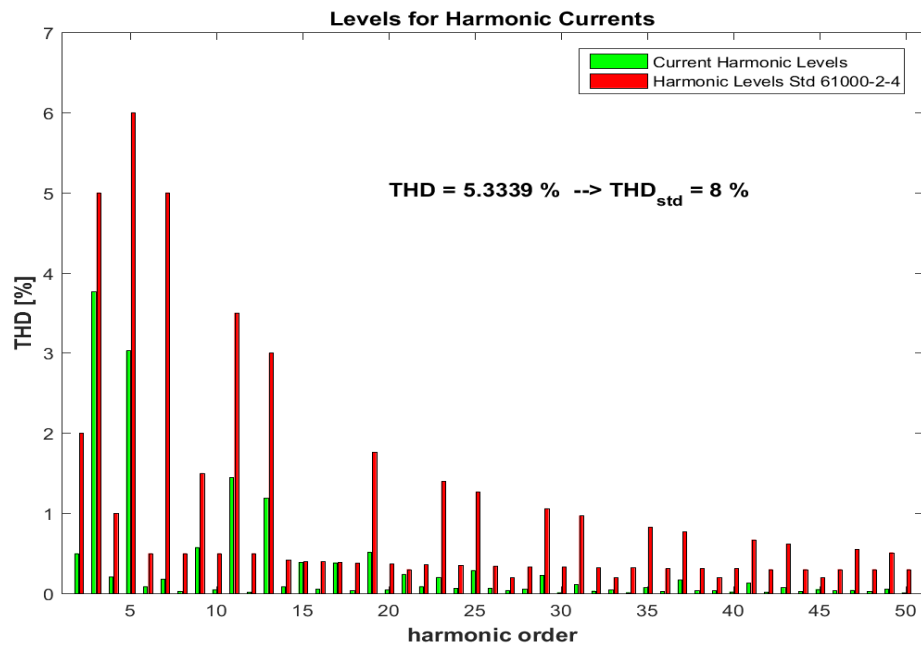


Fig. 5.5: Levels for harmonic currents phase C Pig Farm for point 493.

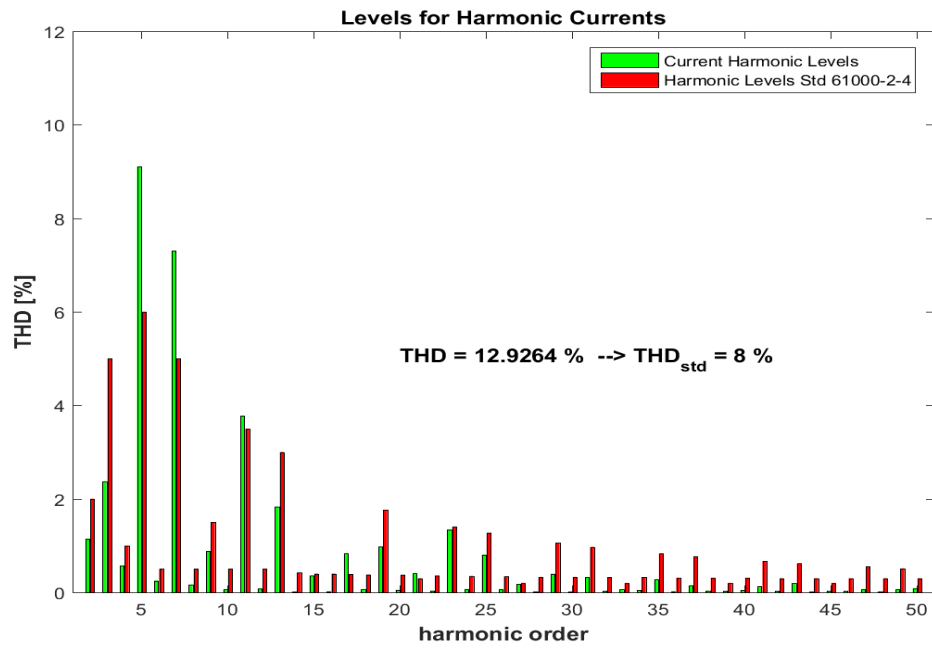


Fig. 5.6: Levels for harmonic currents phase A Pig Farm for point 550.

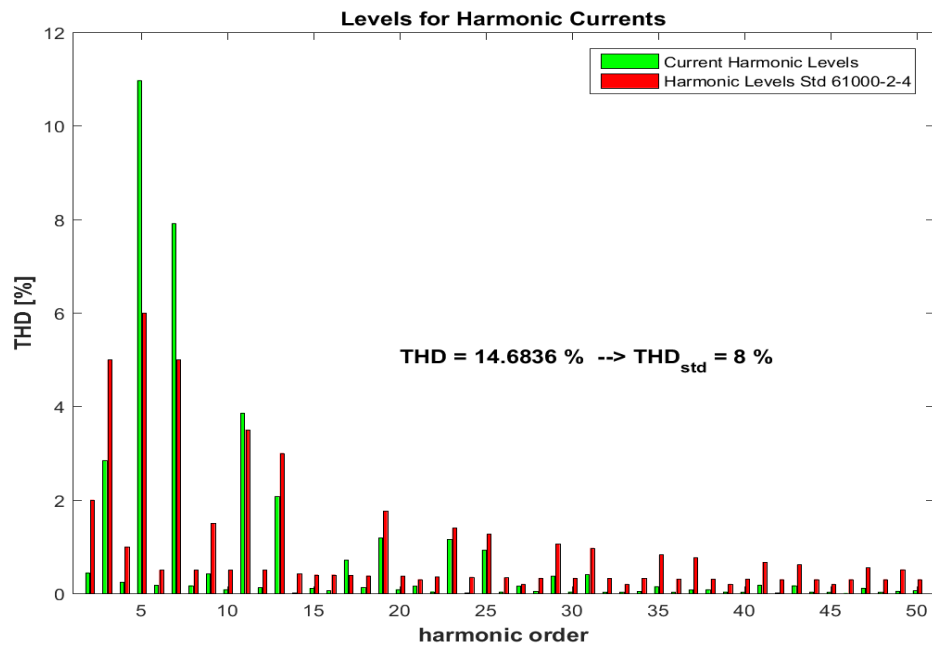


Fig. 5.7: Levels for harmonic currents phase B Pig Farm for point 550.

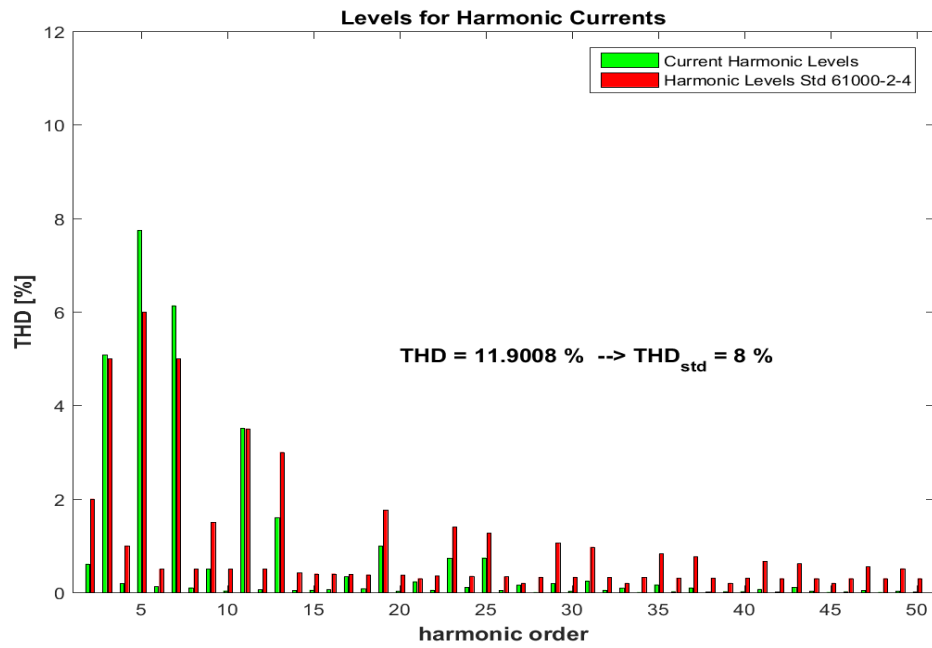


Fig. 5.8: Levels for harmonic currents phase C Pig Farm for point 550.

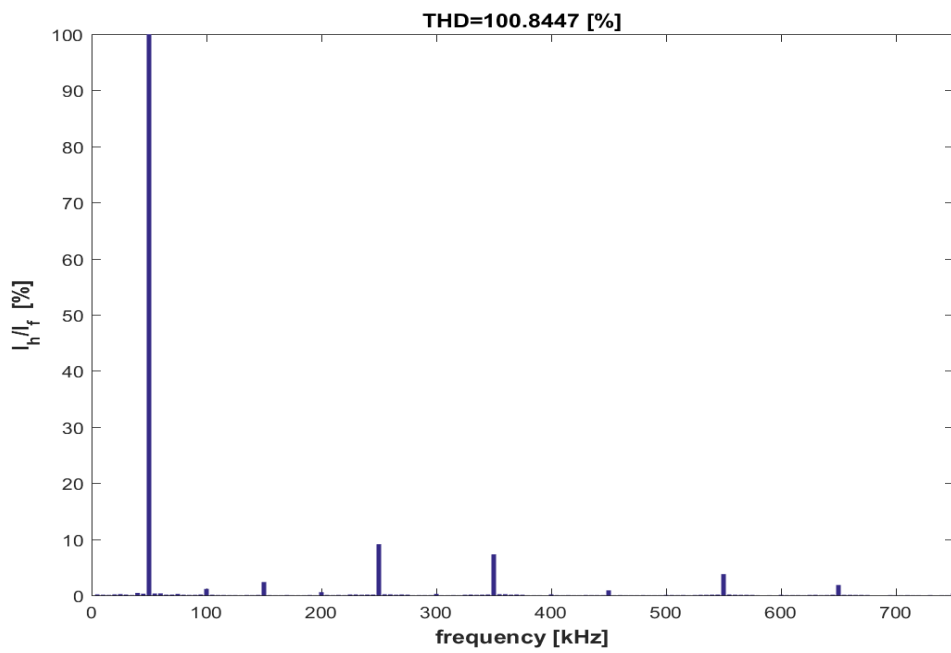


Fig. 5.9: Levels for inter-harmonic currents phase A Pig Farm for point 550.

### 5.3 Harmonic Content of WT

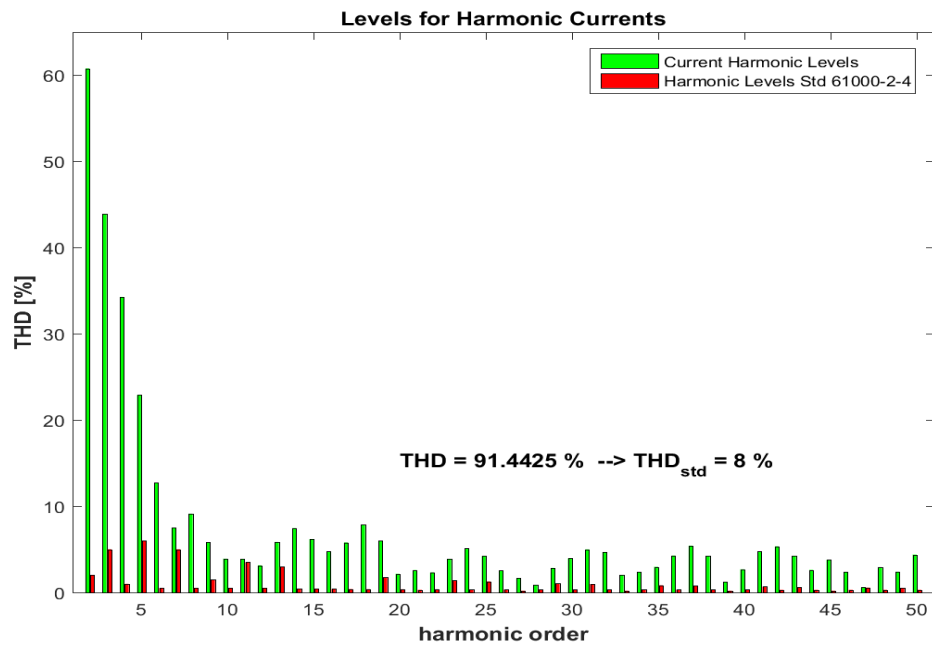


Fig. 5.10: Levels for harmonic currents phase A Wind Turbine for point 493.

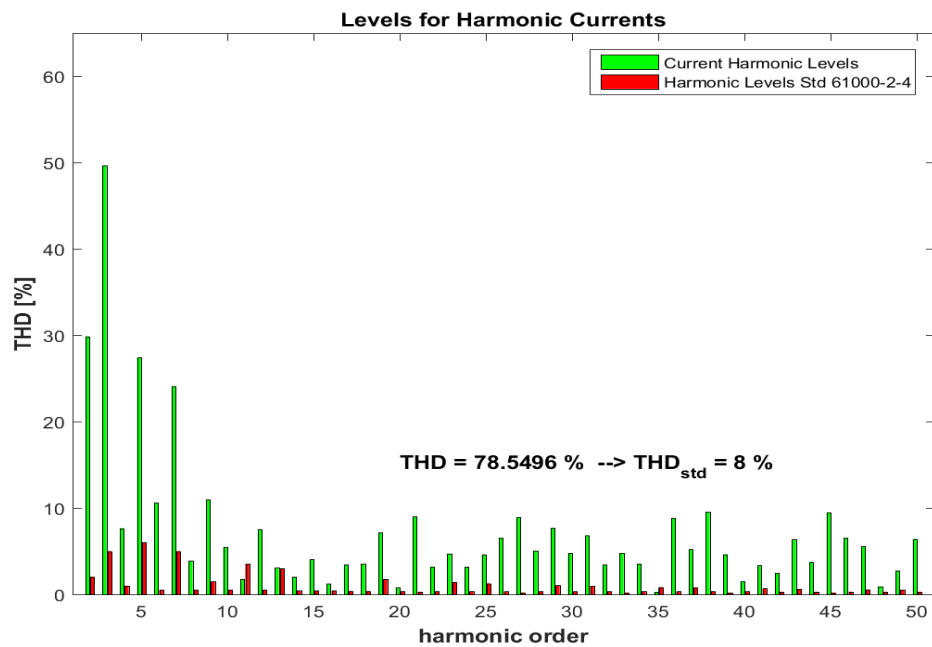


Fig. 5.11: Levels for harmonic currents phase B Wind Turbine for point 493.

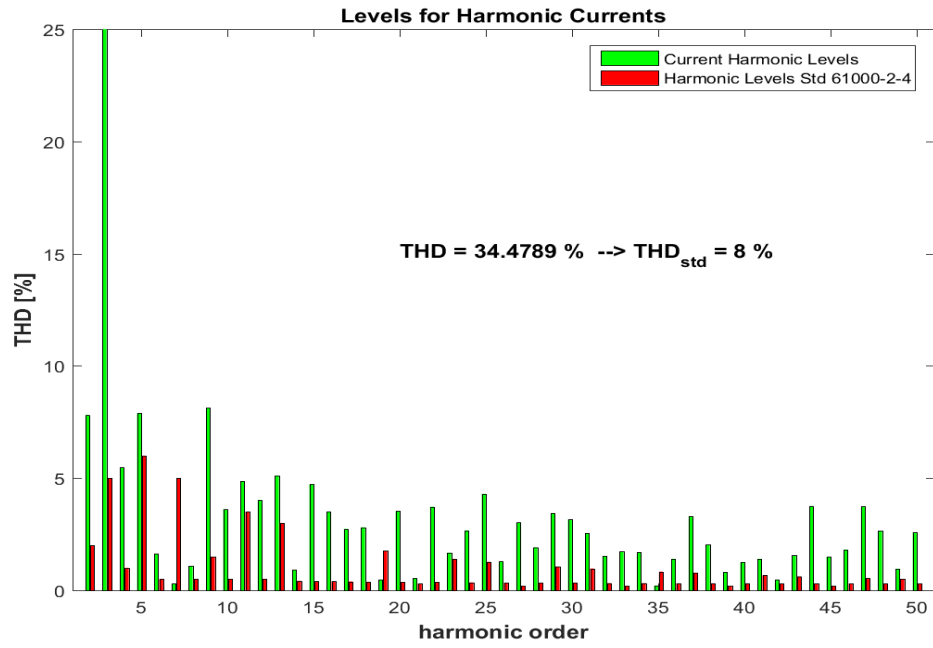


Fig. 5.12: Levels for harmonic currents phase C Wind Turbine for point 493.

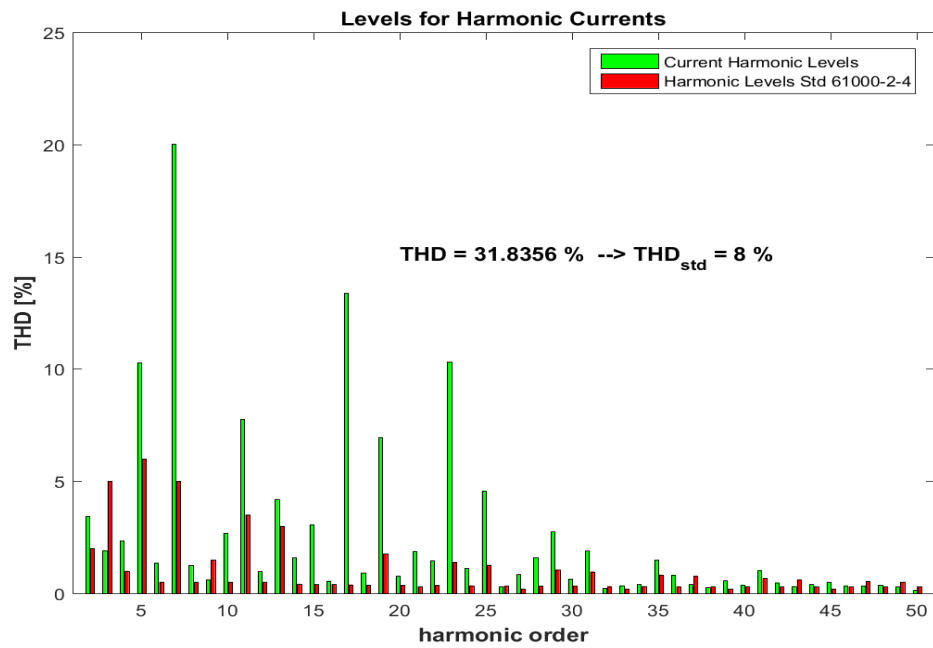


Fig. 5.13: Levels for harmonic currents phase A Wind Turbine for point 550.

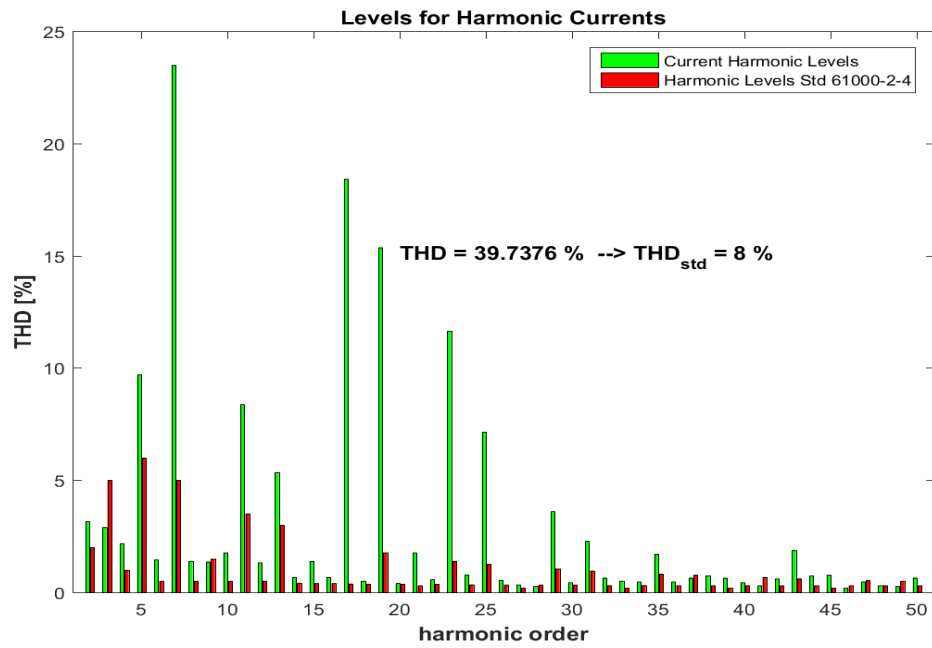


Fig. 5.14: Levels for harmonic currents phase B Wind Turbine for point 550.

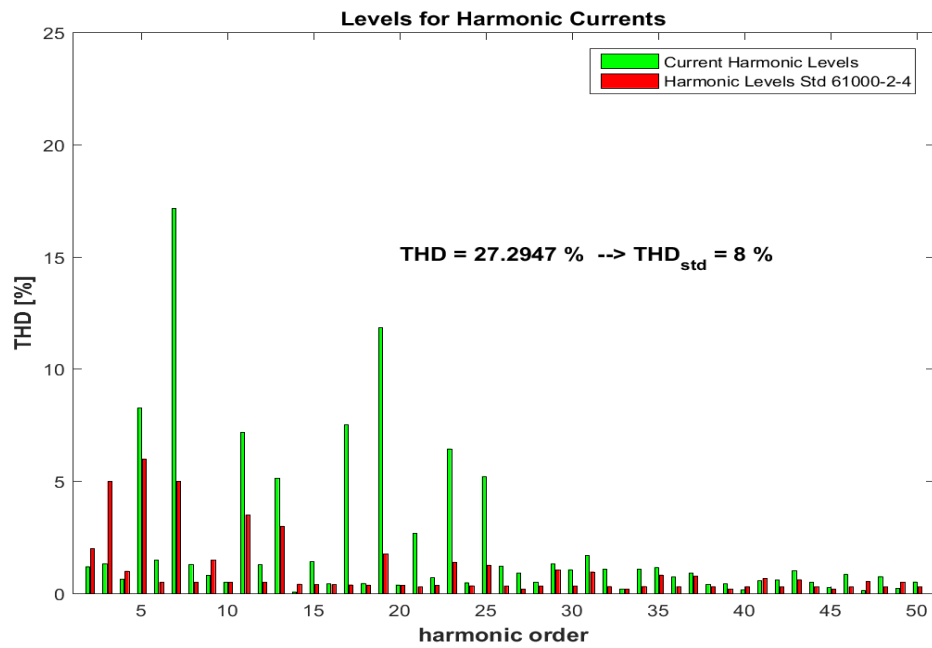


Fig. 5.15: Levels for harmonic currents phase C Wind Turbine for point 550.

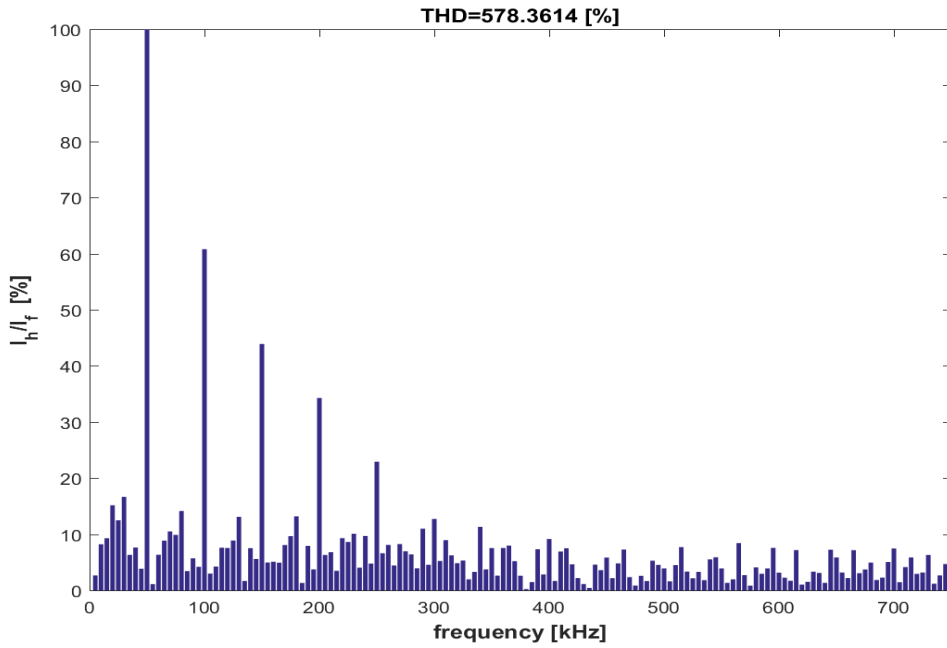


Fig. 5.16: Levels for inter-harmonic currents phase A Wind Turbine for point 493.

For the WT the same harmonic levels are used as for the transformer and PF (IEC61000). It is because that the new from Energinet.dk have lower limits for the harmonics but the WT was installed about 25 years ago. Therefore, it is assumed that IEC61000-2-4 standard is the reference for harmonic levels. The results of DFT for the WT shows that the THD limits are violated for all cases and points. The THD levels for the point 493 are very high 91% in phase A, 78% in phase B and 34% in phase C accordingly Figure.5.10, 5.11 and 5.12. For point 550 the THD levels are smaller compare to the point 493 but still higher than 8% and shown in Figure.5.13, 5.14 and 5.15. The same for the case when looking into inter-harmonics shown in figure Figure.5.16. The whole harmonic spectrum is present. Thus the the limits for harmonic currents are violated.

## 5.4 Harmonic Content in Substation

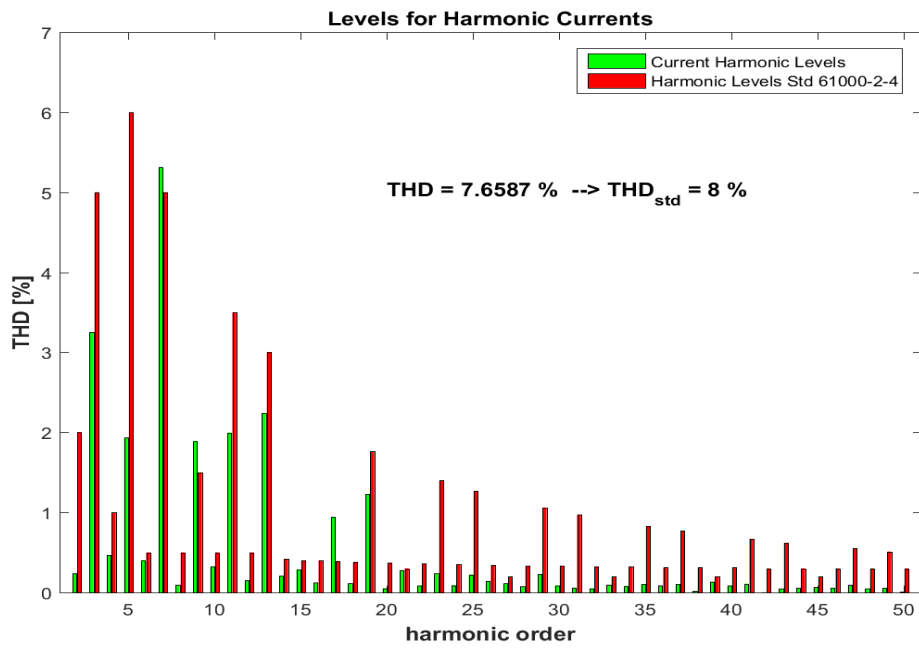


Fig. 5.17: Levels for harmonic currents phase A Transformer for point 493.

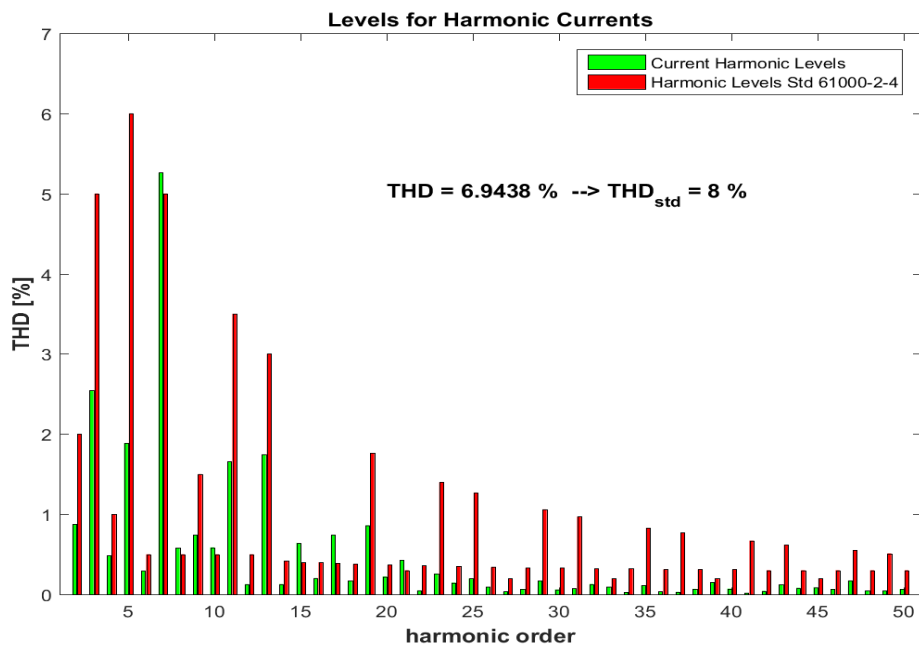


Fig. 5.18: Levels for harmonic currents phase B Transformer for point 493.



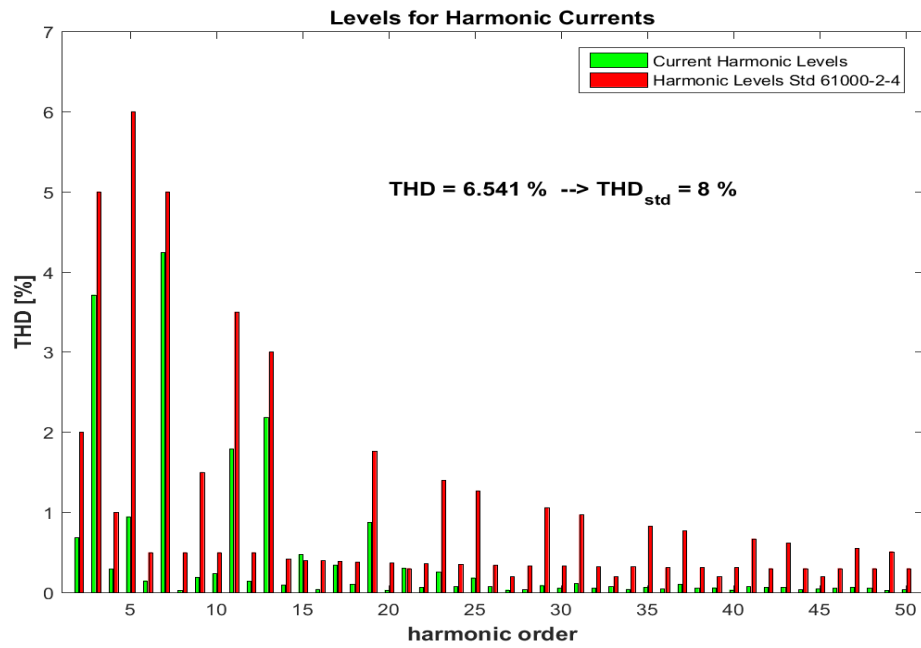


Fig. 5.19: Levels for harmonic currents phase C Transformer for point 493.

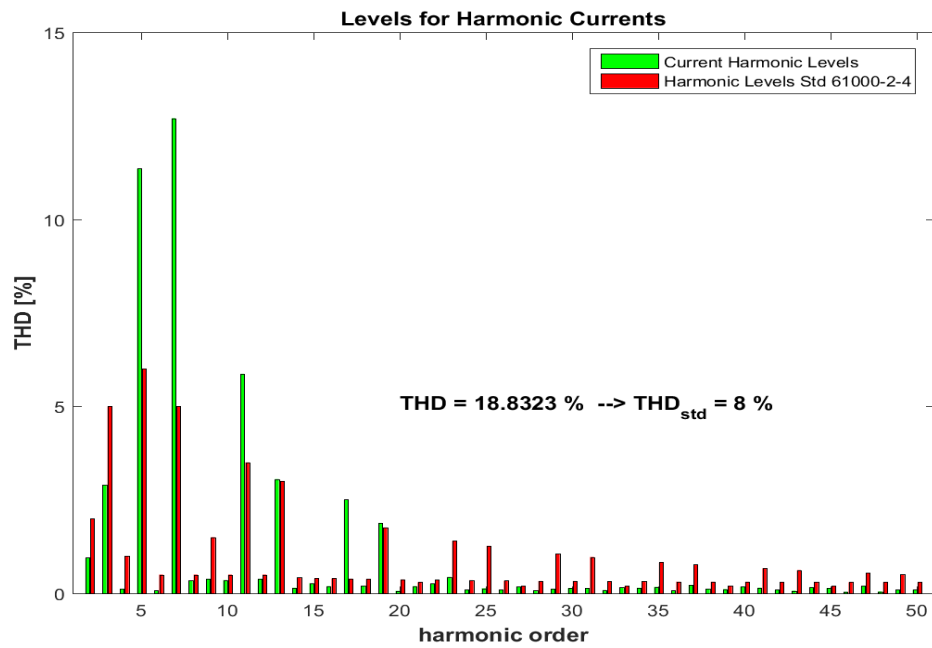


Fig. 5.20: Levels for harmonic currents phase A Transformer for point 550.

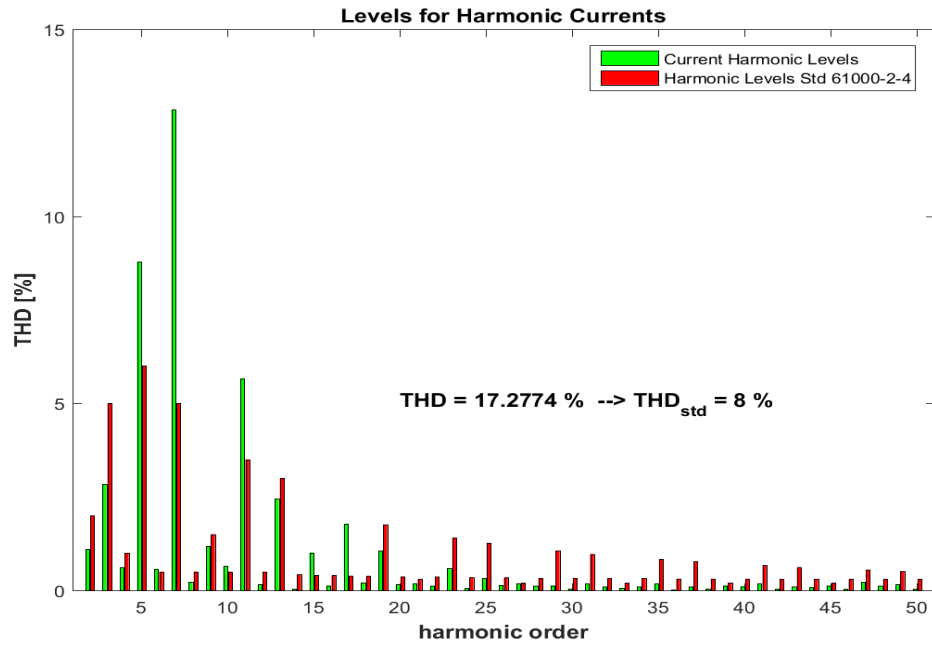


Fig. 5.21: Levels for harmonic currents phase B Transformer for point 550.

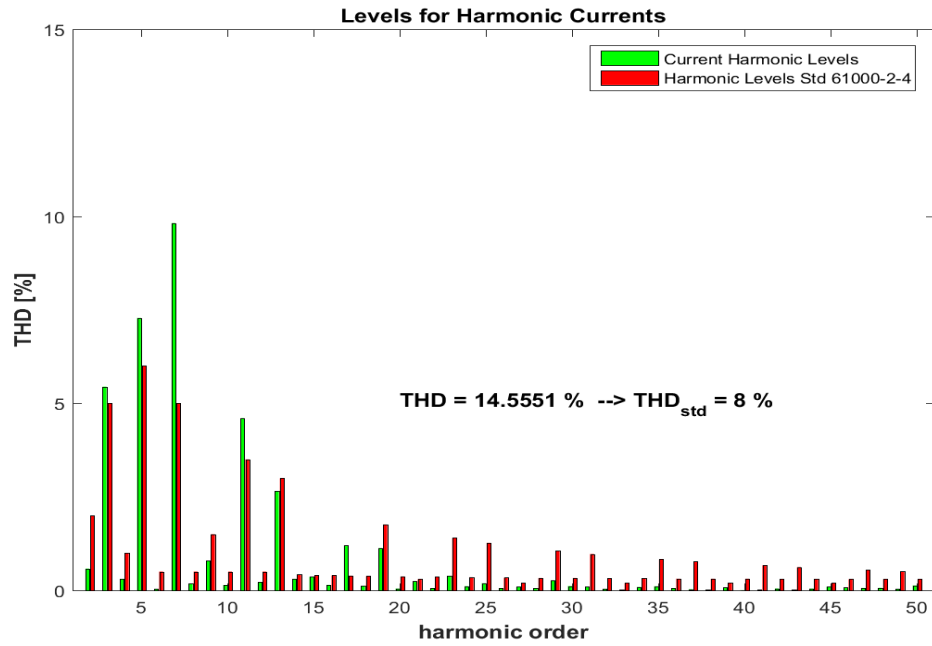


Fig. 5.22: Levels for harmonic currents phase C Transformer for point 550.

It can be observed from the Figure.5.17, 5.18 and 5.19 for the point 493 that THD levels in all three phases are below 8%. However, the levels for harmonic orders

7, 9, 17 are exceeding their limits in phase A. The harmonic levels in phase B Figure.5.18 are also exceeded for the harmonics of the order 7, 8, 10, 15, 17, 21. Finally, in phase C the 17 harmonic is above the limits. When looking at the second point 550 Figure.5.20, 5.21 and 5.22 the THD limits are exceeded in all three phases. The harmonics of the orders 3, 5, 7, 11, 13, 15, 17, 19 are exceeding their levels.

The results for the point 493 with inter-harmonics is presented in Figure.5.23.

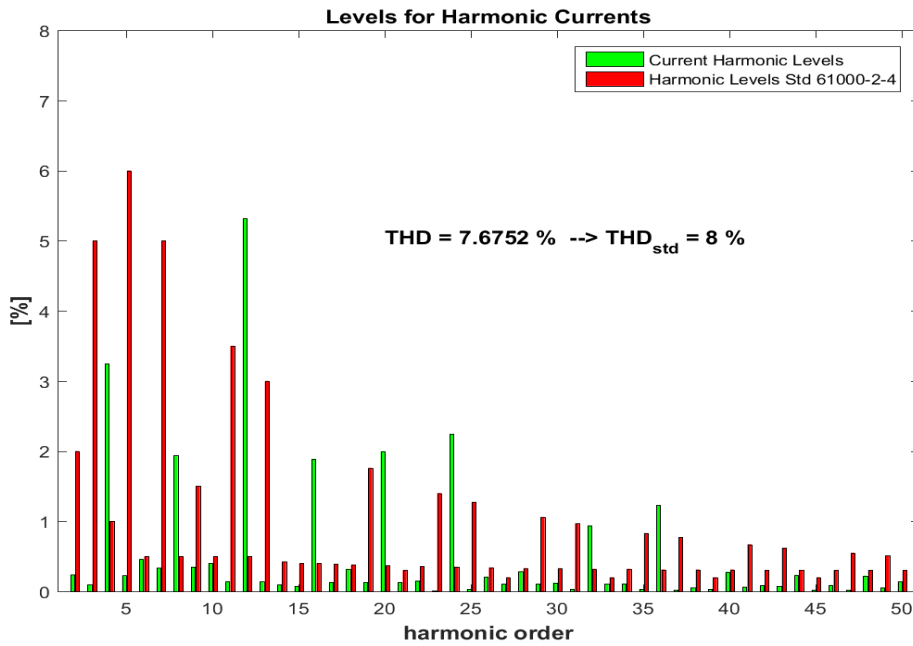


Fig. 5.23: Levels for inter-harmonic currents phase A Transformer for point 493.

To summarize, the high frequency harmonics are eliminated in transformer and underground cables. Thus the remaining content in transformer is from the WT mainly 5, 7, 11, 13, 17<sup>th</sup> harmonics and emissions from PF are seen as the 21<sup>st</sup> harmonic. However, it is difficult to say what kind of harmonic emissions are coming from PV system without looking into the current. The harmonic emissions of PV system needs further investigation.

## 5.5 THD levels in Transformer, WT and PF

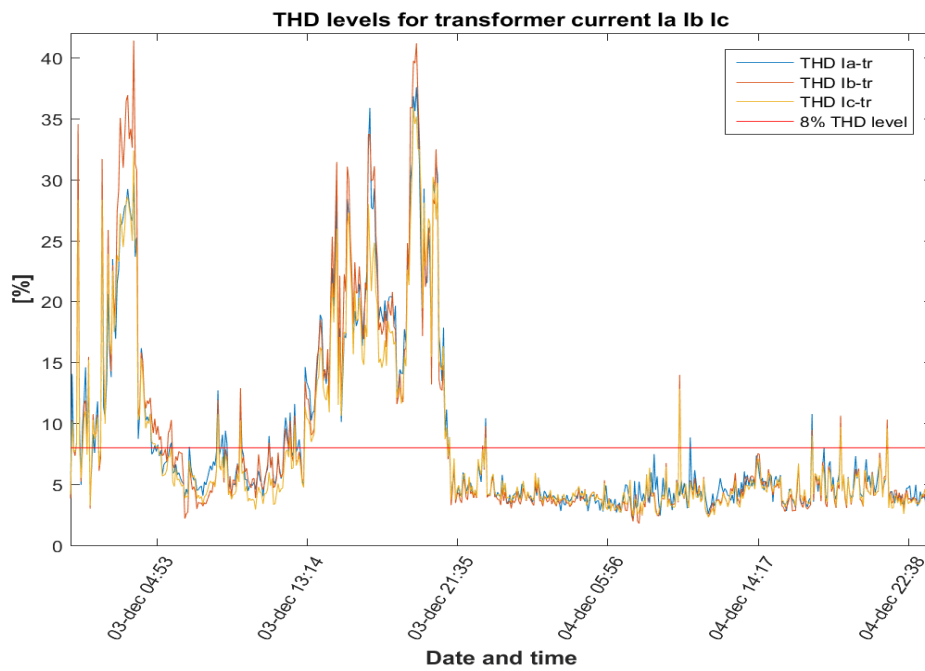


Fig. 5.24: THD levels for transformer current in three phases for measurement period from 3 December to 4 December.

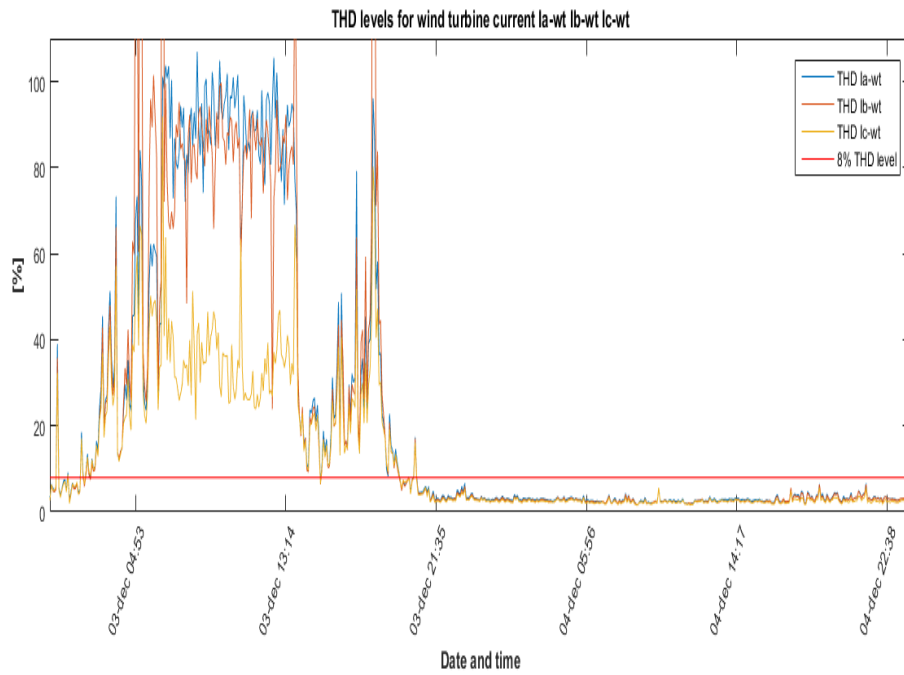


Fig. 5.25: THD levels for wind turbine current in three phases for measurement period from 3 December to 4 December.

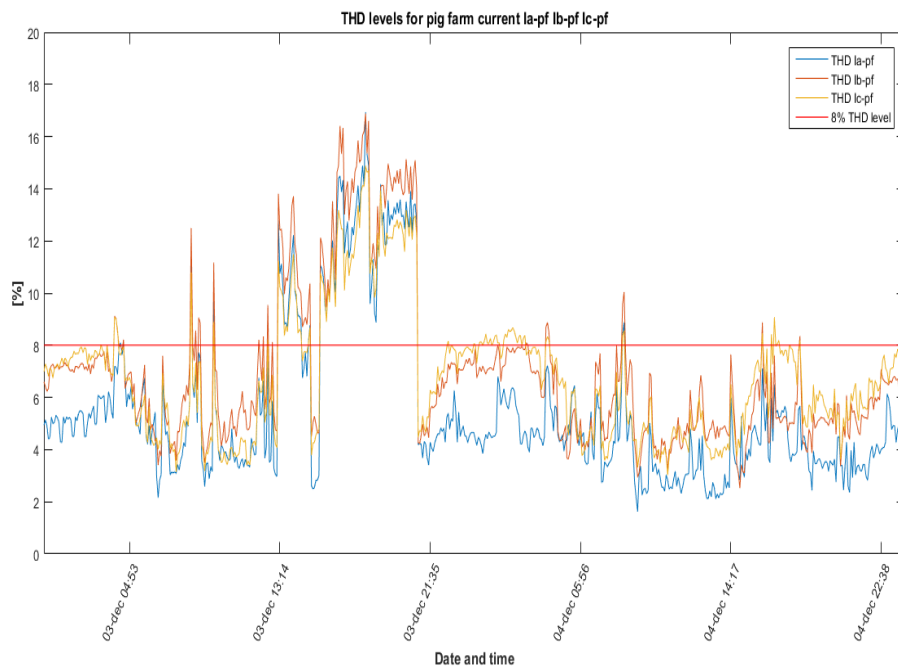


Fig. 5.26: THD levels for pig farm current in three phases for measurement period from 3 December to 4 December.

Finally, the THD levels for two days measurement period are depicted in Figure.5.24, 5.25 and 5.26 respectively for Transformer, WT and PF. It can be seen that for the first day the THD levels are violated for almost the whole day. However, for the second day there are only few point where THD limits are exceeded 8% level. The reason for this that the current from WT was filled with harmonic emissions. It is the period until 04:00am and then from 13:00pm until 21:00pm refer to the Figure.5.24. The picks between 05:00am to 13:00pm on Figure.5.24 are characterized by the harmonics of the PF seen in Figure.5.26. However, the current on PF can be affected by the harmonic emissions from WT as it is seen comparing Figure.5.25 and Figure.5.26 for the period from 13:00pm until 21:00pm. The THD of the WT are close to 100% and even higher.

Starting 3 December from 21:00pm until 4 December 23:00pm the THD limits for WT are not violated Figure.5.25 since the weather conditions are changed from no wind to high wind and storm. The WT has been running at full power and the harmonic content in transformer was mainly due to the PF operations. It has been noticed unbalance in the current of transformer, WT and PF. The unbalance on PF can be explained by the equipment connected on different phases that may work differently(different start and stop time) refer to Figure.5.26.

The amplitude of fundamental and harmonic currents from transformer, WT and PF are listed in Table.5.3 and Figure.. These values will be used in the developed model. Refer to Chapter 6 for more information about the model.

Tab. 5.3: The amplitude of harmonic current in each phase for transformer, wind turbine and pig farm point 493.

Point 493										
Harmonic order	1	5	7	9	11	13	15	17	19	21
Frequency [Hz]	50	250	350	450	550	650	750	850	950	1050
Phase	Amplitude [A]									
la	80,62	1,56	4,28	1,52	1,61	1,81	0,23	0,76	0,99	0,22
lb	84,66	1,60	4,46	0,63	1,40	1,48	0,54	0,63	0,73	0,36
lc	103,71	0,98	4,40	0,20	1,86	2,27	0,49	0,36	0,91	0,32
la_wt	0,17	0,04	0,01	0,01	0,01	0,01	0,01	0,01	0,01	0,00
lb_wt	0,11	0,03	0,03	0,01	0,00	0,00	0,00	0,00	0,01	0,01
lc_wt	1,17	0,09	0,00	0,10	0,06	0,06	0,06	0,03	0,01	0,01
la_pf	254,87	6,13	0,27	1,42	2,89	2,67	0,41	1,10	1,36	0,83
lb_pf	254,87	6,13	0,27	1,42	2,89	2,67	0,41	1,10	1,36	0,83
lc_pf	297,99	9,03	0,54	1,72	4,31	3,54	1,16	1,15	1,54	0,72

Point 550										
Harmonic order	1	5	7	9	11	13	15	17	19	21
Frequency [Hz]	50	250	350	450	550	650	750	850	950	1050
Phase	Amplitude [A]									
la	81,52	9,26	10,35	0,31	4,78	2,49	0,22	2,04	1,53	0,16
lb	83,59	7,34	10,74	0,98	4,74	2,04	0,85	1,49	0,89	0,16
lc	105,47	7,68	10,36	0,84	4,86	2,79	0,38	1,27	1,19	0,26
la_wt	17,13	1,76	3,43	0,11	1,33	0,72	0,53	2,29	1,19	0,32
lb_wt	14,67	1,42	3,45	0,20	1,23	0,78	0,21	2,70	2,26	0,26
lc_wt	16,07	1,33	2,76	0,13	1,16	0,83	0,23	1,21	1,90	0,43
la_pf	244,37	22,26	17,85	2,16	9,24	4,48	0,87	2,04	2,39	0,99
lb_pf	252,82	11,80	1,12	2,09	3,42	3,05	0,83	1,61	1,80	0,63
lc_pf	298,70	23,14	18,33	1,51	10,50	4,79	0,16	1,01	2,99	0,70

Tab. 5.4: The amplitude of harmonic current in each phase for transformer, wind turbine and pig farm point 550.5.4

## 5.6 Summary

With the data gathered in Chapter 5 a result of harmonic content can be processed and analyzed. The harmonics that potentially influence transformer temperature are identified. It was found that harmonic limits are violated in most cases and the main sources are Wind Turbine and Pig Farm. However, the harmonic injections from PV were not covered and left for further research. The values of harmonic currents needed for model validation are found. The inter-harmonics are present in the Pig Farm loads and explained.



## 6 Online Monitoring

This chapter presents the detailed description of the process of modeling the transformer and loads. Moreover, it describes the model verification procedure and introduce the simulation scenarios and its results. Finally, based on the simulation results the explanation of the effect of harmonic distortions on the equipment is given.

### 6.1 Transformer Modeling

Based on the theory presented in section 2 and 2.4 the model is built using PLECS. However, for modeling the other software can be used (Matlab Simulink, LTSpice, etc.). Based on the discussion of modeling in Chapter 2 it was decided to build the model using the three physical domains i.e electrical, magnetic and thermal. Since each of the domains is complement each other i.e combining electrical and thermal model both power losses and the temperature can be seen in one model. To investigate transformer non-linear behavior the combination of three domains has been chosen.

The advantage of circuit combination is that the linear transformer behavior can be modified taking into account non-linear magnetic properties. Thereby, linear and non-linear behavior of transformer core is studied. Consequently, the thermal model is added to see the transformer temperature behavior due to presence of harmonic content. The model used in this work depicted in Figure.6.1. The delta-wye connection is transformed to wye-wye connection for simplifications. It is done to operate with the same quantities of current and voltage. Refer to Appendix 7.2 for the calculations of transformation.

The following description for each domain presented below.

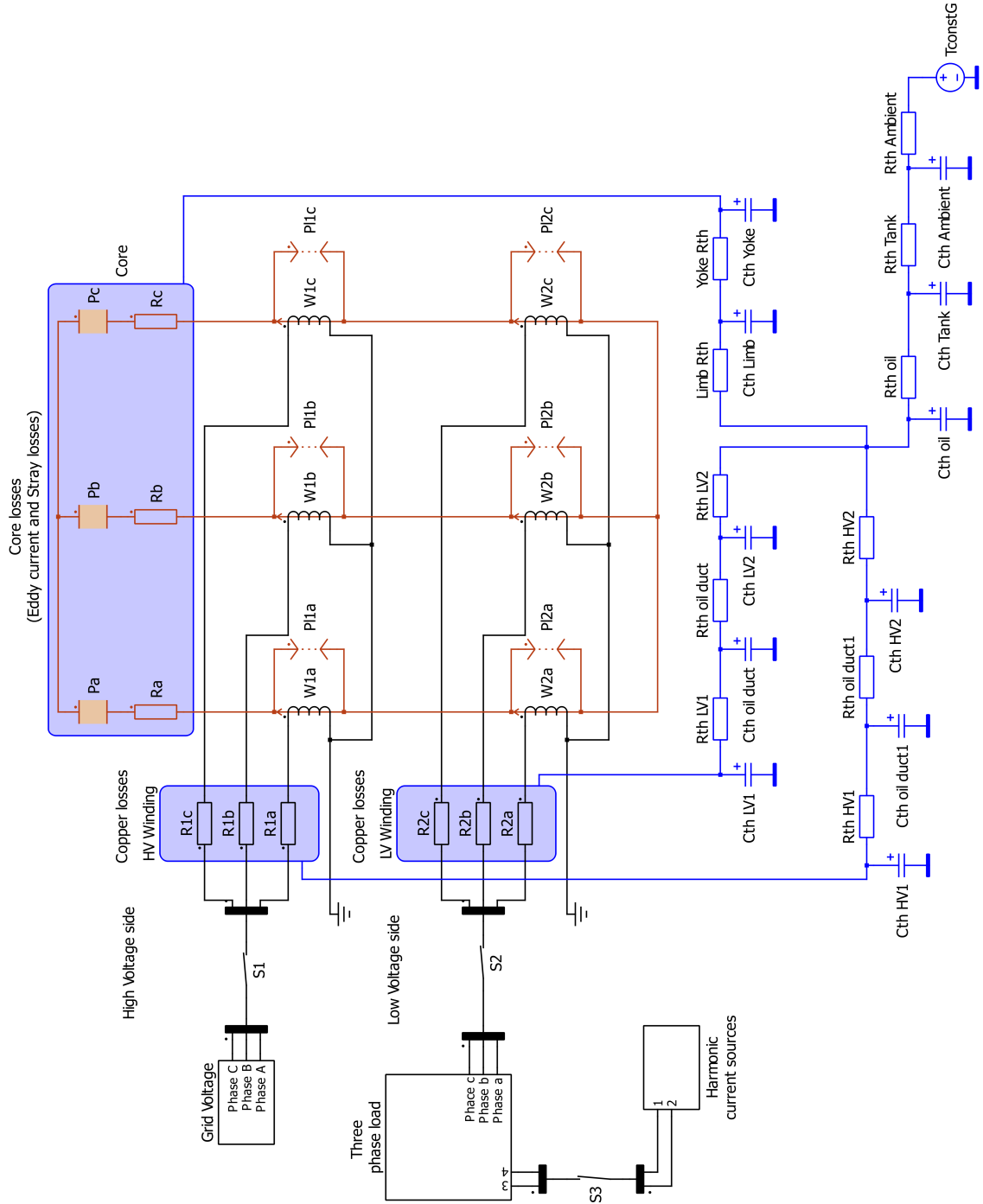


Fig. 6.1: An equivalent electrical-magnetic-thermal model of three phase transformer.

### 6.1.1 Electric domain

The external grid is modeled by the block (Grid Voltage). It has variable settings for the voltage and current. The grid side does not consider any disturbances and voltage is balanced. However, the unbalance of the grid voltage can be modeled by adding the sources of unbalance or sources of harmonic distortions. Primary side input parameters are  $V$ ,  $f$  and offset for phase A, phase B and phase C. The switch  $S1$  is used for no-load loss simulations when the voltage applied on the LV side.

The per-phase transformer model divided into three parts. The first part is to represent the Core losses ( $I^2R$ ) in electrical domain. The primary side winding uses ideal resistors  $R1a$ ,  $R1b$ ,  $R1c$  and secondary  $R2a$ ,  $R2b$ ,  $R2c$  accordingly. Both windings are coupled to magnetic circuit by electro-magnetic interface[11]  $W1a$ ,  $W1b$ ,  $W1c$  and  $W2a$ ,  $W2b$ ,  $W2c$ . Typical representation of the interface by Permeance-capacitance analogy or Reluctance-resistance analogy and described in [11].

### 6.1.2 Magnetic domain

Magnetic domain modeling is used to represent non-linearity of the core. Since the core losses characterized by Eddy current and Hysteresis losses and the ferromagnetic properties of the core. The circuit is modeled using magnetic permeances  $Pa$ ,  $Pb$ ,  $Pc$  in series with magnetic resistances  $Ra$ ,  $Rb$ ,  $Rc$ . It is done to model the core losses since, the magnetic resistance is dissipate heat. It can be seen from the relation of eq.6.1 For the Reluctance- resistance analogy the same approach is applicable.

$$P_{loss} = F \cdot \Phi = R \cdot \Phi^2 [W] \quad (6.1)$$

where  $P_{loss}$  - core loss  $[W]$

$F$  - magnetomotive force  $A \cdot turn$

$\Phi$  - magnetic flux  $[Wb]$

Moreover, the Leakage Flux Path in magnetic core is described by permeances  $Pl1a$ ,  $Pl1b$ ,  $Pl1c$  and  $Pl2a$ ,  $Pl2b$ ,  $Pl2c$   $[Wb]$  refer to Figure.6.1. The permeances are used to show the non-linearity of the core, as the ferromagnetic materials saturate when the magnetic flux has maximum value.

### 6.1.3 Thermal domain

The thermal behavior is captured by adding thermal to the entire circuit. It is done by applying the Heat sink concept [12]. The heat sink absorbs thermal losses and propagates them to the cooling system[12]. Thus the temperature of the element can be determined by thermal flow. It can be seen from Figure.6.1 the heat sinks are applied to each of the phases on electric and magnetic parts. By applying several heat sinks one can determine the heat flow and the temperature rise of each element. For the oil filled transformer, the heat flow is defined as follows:

The heat sources in the circuit are windings and core and heat propagates from those elements to the oil. Than from the oil to the ambient environment through the transformer tank walls. The circuit is modeled by thermal capacitances  $C_{th}$  [J/K] storing heat and thermal resistances  $R_{th}$  [K/W] to resist a heat flow. The overall heat flow in this circuit is defined from the element where heat sink is placed to the ambient environment  $T_{constG}$  through the thermal resistances.

### 6.1.4 Load

The model is completed by adding three phase load. An pure three phase resistive load is used where  $R_{loadA}$ ,  $R_{loadB}$ ,  $R_{loadC}$  [ $\Omega$ ] the loads on each phase connected in star. The block Three phase Load on Figure.6.1. The switch  $S2$  is used for the no-load simulations for the case when the voltage applied on the primary side.

In order to simulate effect of non-linear loads on transformer the block is added that has harmonic sources connected in parallel to the resistances on each phase. It is used to model generation of harmonics on different phases. The block has variable input thus the harmonics can be specified directly. The parameters specified by user are amplitude of harmonic current and harmonic frequency.

All parameters used for simulations in this work are attached in Appendix 7.2.

## 6.2 Model Validation

*Feeding selected data from DFT analysis into transformer model.*

The processed data by DFT will be fitted into the developed transformer model(refer to section with model). The test cases described in section ## will be simulated

and the result of simulations will be validated against temperature measurements from the test campaign.

In order to validate the model the following requirements should be fulfilled.

- Check availability of parameters (i.e. electrical, magnetic, thermal)
- Calculate missing parameters

Run the simulations according to predefined scenarios in section 6.2.1 and compare with:

- Data verification against data sheet from transformer manufacturer (no-load and short-circuit test)
  - Compare electrical quantities with those on the nameplate or from the test report if last is available
- compare and validate transformer temperature with the thermal profiles (thermal sensor and USB thermal logger)

Refer to Appendix A for nameplate and test report.

According to calculations the model has same parameters as on the nameplate.

The magnetic part is verified using the calculations of parameters such as flux -  $\Phi$ , flux leakage -  $\varphi$ , reluctance -  $R$  or permeance -  $P$  as well as the transformer core dimension Appendix A 7.2. Based on the results of calculations of design parameters both electrical and magnetic parts are close to the nameplate values.

Verification of the entire thermal model is done using the temperature measurements which are performed by optic fiber sensor and USB thermal logger measured top and bottom oil temperature.

Since the model required knowledge about thermal resistances and thermal capacitances of the materials used for transformer design ( $Al$ ,  $Cu$ ,  $Fe$ , oil, isolation materials etc.). These data is calculated based on the thermal characteristics of the transformer and its components. Refer to Appendix A7.2 for more information about calculation of thermal capacitances, thermal resistances of the core, windings, transformer oil, tank, other parts and.

### 6.2.1 Simulation Scenarios

This section describes simulation scenarios based on the requirements stated in 3.4. The following scenarios are considered and used for simulations:

### 1. No-Load

This scenario is used to define no-load loss by applying voltage on the primary side. Moreover, the no-load (normal) transformer temperature will be defined.

### 2. Partial load

The simulated scenario is performed for the case when the applied voltage amounts to 10%–50% of rated voltage. The two cases are considered with and without harmonic content drawn from the loads. It will give the information about the transformer temperature under half of load.

### 3. High load

The simulations are performed when the transformer is operated at 100% of its rated voltage. Two sub-cases are considered with and without harmonic content from the loads. The same outcome as for the case 2.

### 4. Worst case

The simulated scenario is consider the transformer that operate at 120% of its rated voltage. Two sub-cases involved one with and second is without harmonic content from the loads.

The first case 1 is simulated to define no-load losses. The other scenarios 2 and 3 are used to define the load losses and the transformer temperature. The worst case scenario 4 when the transformer is forced to operate above name plate rating and the harmonic content is present. Furthermore, the simulation results from combined model will be plotted to visualize transformer temperature rise and compare it with measured data.

Consequently, simulated results will be analyzed and verified in order to provide the guidelines for DSOs actions.

## 6.2.2 Simulation Results

The simulation results cannot be presented in the current work. It is due to the fact that the preparations for the Site-Tests took longer than it was expected. There, was issues with measurement equipment and the date for the measurements was moved one week later. Moreover, the post-processing of measured data is a very complex process since it requires identification of the proper files and loads. The PC used to run Matlab script has less memory and the processing of data was done

taking some parts from raw data and run the script to avoid the memory issues. The other issue that only few points are used from the DFT analysis. Therefore, it is necessary to take more points into account. While looking at Figure.6.2 it was found that the time delay in temperature rise/fall is about 1-5.30 hours. However it is not precise time for temperature rise. Therefore, it is required to use the more points for at least 8-9 hours from single day measurements. The effect of harmonic currents on transformer temperature is shown in Figure.6.2.

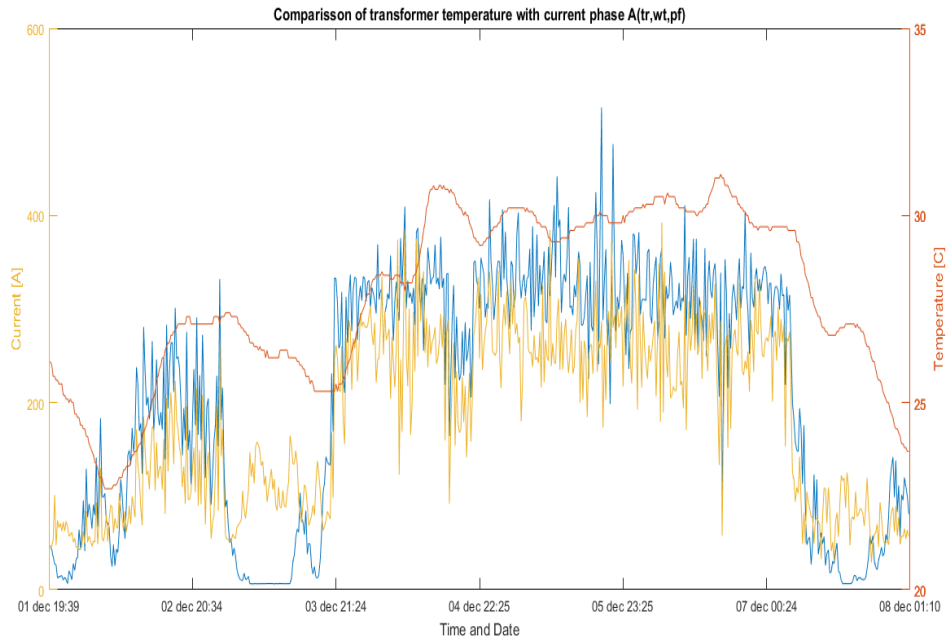


Fig. 6.2: Dependence of transformer temperature due to harmonic currents.

The temperature profile plotted in Figure.6.2 is used for visualization of time delay thus the x-axis is the Time and Date when temperature measured the other axis are current amplitude and transformer top oil temperature. The top tank and bottom tank temperature cannot be plotted in the same figure since it becomes unreadable.

However, one can rely on the simulations that was done in previous project. The model has been validated during the 9<sup>th</sup> semester project and results of simulations and monitoring toll are depicted in Figure.6.3 and Figure.6.4. It means that the model is working and in order to validate the current work the additional time is needed. The further steps are discussed in outlook for this project.

## Simulering Resultater & Effect

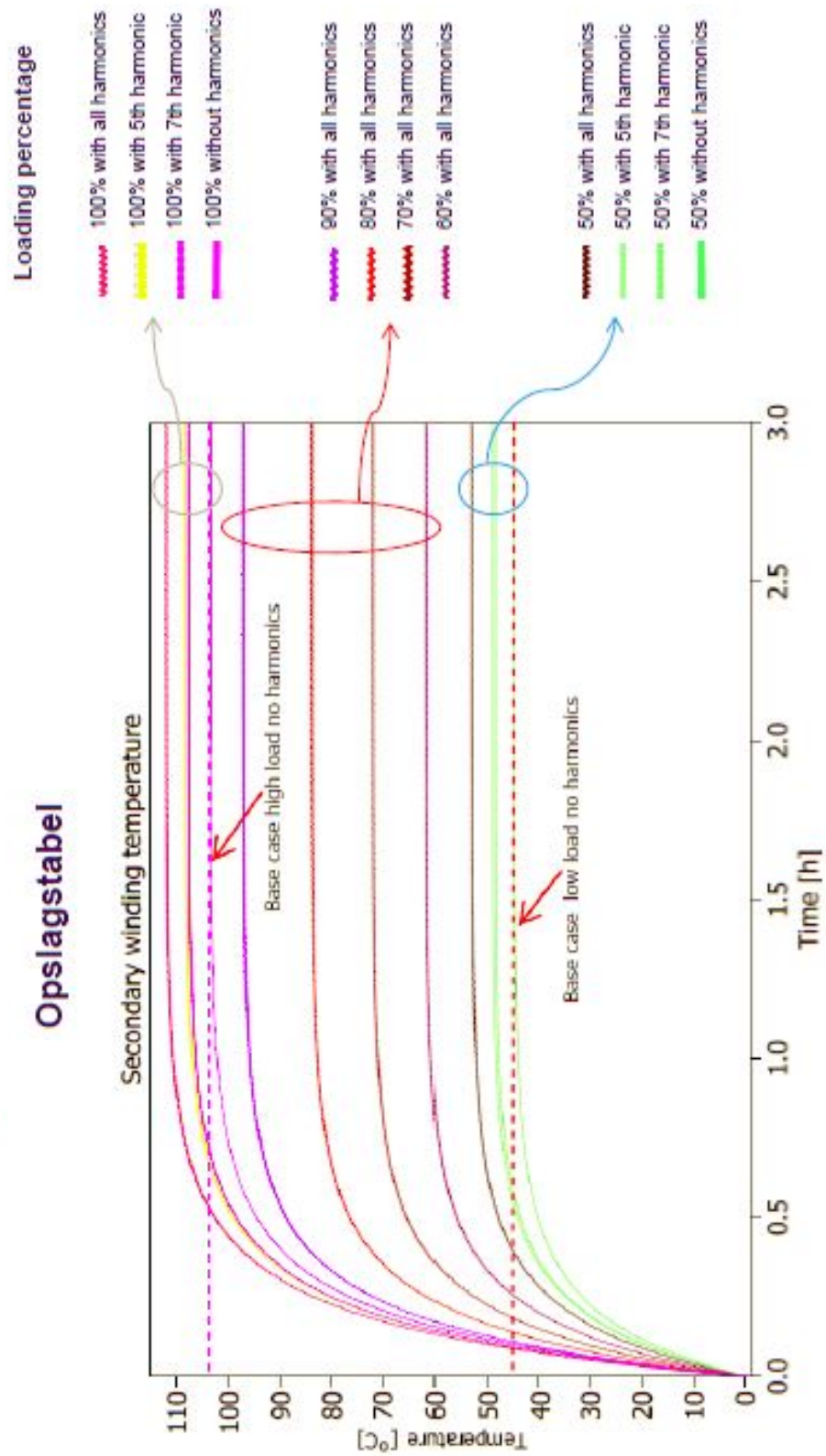


Fig. 6.3: Results of simulations done in previous project.



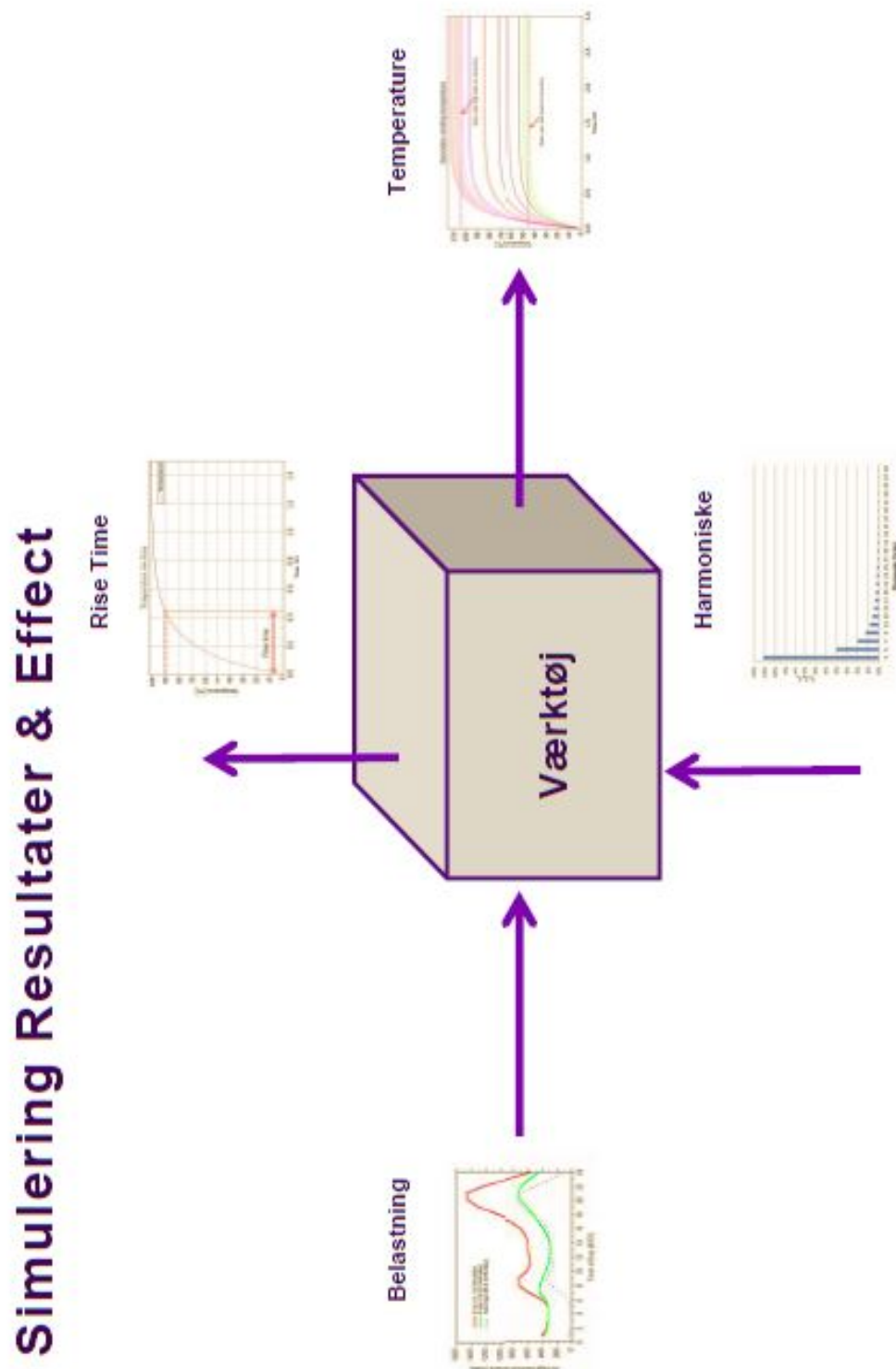


Fig. 6.4: The visualization of monitoring tool developed during the 9th semester project.

### 6.3 Effect of Harmonics on Equipment

The effect of harmonic currents in transformers [3] at harmonic frequencies causes increase in core losses due to eddy currents and hysteresis. Moreover, additional heating is result of increased copper losses and stray losses. The result of it is winding insulation stresses. The vibrations in core lamination due to the presence of harmonics are results in additional audible noise. The high RMS current due to harmonics will increase the copper losses.

The distribution transformers have typically a delta-wye connection, three-phase and neutral. The Triplen (i.e. 3rd, 9th, 15th...) harmonic cannot propagate from primary to secondary and circulate in the primary winding causing overheating. The triplen harmonic will cancel out in the neutral conductor when supplied with linear loading. However, in case of supply the nonlinear loads the triplen harmonics will be accumulated in the neutral conductor. Consequences of it is overheating the transformers and burning of neutral conductors.

The effect of harmonics distortion on induction motors [3] is similar to the transformer and cause increased heating. It is due to the copper and iron losses in the stator winding and rotor lamination. Continuous heating can degrade the windings and bearing lubrication which leads to a damage and reduce the lifetime of the motor. Moreover, the positive sequence components (i.e., 7th, 13th, 19th...) cause in higher torque(rotating in the same direction). However, the negative sequence components (5th, 11th, 17th...) resulting in torque pulsations(against the direction of rotation). Zero sequence components for example, triplen harmonics do not rotate and results in heat dissipation.

The consumers are also influenced by the harmonic distortions. According to [3] the following equipment is affected such as TV receivers, Fluorescent lamp, Computers and Power electronic equipment. The voltage peak and dips caused by harmonics can influence TV, computers and power electronics and leads to malfunction. Moreover, the resonance effect is seen i.e interaction between capacitors and inductance of ballast in fluorescent lamps.

Possible solutions to eliminate the harmonics in transformer is transformer derating to set the maximum allowed current (K -factor). The other approach is to use the

filtering equipment i.e FACT devices or passive and active filters.

$$K = \sqrt{\frac{\sum_h (I_h^2 \cdot h^2)}{\sum_h I_h^2}} \quad (6.2)$$

## 6.4 Summary

An three phase transformer and load electrical-magnetic-thermal model is presented. Additionally, the model is validated using the calculated values for transformer design parameters versus the data sheet for transformer. However, the harmonic content found by use of DFT analysis is not fitted into the model due to the limitations in time and resources. And the additional time is needed to do the simulations. The possible effect of harmonics on the equipment is provided.

# 7 Conclusion and Outlook

## 7.1 Conclusion

The main focus of the project addressed to Online condition monitoring tools and models to investigate thermal behavior of substation transformer exposed to the harmonic content drawn from non-linear loads and renewable sources.

The current work is done in accordance with IEC 61000 Standard series to perform the Site-Tests. The steady-state stability is defined to comply with the connection requirements for equipment connected to low voltage grids  $< 1\text{kV}$ . Since the project based on the measurements taken in substation transformer, the load description including the harmonic emission and its limits was presented.

The Site measurements are done using the oscilloscopes, voltage and current probes and thermal sensors that were placed in predefined places(POM). The Site-Test was performed to define the harmonic content in substation and the harmonic emissions from WT, PF and PV system.

The selected data from measurements was processed and transformed from time domain to the frequency domain by use of DFT algorithm. and the argumentation for selected points are explained. Additionally, the results of DFT was analyzed giving the description for the harmonic content and THD levels in transformer, WT and PF.

Finally, the simulation model was developed combining electrical, magnetic and thermal approaches and further validated against the data sheet. The model parameters were found using the *Transformer design approach*. However, during the entire work the only one sub objective for *Model validation and verification using field measurements* was not achieved. The reasons for this are the long preparations for the test campaign, shifted starting data and the complex process of post processing of measurement data. And last but not least the effect of harmonics

on equipment was described and the guidelines with possible solutions to eliminate the harmonics are given.

Getting this huge amount of data in Aalborg University(AAU) is a step forward in understanding the challenges of DSOs in operating a power grid with renewable energy sources and modern equipment.

Just post processing, extracting and getting on overview of all period of measurement is a tremendous task that require a lot of man power.

Having Thy-Mors willing to provide test site which can be used later on is also great achievement and opportunity for the students to do more in cooperation with DSO.

The other important achievements gathered during the project work are planning and preparations for the test measurements, communications with DSO (technical chef, project coordinator, network chef, operations engineer and construction technician) and consumers(the owner).

## 7.2 Outlook

The future work is required since the sub objectives for Model validation and verification using field measurements was not accomplished. Therefore, several suggestions are listed for improvements:

- Find the current, active and reactive power of PV system.
- Do analysis for single day at least for 8-9 hours.
- Find the harmonic emission from PV system.
- Fit the data from DFT into the model.
- Run simulations according to predefined test cases.
- Validate the model thermal behavior against measured data(transformer top oil temperature and USB thermocouple loggers).
- Develop a stand alone model for DSOs use.
- Provide a guidelines and recommendations based on the simulation results.

# Bibliography

- [1] W.H. Kersting. *Distribution System Modeling and Analysis, Third Edition*. Taylor & Francis, 2012.
- [2] D. Susa, M. Lehtonen, and H. Nordman. Dynamic thermal modelling of power transformers. In *Power Engineering Society General Meeting, 2004. IEEE*, pages 1421 Vol.2–, June 2004.
- [3] J. Arrillaga and N.R. Watson. *Power System Harmonics*. Wiley, 2003.
- [4] Alstom. 2015.
- [5] Areva. 2015.
- [6] Ieee recommended practice for establishing transformer capability when supplying non-sinusoidal load currents. *ANSI IEEE Std C57 1101986*, page 0 1, 1988.
- [7] Remus Teodorescu, Frede Blaabjerg, and Florin Iov. *Modelling and Control of Grid converter: Basic Grid Inverter Control*. Aalborg Universitetsforlag, Denmark, 2006.
- [8] S.V. Kulkarni and S.A. Khaparde. *Transformer Engineering: Design and Practice*. Plant Engineering Series. CRC Press, 2004.
- [9] U.A. Bakshi and V.U. Bakshi. *Electrical Engineering*. Technical Publications, 2009.
- [10] J.O. Smith. *Mathematics of the Discrete Fourier Transform (DFT): With Audio Applicaitons*. BookSurge Publishing, 2007.
- [11] J. Allmeling, W. Hammer, and J. Schonberger. Transient simulation of magnetic circuits using the permeance-capacitance analogy. In *Control and Modeling for Power Electronics (COMPEL), 2012 IEEE 13th Workshop on*, pages 1–6, June 2012.
- [12] Min Luo. Multi-physical domain modeling of a dfig wind turbine system using plects. 2015.

- [13] I. Cioc and C. Nică. *Proiectarea masinilor electrice*. Editura Didactică și Pedagogică, 1994.

# Appendix A

## A.1 Conversion of the parameters

Tab. .1: Delta to star conversion for winding resistance.

$\Delta \rightarrow Y$	$Y - \Delta$
$R_A = \frac{R_{AB} \cdot R_{AC}}{R_{AB} + R_{AC} + R_{BC}}$	$R_{AB} = \frac{R_A \cdot R_B + R_A \cdot R_C + R_B \cdot R_C}{R_C}$
$R_B = \frac{R_{AB} \cdot R_{BC}}{R_{AB} + R_{AC} + R_{BC}}$	$R_{BC} = \frac{R_A \cdot R_B + R_A \cdot R_C + R_B \cdot R_C}{R_A}$
$R_C = \frac{R_{AC} \cdot R_{BC}}{R_{AB} + R_{AC} + R_{BC}}$	$R_{AC} = \frac{R_A \cdot R_B + R_A \cdot R_C + R_B \cdot R_C}{R_B}$

Since the transformer connection is *Dyn5* it was decided to make simplifications and transformed to *Yy* according to Table..1. According to test report Figure.## the winding resistance are measured at temperature of  $75^\circ C$  therefore the following temperature corrections are calculated for winding temperature at  $25^\circ C$ ,  $110^\circ C$  and presented in Tab..2

## A.2 Calculation of transformer design parameters based on the Transformer design approach

The rated parameters for transformer from data sheet: nominal rated power  $S_N = 630 \text{ kVA}$ , primary and secondary nominal voltage respectively  $U_{iN} = 10.5 \text{ kV}$  and  $U_{jN} = 0.42 \text{ kV}$ , number of phases and limbs  $m = 3$ , frequency  $f = 50 \text{ Hz}$ , connection type *Dyn5*, short circuit voltage  $U_k = 4\%$ , no load current  $i_0 = 0.18\%$  tap regulation  $\pm 5\%$ , no load loss  $P_0 = 640 \text{ W}$  and short circuit power  $P_k = 5750 \text{ W}$ , the constant for cold rolled ferromagnetic sheet plates for copper  $p_{10/50} = 0.47 \text{ W/kg}$ . The small subscript letters  $i$  and  $j$  are for the HV and LV windings respectively.



Tab. .2: Temperature corrections for winding resistances on HV and LV side.

phase	HV at 25°C [Ω]	phase	LV at 25°C [Ω]
A	0.5066	a	0.000805
B	0.5076	b	0.00082
C	0.5062	c	0.000795
	HV at 75°C [Ω]		LV at 75°C [Ω]
A	0.6040	a	0.0009598
B	0.6052	b	0.000976
C	0.636	c	0.0009478
	HV at 110°C [Ω]		LV at 110°C [Ω]
A	0.6722	a	0.0011
B	0.6735	b	0.0011
C	0.6717	c	0.0011

### Calculation of magnetic circuit:

1. Cross section of the limb

$$S_c = C_t \cdot \sqrt{\frac{S_1}{f}} = (4 \div 6) \cdot 10^{-4} \cdot \sqrt{\frac{210 \cdot 10^3}{50}} = (0.0259 \div 0.0324) = (25.9 \div 32.4) \cdot 10^{-4} m^2 = (259 \div 324) cm^2$$

$$\text{where } S_1 = \frac{S_N}{3} = 210 kVA$$

$$C_t = (4 \div 6) \cdot 10^{-4} - \text{constant}$$

2. Diameter of the limb

$$D_c = \sqrt{\frac{4 \cdot S_c}{\pi \cdot k_m}} = \sqrt{\frac{4 \cdot (25.9 \div 32.4) \cdot 10^{-4}}{\pi \cdot 0.875}} = 0.1942 \div 0.2171 m = 19.42 \div 21.71 cm$$

$$\text{where } k_m = k_{Fe} \cdot k_g = 0.95 \cdot 0.92 = 0.875$$

$$k_g = 0.92 \text{ and } k_{Fe} = 0.95 - \text{the constants from tab16.1,a[13]}$$

$$\text{From eq.7.2 choose } D_c = 200 mm = 20 cm \text{ with number of sheet plates } n_{tr} = 6$$

3. Dimensions for the plates are width  $a_i$  and thickness  $b_i$  where  $i = 1, 2, 3, 4, 5, 6$  and calculated according Figure.16.1[13, p.798]

$$a_1 = 0.96 \cdot D_c = 0.96 \cdot 20 = 19.2 cm$$

$$a_2 = 0.885 \cdot D_c = 0.885 \cdot 20 = 17.7 cm$$

$$a_3 = 0.775 \cdot D_c = 0.775 \cdot 20 = 15.5 cm$$

$$a_4 = 0.631 \cdot D_c = 0.631 \cdot 20 = 12.62 cm$$

$$a_5 = 0.465 \cdot D_c = 0.465 \cdot 20 = 9.3 cm$$

$$a_6 = 0.28 \cdot D_c = 0.28 \cdot 20 = 5.6 \text{ cm}$$

$$a = a_1 = 14.5 \text{ cm}$$

$$b_1 = \sqrt{R^2 - (a_1/2)^2}, b_2 = ON - b_1, ON = \sqrt{R^2 - (a_2/2)^2}, b_3 = OM - (b_1 + b_2),$$

$$OM = \sqrt{R^2 - (a_3/2)^2},$$

$$b_1 = 2.8 \text{ cm}$$

$$b_2 = 1.9 \text{ cm}$$

$$b_3 = 1.6 \text{ cm}$$

$$b_4 = 1.5 \text{ cm}$$

$$b_5 = 1.1 \text{ cm}$$

$$b_6 = 0.7 \text{ cm}$$

$$b = 19.2 \text{ cm}$$

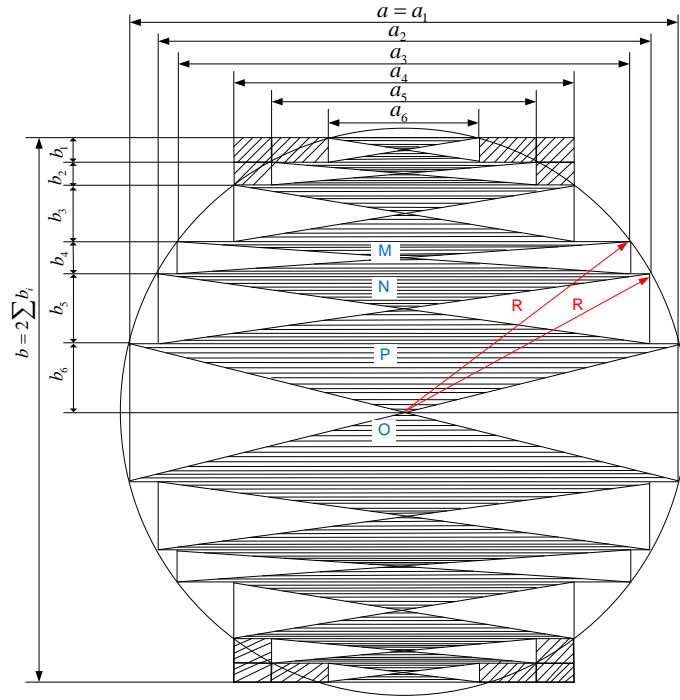


Fig. .1: Core and yoke cross section

4. Cross section of the limb corrected

$$S_c = 2 \cdot k_{Fe} \cdot \sum_{i=1}^{n_{tr}} a_i \cdot b_i = 2 \cdot 0.95 \cdot (19.2 \cdot 12.8 + 17.7 \cdot 1.9 + 15.5 \cdot 1.6 + 12.62 \cdot 1.5 + 9.3 \cdot 1.1 + 5.6 \cdot 0.7) = 276 \text{ cm}^2$$

5. Cross section of the yoke

$$S_j = 2 \cdot k_{Fe} \cdot (a_1 \cdot b_1 + a_2 \cdot b_2 + a_3 \cdot b_3 + a_4 \cdot (b_4 + b_5 + b_6)) = 2 \cdot 0.95 \cdot (19.2 \cdot 12.8 + 17.7 \cdot 1.9 + 15.5 \cdot 1.6 + 12.62 \cdot (1.5 + 1.1 + 0.7)) = 292 \text{ cm}^2$$

6. Height of the limb

$$L_c = \frac{S_i}{100 \cdot A \cdot e_1} = \frac{630 \cdot 10^3}{100 \cdot 300 \cdot 9.19} = 0.76 \text{ m} = 76 \text{ cm}$$

where  $A = 250 \div 400 \text{ A/cm}$  - initial value for the current density in the layer

$B_c = 1.65 \div 1.7 \text{ T}$  - magnetic flux density in limb

$$e_1 = 4.44 \cdot f \cdot S_c \cdot B_c = 4.44 \cdot 50 \cdot 276 \cdot 10^4 \cdot 1.5 = 9.19 \text{ V} - \text{electromotive force (emf)}$$

7. Width of the frame (approximate)

$$T = M - D_c = 40 - 20 = 20 \text{ cm}$$

$$M = 2 \cdot D_c = 2 \cdot 20 = 40 \text{ cm}$$

where  $T$  - width of the window between windings and  $M$  - width between limbs

8. The averaged yoke length

$$L_j = 2 \cdot D_c + 0.9 \cdot D_c = 2 \cdot 20 + 0.9 \cdot 20 = 98 \text{ cm}$$

9. Estimated calculation of no-load loss

$$P_0 \approx P_{Fe} = k_p \cdot p_{10/50} \cdot \left(\frac{f}{50}\right)^{1.3} \cdot (B_c^2 \cdot G_{Fec} + B_j^2 \cdot G_{Fej}) = 1.07 \cdot 0.35 \cdot \left(\frac{50}{50}\right)^{1.3} \cdot (1.5 \cdot 482.43 + 1.41^2 \cdot 437.82) = 572 \text{ W}$$

where  $P_{Fe}$ - iron losses,  $B_j$  - magnetic induction in yoke and  $\beta_j$ - constant for the core in steps immersed in oil  $\beta_j = (1.03 \div 1.1)$

$$B_j = \frac{\Phi}{S_j} = \frac{B_c \cdot S_c}{S_j} = \frac{B_c}{\beta_j} = \frac{1.5}{1.0580} = 1.4178 \text{ T}$$

$$\beta_j = \frac{S_j}{S_c} = \frac{292}{276} = 1.0580$$

$k_p = 1.07$  - coefficient for the core with stepped section and  $k_p = 1.25$  - from practical observations

10. Mass of iron in limb(net)

$$G_{Fec} = 3 \cdot S_c \cdot L_c \cdot \gamma_{Fe} = 3 \cdot 276 \cdot 76 \cdot 7.65 \cdot 10^{-3} = 482.43 \text{ kg}$$

$$\gamma_{Fe} = 7.65 \cdot 10^{-3} \text{ kg/cm}^3 - \text{specific mass for iron sheets}$$

11. Mass of iron in yoke(net)

$$G_{Fej} = 2 \cdot S_j \cdot L_j \cdot \gamma_{Fe} = 2 \cdot 292 \cdot 98 \cdot 7.65 \cdot 10^{-3} = 437.82 \text{ kg}$$

12. Correction of no-load loss for  $k_p = 1.25$

$$P_0 = P_{Fe} \cdot \frac{1.25}{1.07} = 572 \cdot \frac{1.25}{1.07} = 668 \text{ W}$$

### Calculation of windings

1. EMF in primary  $E_i$  and  $E_j$  secondary windings

$$E_i \approx U_{1f} = U_{iN} = 10500 \text{ V} - \text{for Delta connection}$$

$$E_j \approx U_{2f} = \frac{U_{jN}}{\sqrt{3}} = \frac{420}{\sqrt{3}} = 242.5 \text{ V} - \text{for star connection}$$

2. Number of turns in HV windings

$$w_i = \frac{E_i}{e_1} = \frac{10500}{9.19} = 1142 \text{ turns}$$

3. Number of turns for tap  $\pm 5\%$

$$\Delta w_i = \frac{k' \cdot \Delta U\%}{100} \cdot w_i = \frac{5}{100} \cdot 1142 = 57.1 \text{ turns}$$

$$k' \cdot \Delta U\% - \text{regulation for tap changer in percent}$$

4. Total number of turns

$$w_{iT} = w_i + \Delta w_i = 1142 + 57.1 \approx 1199 \text{ turns}$$

5. Number of turns in LV windings

$$w_j = \frac{E_j}{e_1} = \frac{242.5}{9.19} \approx 27 \text{ turns}$$

6. Specify the number of turns from the ratio

$$k = \frac{E_i}{E_j} = \frac{w_i}{w_j}$$

$$w_i = k \cdot w_j = \frac{E_i}{E_j} \cdot w_j = \frac{10500}{242.5} \cdot 27 = 1169 \text{ turns}$$

$$\Delta w_i = \frac{k' \cdot \Delta U\%}{100} \cdot w_i = \frac{5}{100} \cdot 1169 = 58.45 \text{ turns}$$

$$w_{iT} = w_i + \Delta w_i = 1169 + 58.45 \approx 1227 \text{ turns}$$

*Final values of magnetic flux density*

7. Magnetic flux(main)

$$\Phi = \frac{E_i}{4.44 \cdot f \cdot w_i} = \frac{10500}{4.44 \cdot 50 \cdot 1169} = 0.0405 = 4.5 \cdot 10^{-2} \text{ Wb}$$

8. Magnetic induction in the limb

$$B_c = \frac{\Phi}{S_C} = \frac{4.5 \cdot 10^{-2}}{276 \cdot 10^{-4}} = 1.4659 \text{ T}$$

9. Magnetic induction in yoke

$$B_j = \frac{\Phi}{S_j} = \frac{4.5 \cdot 10^{-2}}{292 \cdot 10^{-4}} = 1.3856 \text{ T}$$

10. Specify EMF of one turn

$$e_1 = \frac{E_i}{w_i} = \frac{10500}{1169} = 8.98 \text{ V/turn}$$

*Nominal current in transformer*

11. Current in HV winding

$$I_i = \frac{S_n}{m_i \cdot U_{if}} = \frac{630 \cdot 10^3}{3 \cdot 10500} = 20 \text{ A}$$

12. Current in LV winding

$$I_j = \frac{S_n}{m_j \cdot U_{jf}} = \frac{630 \cdot 10^3}{3 \cdot 242.5} = 866 \text{ A}$$

where  $m_i = m_j = m = 3$  - number of phase

*Cross section of conductor*

13. HV conductor

$$s_{wi} = \frac{I_i}{J_i} = \frac{20}{2.4} = 8.333 \text{ mm}^2$$

14. LV conductor

$$s_{wj} = \frac{I_j}{J_j} = \frac{866}{2.75} = 314.91 \text{ mm}^2$$

where  $J_i = 2.4 \text{ A/mm}^2$  and  $J_j = 2.75 \text{ A/mm}^2$  current density for copper table 16.2[13, p.803]

15. Choosing dimensions of conductors from table 7-I[13, p.1068-1071]

HV Conductor  $O - (1.32 \times 3.55) STAS2873/1 - 86(\text{isolation } 0.3 \text{ mm}) = 8.33 \text{ mm}^2$   
for  $s_{wi} = 8.333 \text{ mm}^2$

LV Conductor  $O - 8(1.25 \times 17) STAS2873/1 - 86(\text{isolation } 0.36 \text{ mm}) = 8 \cdot 39.5 = 316 \text{ mm}^2$  for  $s_{wj} = 314.91 \text{ mm}^2$

Therefor for HV winding conductor cross section  $s_{wi} = 8.33 \text{ mm}^2$  with conductor dimensions  $\frac{1.32 \times 3.55}{1.62 \times 3.85}$  where  $a'xb' = 1.62 \times 3.85 \text{ mm}^2$  - size with isolation

For LV winding conductor cross section  $s_{wj} = 316 \text{ mm}^2$  with conductor dimensions  $\frac{1.25 \times 17}{1.61 \times 17.36}$  where  $a'xb' = 1.61 \times 17.36 \text{ mm}^2$  - size with isolation

*Specify current density*

16. Current density in HV winding

$$J_i = \frac{I_i}{s_{wi}} = \frac{20}{8.33} = 2,4 \text{ A/mm}^2$$

17. Current density in LV winding

$$J_j = \frac{I_j}{s_{wj}} = \frac{866}{316} = 2,74 \text{ A/mm}^2$$

Choosing the conductor type, wiring method and isolation spaces according to [13, p.880]

Choosing isolation distances for  $U_{jN} = 0.42 \text{ kV}$  and  $U_{iN} = 10.5 \text{ kV}$  from table 16.3[13, p.813]

Refer to Figure..2 to see transformer dimensions and design parameters.

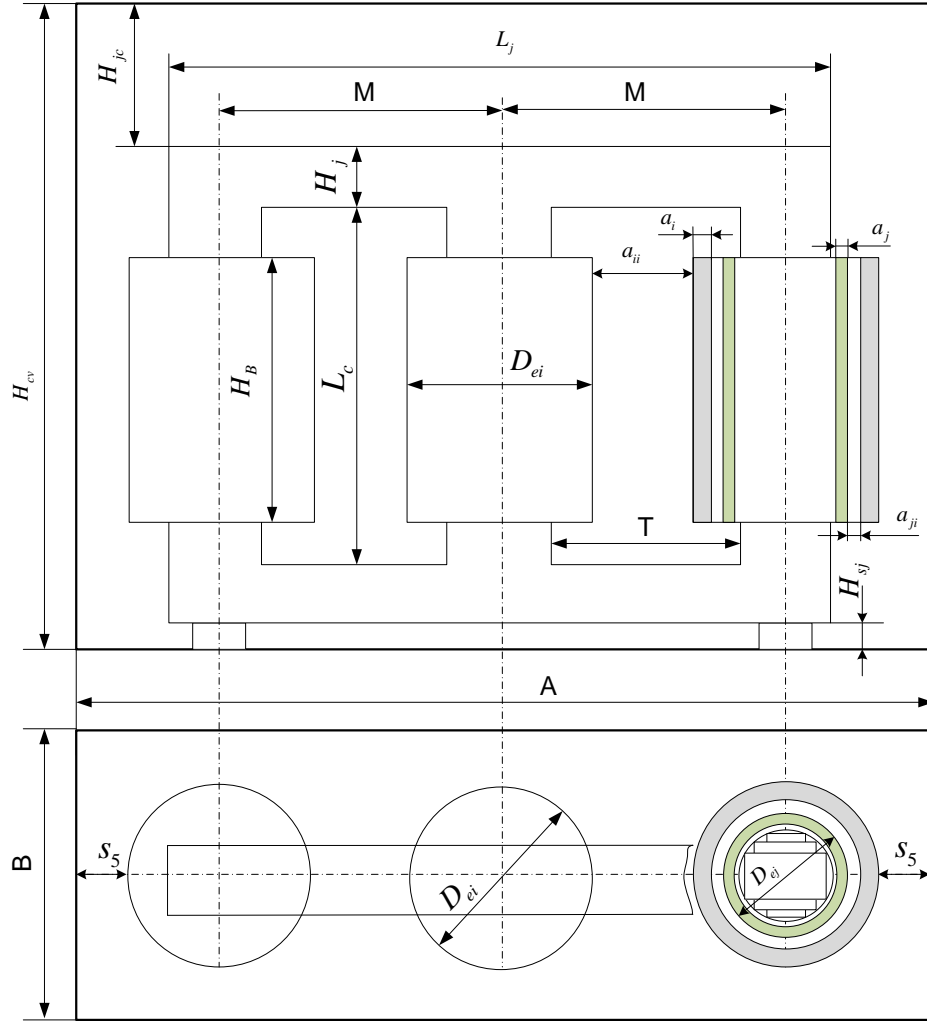


Fig. .2: Transformer design parameters.

$s_{im} = 2.5 \text{ cm}$  - distance from top of HV windings to the yoke

$a_{mj} = 0.4 \text{ cm}$  - distance from the limb to LV windings

$a_{ji} = 0.8 \text{ cm}$  - distance from the limb to HV windings

$a_{ii} = 0.8 \text{ cm}$  - distance between HV windings on the limbs

18. Height of the HV winding(bobbin)

$$H_B = L_c - 2 \cdot s_{im} = 76.16 - 2 \cdot 2.5 = 71.16 \text{ cm}$$

19. Number of turns LV winding

$$w_{sj} = \frac{H_B - n_t \cdot h_s}{h_s \cdot k_\varepsilon} - 1 = \frac{71.16}{34.72 \cdot 1.01} - 1 \approx 19 \text{ turns/layer}$$

where  $h_s = 2 \cdot b' = 2 \cdot 17.36 = 34.72 \text{ cm}$  - thickness of conductor

$k_\varepsilon = 1.01$ - the factor taking into account the actual deviations in insulation thickness  
and  $n_t = 0$  - number of transpositions

20. Height of the LV winding(bobbin)

$$H_{Bj} = (w_{sj} + 1) \cdot h_s \cdot k_\varepsilon + n_t \cdot h_s = (19 + 1) \cdot 3.472 \cdot 1.01 \approx 70 \text{ cm}$$

21. Distance to isolation LV

$$s_{jm} = \frac{L_c - H_{Bj}}{2} = \frac{76.16 - 70}{2} = 3.08 \text{ cm}$$

22. Number of turns HV

$$w_{si} = \frac{H_B}{b'} - 1 = \frac{71.16}{3.85 \cdot 10^{-1}} - 1 \approx 184 \text{ turns/layer}$$

23. Number of layers

$$n_{si} = \frac{w_i T}{w_{si}} = \frac{1227}{184} \approx 7 \text{ layers}$$

24. The tension/voltage in layer

$$U_s = 2 \cdot w_{si} \cdot e_1 = 2 \cdot 184 \cdot 8.98 = 3305 \text{ V}$$

from the table 16.6[13, p.830] choose the insulation thickness  $\delta_s$  of the layers

$$\delta_s = 3 \cdot 0.36 = 0.72 \text{ mm}$$

*Thickness of the windings*

25. LV windings

$$a_j = n_{sj} \cdot a_s + n_a \cdot a_{ja} + (n_s - n_a - 1) \cdot \delta_{iz} = 2 \cdot 3.22 + 1 \cdot 3 + (2 - 1 - 1) \cdot \delta_{iz} = 9.44 \text{ mm} = 0.94 \text{ cm}$$

where  $a_s = 2 \cdot a' = 2 \cdot 1.61 = 3.22 \text{ mm}$  - size of conductor with isolation

$n_{sj} = 2$  - number of conductors in  $a_s$

$n_a = 1$  - number of axial ducts

$a_{ja} = 3$  - cooling duct inside LV windings

Thickness of windings

26. HV winding

$$a_i = n_{si} \cdot d' + a_{ia} + (n_{si} - 2) \cdot \delta_s = 7 \cdot 1.62 + 5 + (7 - 2) \cdot 0.72 = 19.94 \text{ mm} = 1.994 \text{ cm}$$

where  $d' = a'$ - conductor diameter

$$n_s = n_{si}$$

$a_{ia} = 5 \text{ mm}$  - cooling duct inside HV windings

27. Width of the window between windings (refined)

$$T = 2 \cdot (a_{mj} + a_j + a_{ji} + a_i) + a_{ii} = 2 \cdot (0.4 + 0.94 + 0.8 + 1.994) + 0.8 = 9.07 \text{ cm}$$

Considering result obtained by estimated calculations  $T = 9 \text{ cm}$

### Calculation of no-load current

1. Calculate LV winding resistance

$$R_j = \rho_{cu75^\circ} \cdot \frac{w_j \cdot l_{medj}}{s_{wj}} = 0.022 \cdot \frac{27 \cdot 0.6912}{316} = 0.0013 = 1.3 \cdot 10^{-3} \Omega$$

where  $\rho_{cu75^\circ} = 0.022 \Omega \text{ mm}^2 / \text{m}$  - resistivity of copper

$l_{medj}$  - the average length of LV windings

$$l_{medj} = \pi \cdot D_{m2} = \pi \cdot 22 = 69.12 \text{ cm} = 0.6912 \text{ m}$$

$D_{m2}$  - the average diameter of LV windings

$$D_{m2} = D_c + 2 \cdot a_{mj} + a_j = 20 + 2 \cdot 0.4 + 0.9440 \approx 22 \text{ cm}$$

2. Calculate HV winding resistance

$$R_i = \rho_{cu75^\circ} \cdot \frac{w_i \cdot l_{medi}}{s_{wi}} = 0.022 \cdot \frac{1169 \cdot 0.8168}{8.33} = 2.52 \Omega$$

$l_{medi}$  - the average length of HV windings

$$l_{medi} = \pi \cdot D_{m1} = \pi \cdot 26 = 81.68 \text{ cm} = 0.8168 \text{ m}$$

$D_{m1}$  - the average diameter of HV windings

$$D_{m1} = D_c + 2 \cdot (a_{mj} + a_j + a_{ji}) + a_i = 20 + 2 \cdot (0.4 + 0.9440 + 0.8) + 1.994 \approx 26 \text{ cm}$$

*Calculation of losses in windings*

3. Losses in LV windings

$$P_{elj} = m \cdot k_{rj} \cdot R_j \cdot I_j^2 = 3 \cdot 1.0001 \cdot 1.3 \cdot 10^{-3} \cdot 866^2 = 2923 \text{ W}$$

where  $k_{rj}$  - the factor of increase in alternating current losses



$$k_{rj} = 1 + 1.73 \cdot \alpha_p^2 \cdot \left(\frac{f}{\rho \cdot 10^4}\right)^2 \cdot a^4 \cdot (m_s^2 - 0.2) = 1 + 1.73 \cdot 0.9072^2 \cdot \left(\frac{50}{0.22 \cdot 10^4}\right)^2 \cdot 0.125^4 \cdot (4^2 - 0.2) = 1.0001$$

$a = 0.125$  - conductor width in cm

$b = 1.7$  - conductor height in cm

$\alpha_p$  - coefficient for shaped conductor

$$\alpha_p = k_R \cdot \frac{b \cdot n}{H_{Bj}} = 0.9830 \cdot \frac{1.7 \cdot 38}{70} = 0.9072$$

where  $k_R$  - Rogowski coefficient

$n = 2 \cdot w_{sj} = 2 \cdot 19 = 38$  - number of conductors per bobbin

$$k_R = 1 - \frac{a_j + a_i + a_{ji}}{\pi \cdot H_{Bj}} = 1 - \frac{0.9440 + 1.994 + 0.8}{\pi \cdot 70} = 0.9830$$

4. Losses in HV windings

$$P_{eli} = m \cdot k_{ri} \cdot R_i \cdot I_i^2 = 3 \cdot 1.0002 \cdot 2.52 \cdot 20^2 = 3026 \text{ W}$$

$$k_{ri} = 1 + 1.73 \cdot \alpha_p^2 \cdot \left(\frac{f}{\rho \cdot 10^4}\right)^2 \cdot a^4 \cdot (m_s^2 - 0.2) = 1 + 1.73 \cdot 0.9025 \cdot \left(\frac{50}{0.22 \cdot 10^4}\right)^2 \cdot 0.132^4 \cdot (7^2 - 0.2) = 1.0002$$

where  $k_i$  - factor of increase is in alternating current losses

$a = 0.132$  - conductor width in cm

$b = 0.355$  - conductor height in cm

$$\alpha_p = k_R \cdot \frac{b \cdot n}{H_{Bi}} = 0.9833 \cdot \frac{0.355 \cdot 184}{71.16} = 0.9025$$

where  $n = w_{si} = 184$  - conductors per bobbin

$m_s = n_{si} = 7 \text{ layers}$

$H_{Bi} = H_b = 71.16 \text{ cm}$  - height of the bobbin

$$k_R = 1 - \frac{a_j + a_i + a_{ji}}{\pi \cdot H_{Bi}} = 1 - \frac{0.9440 + 1.994 + 0.8}{\pi \cdot 71.16} = 0.9833$$

*Density of the losses on the winding surface*

5. LV side

$$q_j = \frac{P_{elj}}{c \cdot S_{wj}} = \frac{2923.4}{3 \cdot 0.15} = 633 \text{ W/m}^2$$

where  $c = m = 3$  - colons(yoke)

$S_{wj}$  - yoke cross section and calculated as

$$S_{wj} = 0.8 \cdot \pi \cdot (D_{ij} + 2 \cdot D_{m2} + D_{ej}) \cdot H_{Bj} = 0.8 \cdot \pi \cdot (20.8 + 2 \cdot 22 + 22.688) \cdot 70 = 1539.2 \text{ cm}^2 = 0.15 \text{ m}^2$$

where  $D_{ij}$  and  $D_{ej}$  internal and external diameter of LV winding respectively

$$D_{ij} = D_c + 2 \cdot a_{mj} = 2 + 2 \cdot 0.4 = 20.8 \text{ cm}$$

$$D_{ej} = D_{ij} + 2 \cdot a_j = 20.8 + 2 \cdot 0.944 = 22.6880 \text{ cm}$$

6. HV side

$$q_i = \frac{P_{eli}}{c \cdot S_{wi}} = \frac{2923.4}{3 \cdot 1.955} = 516 \text{ W/m}^2$$

$$S_{wi} = \pi \cdot (0.8 \cdot (D_{ii} + 2 \cdot D'_{mi}) + D_{ej}) \cdot H_{Bi} = \pi \cdot (0.8 \cdot (24 + 2 \cdot 25.15) + 22.688) \cdot 71.16 = 1955 \text{ cm}^2 = 1.955 \text{ m}^2$$

where  $D_{ii}$  and  $D_{ei}$  internal and external diameter of HV winding respectively

$$D_{ii} = D_{m1} - a_i = 26 - 1.994 = 24 \text{ cm}$$

$$D'_{m1} = D_{ii} + 2 \cdot n'_s \cdot a' + a_{ia} = 24 + 2 \cdot 2 \cdot 0.162 + 0.5 = 25.15 \text{ cm}$$

$$D_{ei} = D_{m1} + a_i = 26 + 1.994 = 27.99 \text{ cm}$$

$a' = 1.62 \text{ mm}$  - conductor width from cable dimensions

$$n'_s = \frac{1}{3} \cdot n_{si} = \frac{1}{3} \cdot 7 \approx 2 \text{ number of conductors per bobbin}$$

*Total electrical losses*

7. Nominal Short-circuit power

$$P_{kN} = P_{elj} + P_{eli} = 2923.4 + 3026,6 = 5950 \text{ W}$$

8. Active component of short-circuit voltage

$$U_{ka} = \frac{P_{kN}}{S_n} = \frac{5950}{630 \cdot 10^3} = 0.944 \%$$

9. Reactive component of short-circuit voltage

$$U_{kr} = \frac{2 \cdot \pi \cdot \mu_0 \cdot f \cdot w_i \cdot I_i \cdot l_m \cdot \delta' \cdot k_q}{e_1 \cdot H_{Bj}} \cdot k_R \cdot 100 = \frac{2 \cdot \pi \cdot 4 \cdot \pi \cdot 10^{-7} \cdot 50 \cdot 1169 \cdot 20 \cdot 0.9098 \cdot 2.65 \cdot 1}{8.9820 \cdot 70} \cdot 0.9421 \cdot 100 = 3.3484 \%$$

where  $\delta'$  and  $l_m$

$$\delta' = a_{ji} + \frac{a_{ja} + a_{ia}}{4} + \frac{a_j + a_i}{3} = 0.8 + \frac{3 + 0.5}{4} + \frac{0.9940 + 1.994}{3} = 2.6543 \text{ cm}$$

$$l_m = \pi \cdot (D_c + 2 \cdot a_{mj} + a_{ji} + a_i + a_{ia} + \frac{3 \cdot (a_j + a_{ja})}{2}) = \pi \cdot (20 + 2 \cdot 0.4 + 0.8 + 0.994 + 0.5 + \frac{3 \cdot (0.994 + 3)}{2}) = 90.98 \text{ cm} = 0.90 \text{ m}$$

$k_R$  - Rogowski coefficient

$$k_q = 1 + \frac{x^2 \cdot H_B}{r \cdot \delta' \cdot k_R} = 1 + \frac{0.0163^2 \cdot 33}{3 \cdot 3.245 \cdot 0.9421} = 1.0025$$

$$x = \frac{H_x}{H_B} = \frac{-1.163}{71.16} = -0.0163$$

$$H_x = H_{Bj} - H_{Bi} = 70 - 71.163 = -1.163 \text{ cm}$$

$$r = 3$$

$$\mu_0 = 4 \cdot \pi \cdot 10^{-7} \text{ H/m} - \text{magnetic permeability}$$

10. Short-circuit voltage

$$U_k = \sqrt{U_{ka}^2 + U_{kr}^2} = \sqrt{0.944^2 + 3.3484^2} = 3.479 \%$$

*Mass of conductors in coil*

11. Mass of LV windings

$$G_{wj} = \gamma_{cu} \cdot s_{wj} \cdot w_j \cdot l_{medj} = 8.9 \cdot 10^{-3} \cdot 3.16 \cdot 27 \cdot 69.12 = 52.48 \text{ kg}$$

where  $\gamma_{cu} = 8.9 \cdot 10^{-3} \text{ kg/cm}^3$  - specific mass of copper

The values used for  $s_{wj} = 3.16 \text{ cm}^2$  and  $s_{wi} = 0.0833 \text{ cm}^2$  are converted from  $\text{mm}^2$  to  $\text{cm}^2$

For  $L_{medj} = 69.12 \text{ cm}$  and  $L_{medi} = 81.68 \text{ cm}$  converted from  $m$  to  $\text{cm}$

12. Mass of HV windings

$$G_{wi} = \gamma_{cu} \cdot s_{wi} \cdot w_{iT} \cdot l_{medi} = 8.9 \cdot 10^{-3} \cdot 0.0833 \cdot 1227 \cdot 81.68 = 74.30 \text{ kg}$$

$$w_{iT} = 1227 \text{ turns}$$

*Determination of no-load current*

13. Active component of no-load current

$$I_{0a} = \frac{P_{Fe}}{m \cdot U_{if}} = \frac{572}{3 \cdot 10500} = 0.0182 \text{ A} = 18.2 \mu\text{A}$$

14. Reactive component of no-load current

$$I_{0r} = I_{\mu} = \frac{H_c \cdot L_c + H_j \cdot L_j + n_{\delta} \cdot \frac{B_i}{\mu_0} \cdot \delta_i}{\sqrt{2} \cdot w_i} = \frac{2.5 \cdot 76.16 + 1.98 + 2 \cdot \frac{1.0366}{4 \cdot \pi \cdot 10^{-7}} \cdot 0.025 \cdot 10^{-3}}{\sqrt{2} \cdot 1169} = 0.1994 \text{ A} = 199.4 \mu\text{A}$$

where  $n_{\delta} = 2$  constant for ferromagnetic cores with normal construction

For  $B_c = 1.4659 \text{ T}$  and  $B_j = 1.3856 \text{ T}$  - magnetic induction in limb and yoke find the corresponding values for magnetic field strengths from annex [13, p.1065]

$H_c = 2.5 \text{ A/cm}$  and  $H_j = 1 \text{ A/cm}$  - magnetic field strength in limb and yoke

$B_i$  - amplitude of magnetic induction

$$B_i = B_c \cdot \cos \alpha = 1.4659 \cdot \frac{\sqrt{2}}{2} = 1.0366 \text{ T}$$

where  $\alpha = 45^\circ$  - the angle between colons and clamp plates

15. Total no-load current

$$I_{10} = \sqrt{I_{0a}^2 + I_{\mu}^2} = \sqrt{0.0182^2 + 0.1994^2} = 0.2002 A = 200\mu A$$

16. That in percent is

$$I_{10}[\%] = \frac{I_{10}}{I_i} \cdot 100 = \frac{0.2002}{20} = 1.0011 \%$$

### Thermal calculations

*Estimation of transformer temperature*

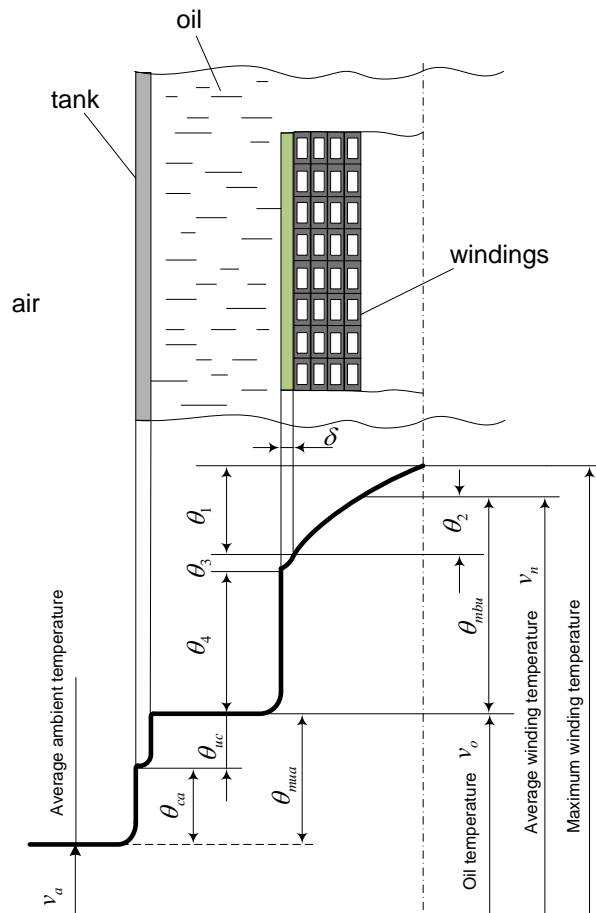


Fig. .3: The temperature drop from windings to the ambient in oil filled transformer.

1. Temperature of windings and oil

For LV winding, cylindrical type, the average temperature of bobbin  $\Theta_2$  is equal to the max. temperature of the core and windings  $\Theta_1$

$$\Theta_1 = \Theta_2 = 0$$

2. Temperature in isolation of conductor

$$\Theta_3 = q_j \cdot \frac{\delta}{\lambda_{iz}} \cdot 10^{-4} = 633 \cdot \frac{0.018}{0.0014} = 0.814^\circ C$$

where  $\delta = 0.018 \text{ cm}$  - constant for paper insulation

$\lambda_{iz} = 0.0014 \text{ W/cm}^\circ C$  constant for paper impregnated in oil from table 18.2[13, p.857]

3. For HV windings

$$\Theta_1 = \frac{p \cdot a_b^2}{8 \cdot \lambda_m} = \frac{1.7 \cdot 10^{-2} \cdot 3.69^2}{8 \cdot 1.8 \cdot 10^{-3}} = 15.85^\circ C$$

where  $p$  - specific losses produced in  $\text{cm}^3$ ,  $\lambda_m$  - average conductivity

$$p = k_p \cdot \frac{J_i^2 \cdot a \cdot b}{(a' + \delta_s) \cdot b'} \cdot 10^{-2} = 2.14 \cdot \frac{2.4^2 \cdot 0.132 \cdot 0.355}{(0.162 + 0.072) \cdot 0.385} = 1.7 \cdot 10^{-2} \text{ W/cm}^3$$

$k_p = 2.14$  - constant for copper

$$\delta_s = \delta_s = 3 \cdot 0.36 = 0.72 \text{ mm} = 0.072 \text{ cm}$$

$$\lambda_m = \lambda_i \cdot \frac{(a' + \delta_s) \cdot b}{(2\delta + \delta_s) \cdot b'} = 1.7 \cdot 10^{-3} \cdot \frac{(0.162 + 0.072) \cdot 0.355}{(0.03 + 0.072) \cdot 0.385} = 1.8 \cdot 10^{-3} \text{ W/cm}^3$$

with thermal conductivity equivalent to

$$\lambda_i = \frac{\lambda \cdot \lambda_s (2\delta + \delta_s)}{\lambda_s \cdot 2\delta + \lambda \cdot \delta_s} = \frac{1.4 \cdot 10^{-3} \cdot 1.7 \cdot 10^{-3} (0.03 + 0.072)}{1.7 \cdot 10^{-3} \cdot 0.03 + 1.4 \cdot 10^{-3} \cdot 0.072} = 1.7 \cdot 10^{-3} \text{ W/cm}^\circ C$$

where  $\lambda = 1.4 \cdot 10^{-3} \text{ W/cm}^\circ C$  - constant for isolation impregnated in oil

$\lambda_s = 1.7 \cdot 10^{-3} \text{ W/cm}^\circ C$  - constant for isolation impregnated in lac

$$2\delta = a' - a = b' - b = 0.3 \text{ mm} = 0.03 \text{ cm}$$

$n_s'' = 5 \text{ layers}$  - out of 7 since  $n_s' = 7 \text{ layers}$

$$a_b = n_s'' \cdot a' + (n_s'' - 1) \cdot \delta_s = 5 \cdot 0.162 + (5 - 1) \cdot 0.072 = 3.69 \text{ cm}$$

4. The average temperature drop

$$\Theta_2 = \frac{2}{3} \cdot \Theta_1 = \frac{2}{3} \cdot 15.85 = 10.56^\circ C$$

5. Temperature drop between the LV windings surface and the oil

$$\Theta_{4j} = 0.285 \cdot q_j^{0.6} = 0.285 \cdot 633^{0.6} = 13.66^\circ C$$

6. Temperature drop between the HV windings surface and the oil

$$\Theta_{4i} = 0.285 \cdot q_i^{0.6} = 0.285 \cdot 516^{0.6} = 12.09^\circ C$$

7. The average temperature drop winding to oil

$$\Theta_{mbu} = \Theta_2 + \Theta_3 + \Theta_{4i} = 10.56 + 0.814 + 12.09 = 23.47^\circ C$$

8. The maximum average temperature drop core to oil

$$\Theta_{maxfu} = \Theta' \cdot \frac{\Theta_4'' + 1.5 \cdot \Theta_1''}{\Theta' + \Theta_4'' + 1.5 \cdot \Theta_1''} = 8.13 \cdot \frac{6.56 + 1.5 \cdot 10.5}{8.13 + 6.56 + 1.5 \cdot 10.5} = 5.96^\circ C$$

where

$$\Theta_1' = \frac{p \cdot a^2}{8 \cdot \lambda_l} = \frac{6.8 \cdot 10^{-3} \cdot 19.2^2}{8 \cdot 0.2} = 1.57^\circ C$$

$$p = p_{Fe} \cdot \gamma_{Fe} \cdot k_{Fe} = k_p \cdot p_{10/50} \cdot \left(\frac{f}{50}\right)^{1.3} \cdot B_c^2 \cdot \gamma_{Fe} \cdot k_{Fe} = 1.25 \cdot 0.35 \cdot \left(\frac{50}{50}\right)^{1.3} \cdot 1.467^2 \cdot 7.65 \cdot 10^{-3} \cdot 0.95 = 6.8 \cdot 10^{-3} W/cm^3$$

$$k_p = 1.07 \div 1.25$$

Dimensions for the plates  $a$  and  $b$

$$a = a_1 = 19.2 cm$$

$$b = 2 \cdot \sum b_i = 19.2 cm$$

the values for  $\lambda_l = 0.2 W/cm^\circ C$  and  $\lambda_t = 0.03 W/cm^\circ C$  are found from table 18.4 [13, p.860]

$$\Theta_4' = \frac{p \cdot a}{2 \cdot \lambda_{conv}} = \frac{6.8 \cdot 10^{-3} \cdot 19.2}{2 \cdot 0.01} = 6.56^\circ C$$

where  $\lambda_{conv} = 100 W/m^2^\circ C = 0.01 W/cm^2^\circ C$

$$\Theta' = \Theta_1' + \Theta_4' = 1.57 + 6.56 = 8.13^\circ C$$

$$\Theta_1'' = \frac{p \cdot b^2}{8 \cdot \lambda_t} = \frac{6.8 \cdot 10^{-3} \cdot 19.2^2}{8 \cdot 0.03} = 10.5^\circ C$$

$$\Theta_4'' = \Theta_4' \cdot \frac{b}{a} = 6.56 \cdot \frac{19.2}{19.2} = 6.56^\circ C$$

9. Calculation of the internal surface of transformer tank and heat dissipation

$$A = 2 \cdot M + D_{ei} + 2 \cdot s_5 = 2 \cdot 30 + 27.99 + 2 \cdot 3 \approx 114 cm$$

$$B = D_{ei} + s_1 + s_2 + d_1 + s_3 + s_4 + d_2 = 27.99 + 2.5 + 2.5 + 0.3 + 2 + 2 + 1 \approx 38 cm$$

$$H_{cv} = L_c + 2 \cdot H_j + H_{jc} + H_{sj} = 76.16 + 2 \cdot 1 + 30 + 3 \approx 111 cm$$

where minimum isolation distances  $s_1, s_2, \dots, s_5$  and  $d, d_2$  dimensions for conductor size for winding direction are taken from table 18.5 [13, p.864] and minimum distance from the yoke to the top  $H_{jc}$  and bottom  $H_{sj}$  tank surface from table 18.6 [13, p.864].

$$s_1 = s_2 = 2.5 cm$$

$$s_3 = s_4 = 2 cm$$

$$s_5 = 3 cm$$

$$d_1 = 3 mm = 0.3 cm$$

$$d_2 = 10 mm = 1 cm$$

10. Temperature drop tank to air

$$\Theta_{ca} \leq 55 - \Theta_{mbu} = 55 - 23.47 = 31.52^\circ C$$

11. Vertical surface area of the tank

$$S_{cv} = 2 \cdot (A + B) \cdot H_{cv} = 2 \cdot (114 + 38) \cdot 111 = 3.39 \cdot 10^4 \text{ cm}^2 = 3.39 \text{ m}^2$$

12. The surface of radiation considered to be about 50% bigger

$$S_r = k \cdot S_{cv} = 1.5 \cdot 3.39 = 5.0786 \text{ m}^2$$

where  $k = 1.5$

13. Surface area of convection

$$S_{co} = \frac{1.05 \cdot (P_{kN} + P_0)}{2.5 \cdot \Theta_{ca}^{1.25}} - 1.12 \cdot S_r = \frac{1.05 \cdot (5950 + 668)}{2.5 \cdot 31.52^{1.25}} - 1.12 \cdot 5.0786 = 30.39 \text{ m}^2$$

14. Surface area elements of cooling

$$S_{er} = S_{co} - S_{cv} = 30.39 - 3.39 = 27 \text{ m}^2$$

15. Refine convective area

$$S'_{ct} = S_{ct} + S_{cc} = 2.60 + 0.4 = 3 \text{ m}^2$$

where from the table 15.3 [13, p.788] the base dimensions for radiator are

$L = 90 \text{ cm}$  - collector length

$$S_{ct} = 2.60 \text{ m}^2$$

$S_{cc} = 0.4 \text{ m}^2$  - area of collector cooling

16. Number of radiators

$$\frac{S_{er}}{S'_{ct}} = \frac{27}{3} \approx 9 \text{ radiators}$$

17. Thus area related to convection

$$S_{co} = S_{cv} + 9 \cdot S'_{ct} = 3.39 + 9 \cdot 3 = 30.39 \text{ m}^2$$

$$S_r = 2 \cdot ((A + 30) + (B + 60)) \cdot H_{cv} \cdot 10^{-4} = 2 \cdot ((113 + 30) + (38 + 60)) \cdot 111 \cdot 10^{-4} = 5.38 \text{ m}^2$$

*Finalizing the transformer temperature drop*

18. Temperature drop tank to air

$$\Theta_{ca} = \left[ \frac{1.05 \cdot (P_{kN} + P_0)}{2.8 \cdot S_r + 2.5 \cdot S_{co}} \right]^{0.8} = \left[ \frac{1.05 \cdot (5950 + 668)}{2.8 \cdot 5.38 + 2.5 \cdot 30.39} \right]^{0.8} = 32.06^\circ C$$

19. Temperature drop oil to tank

$$\Theta_{uc} = 0.165 \cdot k_1 \cdot \left[ \frac{1.05 \cdot (P_{kN} + P_0)}{S_{co}} \right]^{0.6} = 0.165 \cdot 1 \cdot \left[ \frac{1.05 \cdot (5950 + 668)}{30.39} \right]^{0.6} = 4.21^\circ C$$

where  $k_1 = 1$  coefficient for transformers with natural cooling

20. The average temperature drop oil to air

$$\Theta_{mua} = 1.2 \cdot (\Theta_{uc} + \Theta_{ca}) = 1.2 \cdot (4.21 + 32.06) = 43.53^\circ C < 60^\circ C$$

21. Temperature drop winding to air

$$\Theta_{ba} = \Theta_{mbu} + \Theta_{uc} + \Theta_{ca} = 23.47 + 4.21 + 32.06 = 59.75^\circ C$$

22. The winding temperature  $\Theta_n$  is calculated according to the standard for class A with ambient temperature  $\Theta_a = 40^\circ C$

$$\Theta_n = \Theta_{ba} + \Theta_a = 59.75 + 40 = 99.75^\circ C < 105^\circ C = \Theta_{N class A}$$

### Calculation of thermal resistance

1. Thermal resistance for HV windings

$$R_{th HV1} = \frac{n'_{si} \cdot a_i \cdot 10^{-2}}{k \cdot s_{wi} \cdot 10^{-6} \cdot w'_{iT}} = \frac{3 \cdot 1.32 \cdot 10^{-2}}{401 \cdot 8.33 \cdot 10^{-6} \cdot 765} = 0.0088 K/W$$

$$R_{th HV2} = \frac{n''_{si} \cdot a_i \cdot 10^{-2}}{k \cdot s_{wi} \cdot 10^{-6} \cdot w''_{iT}} = \frac{4 \cdot 1.32 \cdot 10^{-2}}{401 \cdot 8.33 \cdot 10^{-6} \cdot 1145} = 0.0087 K/W$$

where

$k = 401 W/m \cdot K$  - thermal conductivity of copper

$$n'_{si} = 40\% \cdot n_{si} = 0.4 \cdot 7 = 3 \text{ turns/layer}$$

$$n''_{si} = 60\% \cdot n_{si} = 0.6 \cdot 7 = 4 \text{ turns/layer}$$

$$w'_{iT} = 40\% \cdot w_{iT} = 0.4 \cdot 1227 = 491 \text{ turns}$$

$$w''_{iT} = 60\% \cdot w_{iT} = 0.6 \cdot 1227 = 736 \text{ turns}$$

2. Thermal resistance for LV windings

$$R_{th LV1} = \frac{n'_{sj} \cdot a_j \cdot 10^{-2}}{k \cdot s_{wj} \cdot 10^{-6} \cdot w'_j} = \frac{1 \cdot 1.25 \cdot 10^{-2}}{401 \cdot 316 \cdot 10^{-6} \cdot 13.5} = 0.009 K/W$$

$$R_{th LV2} = \frac{n''_{sj} \cdot a_j \cdot 10^{-2}}{k \cdot s_{wj} \cdot 10^{-6} \cdot w''_j} = \frac{1 \cdot 1.25 \cdot 10^{-2}}{401 \cdot 316 \cdot 10^{-6} \cdot 13.5} = 0.0062 K/W$$

where for LV windings the bobbin can be spread equally

$$n'_{sj} = 50\% \cdot n_{sj} = 0.5 \cdot 2 = 1 \text{ turns/layer}$$

$$n''_{sj} = 50\% \cdot n_{sj} = 0.5 \cdot 2 = 1 \text{ turns/layer}$$

$$w'_j = 50\% \cdot w_j = 0.5 \cdot 27 = 13.5 \text{ turns}$$

$$w''_j = 50\% \cdot w_j = 0.5 \cdot 27 = 13.5 \text{ turns}$$

$$R_{th Air} = 5.76 \cdot 10^{-4} K/W \text{ - air thermal resistance}$$

$$R_{th oil} = 0.05 K/W \text{ - oil thermal resistance}$$



## Appendix B Transformer rated data and test report

**KONČAR D&ST**

**TRANSFORMER**

Type	5TBNO 630-12/I	
No.	DT0977-512431	Year 2014
Power	630 kVA	Connect Dyn5
Standard	DEFU, IEC 60076	
Freq.	50 Hz	Cooling ONAN
Phases	3	
$U_k$	4.3 %	Mass of oil 335 kg
		Total mass 1800 kg

279163

Pos. ①	+5%	11025	
②	+2.5%	10763	
③	Rated voltages	10500	420 V
④	-2.5%	10238	
⑤	-5%	9975	
Rated currents	34.6	866	A
Insulation level	LI75 AC28	AC3	

MADE IN CROATIA

**ZK**

Fig. .4: Transformer rated data

# Appendix A

<b>KONČAR</b>		<b>TRANSFORMER TEST REPORT</b>		Part No. DT0977	
<b>D&amp;ST</b>		Type 5TBNO 630-12/I		Year of manufacturing 2014	
Serial No. 612431		Tested according to DEFU, IEC 60076			
Power 630 kVA		H.V. 10500±2x2,5% V		Currents 34,6 A	
Connection symbol Dyn5		L.V. 420 V		866 A	
Frequency 50 Hz		Temperature class A		Oil 335 kg Total mass 1800 kg	
1 Temperature of transformer during testing 22 °C		Ambient temperature during testing 22 °C			
2 Vector-group checked and found Dyn5		Tolerance of voltage ratio checked and found < 0,5 %			
3 Winding resistances at H.V. tap-changer position 3					
H.V. winding		A - B 1,522		A - C 1,521	
		B - C 1,518		L.V. winding	
		a - b 0,00161		a - c 0,00164	
				b - c 0,00159	
4 Winding insulation resistances					
H.V. - L.V. (≡) >2000 MΩ		H.V. - ≡ (L.V.) >2000 MΩ		L.V. - ≡ (H.V.) >2000 MΩ	
5 Dielectric strenght of oil 55 kV Type of oil Hyvolt I					
6 Separate source voltage withstand tests					
H.V. winding - L.V. winding and earthed parts		28 kVef		Duration 1 min 50 Hz	
L.V. winding - earthed parts		3 kVef		Duration 1 min	
7 Induced overvoltage withstand test (voltage applied to L.V. winding terminals)					
Voltage 2 Un		Frequency 150 Hz		Duration 40 sec	
8 Load loss and impedance voltage at short - circuited LV winding and position of tap - changer 3					
Voltage V		Current A		Loss W	
Measured 400		31,26		3898	
Calculated to 443		34,6		4775	
9 No-load loss and current at rated voltage and frequency					
Voltage Vavr 420		Current Arms 1,6		Loss W 635	
				Correction W 0	
				Corr. Loss W 635	
Following currents have been measured per phases					
Phase a 1,76 A		Phase b 1,18 A		Phase c 1,85 A	
10					
Impedance voltage at 75 °C		RATED		GUARANTEED	
Load loss at 75 °C		W		P <sub>k</sub> ≤	
No-load loss		W		P <sub>0</sub> ≤	
Total losses		W		P <sub>0</sub> + P <sub>k</sub> ≤	
No-load current		%		i <sub>0</sub> ≤	
Remarks					
Zagreb, 16.1.2014.		Tested by Z.Pršec, ing.		Approved by K.Gluhak, dipl.ing.	
				Page 1/1	

Fig. .5: Transformer test report.

# Appendix C Harmonic levels standard

## 1. DS/EN61000-2-4

Tab. .3: Summary of harmonic levels from DS/EN61000-2-4 for Class 2

Order $h$	5	7	11	13	17	$17 < h \leq 49$
Class 2	6	5	3.5	3	2	$2.27 \cdot (17/h) - 0.27$

Order $h$	3	9	15	21	$21 < h \leq 45$
Class 2	5	1.5	0.4	0.3	0.2

Order $h$	2	4	6	8	10	$10 < h < 50$
Class 2	2	1	0.5	0.5	0.5	$0.25 \cdot (10/h) + 0.25$

## 2. Teknisk forskrift 3.2.2 for solcelleanlæg større end 11 kW

#### 4.5.2.2 Krav til solcelleanlæg kategori B

Grænseværdierne for emission af harmoniske strømme for forskellige ordener  $h$  fremgår af nedenstående tabel.

Spændings-niveau	SCR	Ulige harmonisk orden $h$ (ikke multiplum af 3)					Lige harmonisk orden $h$		
		5	7	11	13	$17 \leq h \leq 39$	2	4	$8 \leq h \leq 40$
$U_c \leq 1 \text{ kV}$	<33	3,6	2,5	1,0	0,7	-	-	-	-
	$\geq 33$	4,1	2,8	1,1	0,8	-	-	-	-
	$\geq 66$	5,3	3,5	1,7	1,2	-	-	-	-
	$\geq 120$	7,2	4,6	2,6	1,6	-	-	-	-
	$\geq 250$	11,7	7,5	4,4	3,0	-	-	-	-
	$\geq 350$	15,2	9,6	5,9	4,1	-	-	-	-
$U_c > 1 \text{ kV}$	-	4,0	4,0	2,0	2,0	$\frac{400}{h^2} \text{ *)}$	0,8	0,2	0,1

\*) Dog ikke mindre end 0,1 %.

Note: for SCR  $\geq 33$  må interpoleres imellem tabelværdierne.

Tabel 5 Grænseværdier for harmonisk strøm  $I_h/I_n$  (% af  $I_n$ ).

Grænseværdierne for emission af samlet harmonisk strømforvrængning fremgår af nedenstående tabel.

Spændings-niveau	SCR	THD <sub>I</sub>	PWHD <sub>I</sub>
$U_c \leq 1 \text{ kV}$	<33	4,5	7,9
	$\geq 33$	4,9	8,1
	$\geq 66$	6,0	9,0
	$\geq 120$	8,3	10,5
	$\geq 250$	13,9	14,3
	$\geq 350$	18,0	17,3
$U_c > 1 \text{ kV}$	-	-	-

Tabel 6 Grænseværdier for samlet harmonisk strømforvrængning (% af  $I_n$ ) for alle harmoniske forstyrrelser.

# Appendix D PV system rated data

<b>Fronius Agilo 100.0-3</b>	Input data	
	MPP voltage range	460 - 820 V DC
	Max. input voltage (at 1000 W/m <sup>2</sup> , -10 °C in an open circuit)	950 V DC
	Max. input current	227.0 A
	Max. short circuit current of the solar modules	340.5 A
	Output data	
	Nominal output power ( $P_{nom}$ )	100 kVA
	Max. output power	100 kVA
	Nominal grid voltage	3 ~ NPE 400 V / 230 V
	Grid voltage tolerance	+10 / -5 % <sup>1)</sup>
	Nominal output current (three-phase)	150.2 A
	Nominal frequency	50 - 60 Hz <sup>1)</sup>
	Total harmonic distortion	< 3 %
	Power factor cos phi	<sup>1)</sup> 0.8 - 1 ind./cap. <sup>2)</sup>
	Max. permitted mains impedance $Z_{max}$ at PCC <sup>3)</sup>	52 mOhm
	Max. feedback current <sup>4)</sup>	0 A <sup>5)</sup>
	Starting current pulse <sup>5)</sup>	0 A <sup>5)</sup>
	Max. output fault current per period	522 A / 2.47 ms
	General data	
	Maximum efficiency	97.2 %
	Europ. efficiency	96.6 %
	Overnight internal consumption	36 W
	Cooling	Controlled forced-air ventilation
	Degree of protection	IP 30
	Dimensions l x w x h	1100 x 700 x 1884 mm
	Weight	834 kg
	Permitted ambient temperature (at 95% rel. humidity)	- 20 °C - +50 °C
	EMC emission class	A
	Over-voltage category AC / DC	3 / 2
	Degree of pollution	3
	Protection devices	
	DC insulation measurement	Warning/shutdown <sup>7)</sup> at $R_{iso}$ < 31.66 kOhm
	Manifestation of DC overload	Operating point shift power limitation
	DC circuit breaker	Integrated

110

Fig. .6: Inverter rated data.

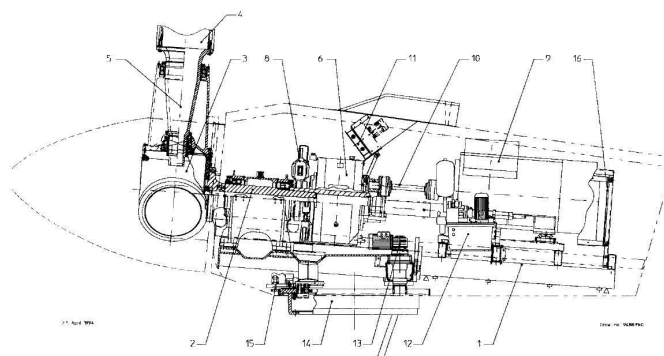


# Appendix E Vestas V29 255kW Wind Turbine

General Specification V29-225 kW				
Date: 28. Nov 1996	Class: 1	Item no.: 941521.R3	Page: 10 of 22	

## 6. General Specification

### 6.1 Structure of machinery



- |                      |                          |
|----------------------|--------------------------|
| 1. Nacelle bed plate | 9. Generator             |
| 2. Main shaft        | 10. Transmission shaft   |
| 3. Blade hub         | 11. Hydraulic unit       |
| 4. Blade             | 12. Gear oil system      |
| 5. Blade bearing     | 13. Yaw gears            |
| 6. Gearbox           | 14. Yaw ring             |
| 7. Torque arm system | 15. Yaw control          |
| 8. Disc brake        | 16. VMP-top control unit |

Fig. .7: Vestas V29 255kW Wind Turbine (1)



		General Specification V29-225 kW		
Date:	28. Nov 1996	Class:	I	Item no.: 941521.R3
				Page: 13 of 22
<b>7.5</b>	<b>Machinefoundation</b>	Manufacturer:	VESTAS	
		Type:	Tubular construction	
		Material:	Steel 44.2 DIN 17100	
<b>7.6</b>	<b>Yaw System</b>	Manufacturer:	VESTAS	
		Type:	Slideblocksystem with build in friction	
<b>7.6.1</b>	<b>Yaw gear, 2 units</b>	Type:	Planet and worm gear	
		Rated torque:	2 x 500 Nm	
		Manufacturer:	Bonfiglioli-Transmittal, or corresponding	
<b>7.6.2</b>	<b>Yaw motors</b>	Rotational Speed:	950 RPM	
		Rated power:	0.55 kW	
<b>7.7</b>	<b>Tower</b>	Type:	Conical tubular	
		Height:	31 m	
		Manufacturer:	VESTAS	
		Surface treatment:	Metallized + painting	
		Weight:	12,000 kg	
<b>7.7.1</b>	<b>Paintsystem, outside</b>	Sandblasting:	SA3 (ISO 8501)	
		Metallizing:	DSI/ISO 2063 Zn 80	
		Epoxy coating:	Min. 120 µ (2 layers)	
		Polyurethane coat:	UV resistant min. 40 µ (1 layer)	
<b>7.7.2</b>	<b>Paintsystem, inside</b>	Sandblasting:	SA2.5 (DS8501)	
		Zinciferous first coat:	Min. 50 µ (1 layer)	
		Epoxy coating:	Min. 100 µ (1 layer)	
<b>7.7.3</b>	<b>Lattice tower</b>	Type:	Lattice	
		Height:	31 m	
		Manufacturer:	VESTAS	
		Surface treatment:	Hot galvanized	

Fig. .8: Vestas V29 255kW Wind Turbine (2)



				General Specification V29-225 kW			
Date:	28. Nov 1996	Class:	I	Item no.:	941521.R3	Page:	14 of 22

## 7.8 Gearbox

Nominal power:	450 kW
Ratio:	1:24,6
Type:	Two stage, parallel shafts
Oil quantity:	53 l
Slowspeed shaft:	Hollow shaft
Manufacturer:	Valmet or corresponding

## 7.9 Couplings

### 7.9.1 Main shaft gear

Type:	Conical shrink disc
-------	---------------------

### 7.9.2 Gear - Generator

Type:	Transmission shaft
-------	--------------------

## 7.10 Generator

Type:	Doublewinding, asynchronous		
Manufacturer:	Siemens corresponding		
Rated power, 6 poles:	225 kW		
Voltage:	3x400 V		
Frequency:	50 Hz		
Class of insulation:	F		
Rotational speed (225 kW):	1016 RPM		
Rated current:	390A/225A		
Power factor:	0.83		
Reactive power no load:	95 kVAr		
Power Factor correction:	100 kVAr		
Resulting power factor at:	1/1 load:	0.98	
	3/4 load:	0.99	
	1/2 load:	0.99	
	1/4 load:	1.00	
Resulting power at full load:	333/193 A		
Rated power, 8 poles:	50 kW		
Voltage:	3x400 V		
Frequency:	50 Hz		
Class of insulation:	F		
Rotational speed (50 kW):	760 RPM		
Rated Power:	98A/57A		
Power factor:	0.74		
Reactive power no. load:	34 kVAr		
Power factor correction:	37,5 kVAr		
Resulting power factor at:	1/1 load	0.99	
	3/4 load	0.99	
	1/2 load	1.00	
	1/4 load	0.99	
Resulting current:	73A/42A		

Fig. .9: Vestas V29 255kW Wind Turbine (3)

# Appendix F PV inverter Fronius Agilo

Fronius Agilo 100.0-3	Input data	
	MPP voltage range	460 - 820 V DC
	Max. input voltage (at 1000 W/m <sup>2</sup> / -10 °C in an open circuit)	950 V DC
	Max. input current	227.0 A
	Max. short circuit current of the solar modules	340.5 A
	Output data	
	Nominal output power (P <sub>nom</sub> )	100 kVA
	Max. output power	100 kVA
	Nominal grid voltage	3 ~ NPE 400 V / 230 V
	Grid voltage tolerance	+10 / -5 % <sup>1)</sup>
	Nominal output current (three-phase)	150.2 A
	Nominal frequency	50 - 60 Hz <sup>1)</sup>
	Total harmonic distortion	< 3 %
	Power factor cos phi	1
		0.8 - 1 ind./cap. <sup>2)</sup>
	Max. permitted mains impedance Z <sub>m</sub> at PCC <sup>3)</sup>	52 mΩ
	Max. feedback current <sup>4)</sup>	0 A <sup>5)</sup>
	Starting current pulse <sup>6)</sup>	0 A <sup>5)</sup>
	Max. output fault current per period	522 A / 2.47 ms
	General data	
	Maximum efficiency	97.2 %
	Europ. efficiency	96.6 %
	Overnight internal consumption	36 W
	Cooling	Controlled forced-air ventilation
	Degree of protection	IP 30
	Dimensions l x w x h	1100 x 700 x 1884 mm
	Weight	834 kg
	Permitted ambient temperature (at 95% rel. humidity)	- 20 °C - +50 °C
	EMC emission class	A
	Over-voltage category AC / DC	3 / 2
	Degree of pollution	3
	Protection devices	
	DC insulation measurement	Warning/shutdown <sup>7)</sup> at R <sub>ISO</sub> < 31.66 kΩ
	Manifestation of DC overload	Operating point shift power limitation
	DC circuit breaker	Integrated

## Appendix G Structure of Matlab files

	Transformer Voltage	Transformer Current	Wind Turbine Current	Pig farm Current	File length
Saved file with raw data	rawDataVoltage.mat	rawDataCurrent_tr.mat	rawDataCurrent_wt.mat	rawDataCurrent_pf.mat	
Structure file	rawData	rawData_la_lb_lc	rawDataCurrent_wt	rawDataCurrent_pf	
Phase A	Va	la	la_wt	la_pf	1x1876
Phase B	Vb	lb	lb_wt	lb_pf	1x1876
Phase C	Vc	lc	lc_wt	lc_pf	1x1876
Information inside the file	Time and Amplitude	Time and Amplitude	Time and Amplitude	Time and Amplitude	
Saved file with rms data	Voltage_rms.mat	rmsDataCurrent_tr.mat	rmsDataCurrent_wt.mat	rmsDataCurrent_pf.mat	
Phase A	Va_rms	la_rms	la_wt_rms	la_pf_rms	1x1876
Phase B	Vb_rms	lb_rms	lb_wt_rms	lb_pf_rms	1x1876
Phase C	Vc_rms	lc_rms	lc_wt_rms	lc_pf_rms	1x1876
Information inside the file	Amplitude	Amplitude	Amplitude	Amplitude	
Saved file with vectorized rms data	Voltage_rms_vec.mat	rmsDataCurrent_tr_vec.mat	rmsDataCurrent_wt_vec.mat	rmsDataCurrent_pf_vec.mat	
Phase A	Va_rms_vec	la_rms_vec	la_wt_rms_vec	la_pf_rms_vec	1x1876
Phase B	Vb_rms_vec	lb_rms_vec	lb_wt_rms_vec	lb_pf_rms_vec	1x1876
Phase C	Vc_rms_vec	lc_rms_vec	lc_wt_rms_vec	lc_pf_rms_vec	1x1876
Information inside the file	Amplitude	Amplitude	Amplitude	Amplitude	
	Power	Time	Time	Data file information	
Saved file	Power.mat	Saved file	Time.mat	Saved file	Files_info.mat
Structure file for power P and Q	Power	Structure file for Time of 10 cycles	Time	Structure Info file date and time C1	files_C1
Time stamp for measurements	Time_stamp			Structure Info file date and time C2	files_C2
Active power transformer	active_tr			Structure Info file date and time C3	files_C3
Active power Wind Turbine	active_wt			Structure Info file date and time C4	files_C4
Active power Pig Farm	active_pf				
Reactive power transformer	reactive_tr				
Reactive power Wind Turbine	reactive_wt				
Reactive power Pig Farm	reactive_pf				

Fig. .10: The structure of files saved for easy processing using the Matlab script.

